imgew (Lon)

THE BEHAVIOUR OF BEAM-COLUMN JOINT UNDER REVERSAL LOADING

by

Handy Sutanto

A Report
presented to the University of Ottawa
in partial fulfillment of the
requirements for the degree of
Master of Engineering
in
Department of Civil Engineering

January 1981
Ottawa, Ontario,
Canada.

TABLE OF CONTENTS

LIST OF FIGURES

Figure		Page
27	Joint Condition (front) When Test Was Terminated	46
28	Joint Condition (back) When Test Was Terminated	46
29	Joint Reinforcement, Specimen 3	49
30	Joint Condition of Specimen 3 at Second Cycle	49
31	Specimen 3 at Third Cycle	50
32	Specimen 3 When Test Was Terminated	50
33	Specimen 5 at The End of Cycle 2	54
34	Specimen 5 When Test Was Terminated	55
35	Specimen 4 When Test Was Terminated (front)	57
36	Specimen 4 When Test Was Terminated (back)	58
37	Specimen 6 When Test Was Terminated (front)	61
38	Specimen 6 When Test Was Terminated (back)	62
A 1a	Beam Tip Load Versus Beam Tip Deflection (left),Specimen 1	70
A 1b	Beam Tip Load Versus Beam Tip Deflection (right),Specimen 1	71
A 2a	Beam Tip Load Versus Beam Tip Deflection (left),Specimen 2	72
A 2b	Beam Tip Load Versus Beam Tip Deflection(right),Specimen 2	73
A 3	Beam Tip Load Versus Beam Tip Deflection, Specimen 3	74
A 4	Beam Tip Load Versus Beam Tip Deflection, Specimen 4	75
A 5	Beam Tip Load Versus Beam Tip Deflection, Specimen 5	76
A 6	Beam Tip Load Versus Beam Tip Deflection, Specimen 6	77
A 7	Beam Curvature Versus Joint Moment, Specimen 1	78
A 8	Beam Curvature Versus Joint Moment, Specimen 2	79
A 9	Beam Curvature Versus Joint Moment, Specimen 3	80
A10	Beam Curvature Versus Joint Moment, Specimen 4	81
A11	Beam Curvature Versus Joint Moment, Specimen 5	82
A12	Beam Curvature Versus Joint Moment, Specimen 6	83
A13a	Diagonal Joint Strain (LT-RB) Versus Joint Moment, Sp. 1	84
A13b	Diagonal Joint Strain (RT-LB) Versus Joint Moment, Sp. 1	85
A14a	Diagonal Joint Strain (LT-RB) Versus Joint Moment, Sp. 2	86
A14b	Diagonal Joint Strain (RT-LB) Versus Joint Moment, Sp. 2	87
A15a	Diagonal Joint Strain (LT-RB) Versus Joint Moment, Sp. 3	88
A15b	Diagonal Joint Strain (RT-LB) Versus Joint Moment, Sp. 3	89

Figure		Page
A16a	Diagonal Joint Strain (LT-RB) Versus Joint Moment, Sp. 4	90
A16b	Diagonal Joint Strain (RT-LB) Versus Joint Moment, Sp. 4	91
A17a	Diagonal Joint Strain (LT-RB) Versus Joint Moment, Sp. 5	92
A17b	Diagonal Joint Strain (RT-LB) Versus Joint Moment, Sp. 5	93
A18a	Diagonal Joint Strain (LT-RB) Versus Joint Moment, Sp. 6	94
A18b	Diagonal Joint Strain (RT-LB) Versus Joint Moment, Sp. 6	95
A19a	Diagonal Joint Strain (LT-RB) Versus Beam Tip Defl., Sp.3	96
A19b	Diagonal Joint Strain (RT-LB) Versus Beam Tip Defl., Sp.3	97
A20a	Diagonal Joint Strain (LT-RB) Versus Beam Tip Defl., Sp.4	98
A20b	Diagonal Joint Strain (RT-LB) Versus Beam Tip Defl., Sp.4	99
A21a	Diagonal Joint Strain (LT-RB) Versus Beam Tip Defl., Sp.5	100
A21b	Diagonal Joint Strain (RT-LB) Versus Beam Tip Defl., Sp.5	101
A22a	Diagonal Joint Strain (LT-RB) Versus Beam Tip Defl., Sp.6	102
A22b	Diagonal Joint Strain (RT-LB) Versus Beam Tip Defl., Sp.6	103
A23a	Diagonal Joint Strain (LT-RB) Versus Beam Curvature, Sp.1	104
A23b	Diagonal Joint Strain (RT-LB) Versus Beam Curvature, Sp.1	105
A24a	Diagonal Joint Strain (LT-RB) Versus Beam Curvature, Sp.2	106
A24b	Diagonal Joint Strain (RT-LB) Versus Beam Curvature, Sp.2	107
A25a	Diagonal Joint Strain (LT-RB) Versus Beam Curvature, Sp.3	108
A25b	Diagonal Joint Strain (RT-LB) Versus Beam Curvature, Sp.3	109
A26a	Diagonal Joint Strain (LT-RB) Versus Beam Curvature, Sp.4	110
A26b	Diagonal Joint Strain (RT-LB) Versus Beam Curvature, Sp.4	111
A27a	Diagonal Joint Strain (LT-RB) Versus Beam Curvature, Sp.5	112
A27b	Diagonal Joint Strain (RT-LB) Versus Beam Curvature, Sp.5	113
A28a	Diagonal Joint Strain (LT-RB) Versus Beam Curvature, Sp.6	114
A28b	Diagonal Joint Strain (RT-LB) Versus Beam Curvature, Sp.6	115
A29	Beam Curvature Versus Beam Tip Deflection, Specimen 3	116
A30	Beam Curvature Versus Beam Tip Deflection, Specimen 4	117
A31	Beam Curvature Versus Beam Tip Deflection, Specimen 5	118
A32	Beam Curvature Versus Beam Tip Deflection, Specimen 6	119
A33	Cumulative Energy, Specimens 3, 5	120
A34	Cumulative Energy, Specimens 4, 6	121

Chapter I

INTRODUCTION

1.1 INTRODUCTORY REMARKS

Over the past two decades with increasing urbanisation and city centre redevelopment the trend has been to build taller structures to minimise land costs and the cost of the provision of services. Together with the trend for taller bulidings has been the development of higher strength structural elements of lower stiffness. These trends have resulted in buildings which are susceptible to dynamic loads, principally lateral loads. Many parts of the world are seismically active to some extent and high winds are possible in all parts of the world, and both physical phenomena apply time varying lateral loads to structures. Consequently the behaviour of structures to lateral loads has to be considered in the design of such structures.

It is generally accepted that the integrity of a structure will be greatly joepardized if the joint(s) connecting various members fails. Recent studies have concluded [8,9,13] that a joint under severe earthquake shaking may well be the weakest spot in the struture members.

The behaviour of multistory structures under earthquake action has not received much attention in the past; however, several projects have been initiated during the last few years. Over the past two years a research program has been underway at the University of Ottawa to study the behaviour of beam-column joints. Six beam-column subassemblages of an isolated interior joint, with 8x7 in. column and 6.25x5.25 in. beam, have been studied and the results are presented in this report.

1.2 OBJECTIVE OF STUDY

The main objective is to study in general the behaviour of an interior beam-column joint under earthquake load, and in particular the effect of joint bond forces on its behaviour. The study also includes observations and brief assessments on the effect of column compressive forces, the amount of column reinforcements and joint lateral ties toward the behaviour of the subassembly.

Chapter II

THE BEHAVIOUR OF STRUCTURES UNDER LATERAL LOADS

2.1 THE BEHAVIOUR OF MULTISTORY STRUCTURES UNDER LATERAL LOADING

When a multistory building undergoes lateral load, the manner in which the frame responds to load depends to a large extent on the relative stiffnesses of the beams and columns. Two extreme cases are illustrated in Figure 1. In Figure 1a, the bending stiffness of the floor is very much greater than that of the columns, and the frame is forced to deflect with the points of contraflexure in the columns near mid-height, thus giving a 'shear' mode deformation. The reverse situation called a 'cantilever' mode is shown in Figure 1b, where the points of contraflexure occur in the floors near mid-span. In a typical frame a combined deformation mode occurs in which points of contraflexure form in both beams and columns. A typical frame moment diagram due to lateral forces and service loads with its critical regions is shown in Figure 2.

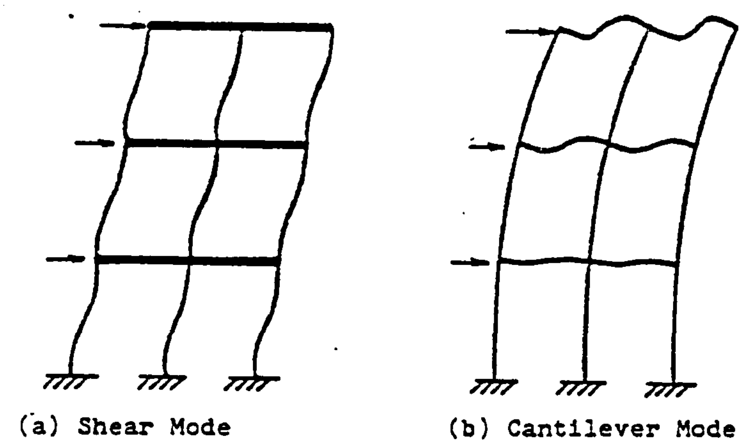

FIG. 1 DEFORMATION MODES

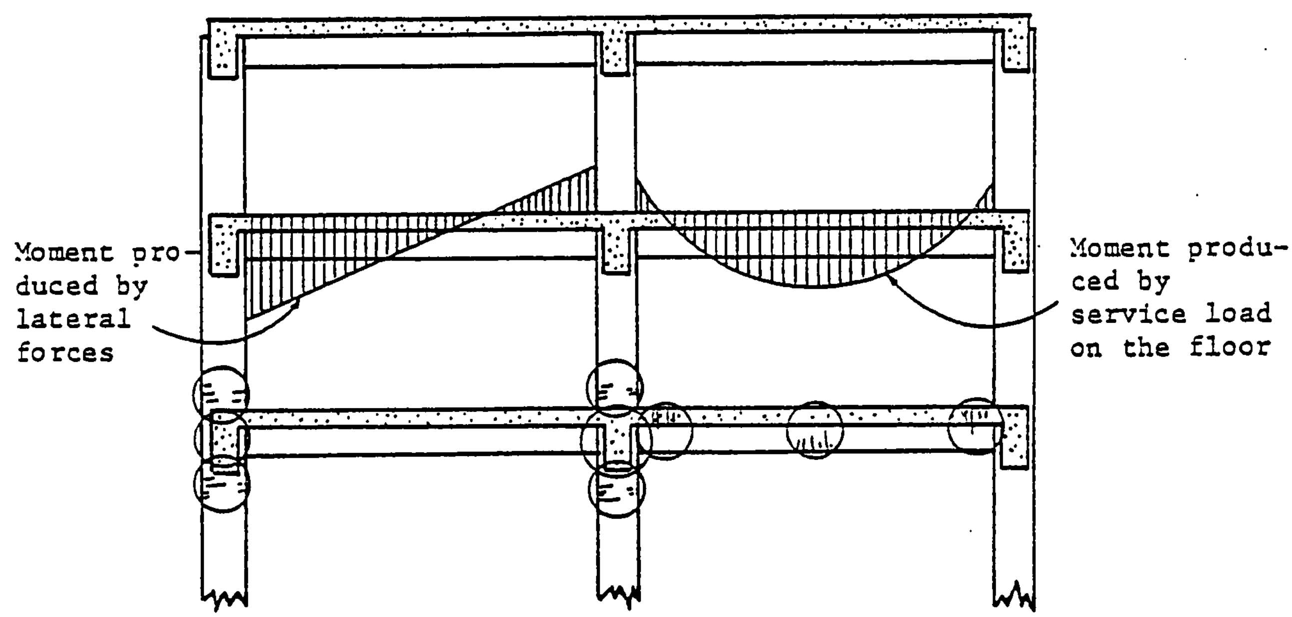

FIG. 2 CRITICAL REGIONS

2.2 THE BEHAVIOUR OF MULTISTORY CONCRETE STRUCTURES UNDER EARTHQUAKE LOADING

During the earthquake motion, a building serves as a mass and receives a large amount of energy, and this energy, one way or another, must be absorbed or dissipated. In other words, the kinetic energy demand caused by the earthquake has to be met by the energy capacity of the structure. Although the demand, which depends on the intensity, frequency of occurance and duration of shaking, is a random variable beyond the control of the designer, the absorption capacity of the structure is, to large extent, in his hands.

It is more meaningful as Blume [1] points out to measure the earthquake capacity of the structure in terms of energy absorption instead of strength alone. Within the elastic or linear range of structural response, energy capacity is proportional to the applied force. If the code lateral forces are exceeded during actual earthquakes and the unit deformations associated with the yield point are exceeded, the performance of the structure in such cases depends upon its properties beyond the initial yield point. If there is no ductility and if there is no inelastic stress path, the structure collapses under continued earthquake demands of greater magnitude. However, ductility and reserve inelastic energy capacity and/or alternate and stronger stress paths may be available to save the structure.

Since what they lack in elastic strength can be made up by their capacity to absorb the energy through inelastic movement, the design of seimic resistant structures therefore leaves us to two alternatives approaches.

1. Design stronger members so as to take up the total force.

2. Design ductile members to absorb part of the total force and sufficient ductility to absorb the total energy demand.

However, in designing a building against severe earthquake, economic considerations always require that the large seismic energy input to the building be absorbed and dissipated through inelastic deformation[1] of its structure. To achieve a large energy absorption and dissipation capacity, ductile or high ductility joint members must be designed.

2.3 DUCTILITY AND SOFTENING

The ultimate ductility (μ) is defined as the ratio of the maximum deformation prior to failure (Δ_u) to the deformation at initial yield (Δ_y).

According to Clough and Penzien [2], the nonlinear response analysis of deformations is nearly identical with the

---

[1]These deformations should be constrained to a limit which would avoid causing severe damage to the structural and nonstructural elements of the building.

elastic analysis. This conclusion is very convenient in that the inelastic deformation behaviour can be interpreted directly from a linear elastic response analysis. Consider, for example, the member force displacement relation shown in Figure 3. The following expressions therefore can be deduced

$$\frac{\Delta_{max.}}{\Delta_y} = \frac{f_{max.}}{f_y}$$

$$f_y = \frac{f_{max.}}{\mu} \qquad (1)$$

where μ may be established by direct stress, by buckling, by local failure, or by whatever condition or combination of conditions which leads to the minimum value of μ.

Softening is defined as the weakening of the joint in resisting the load particularly at the starting of reversal loading. This phenomena is demonstrated by using the elasto-plastic hysteresis loop in Figure 4. For a given deflection, the softening would reduce the energy absorption capacity (area dd'e'fgg' of Figure 4b < defgd of Figure 4a); in other words it requires a larger deflection to give the same amount of energy (area d'e'f'gd' of Figure 4c = defgd of Figure 4a).

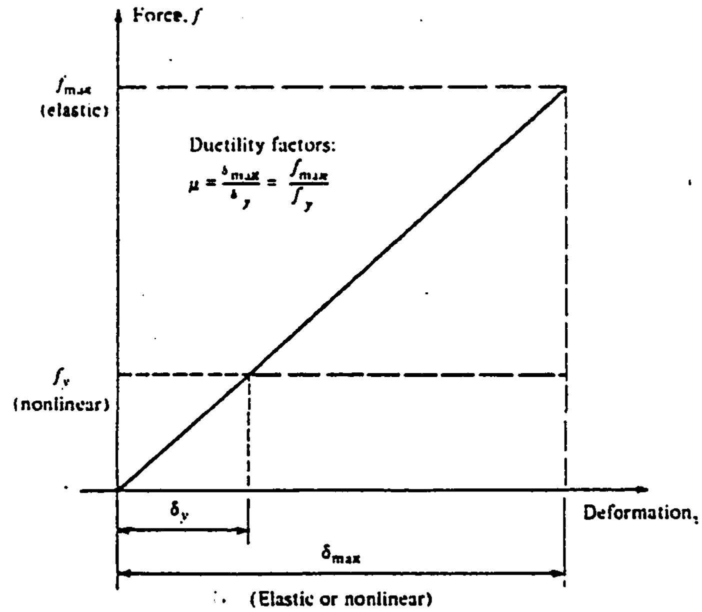

FIG. 3 DUCTILITY FACTOR, μ

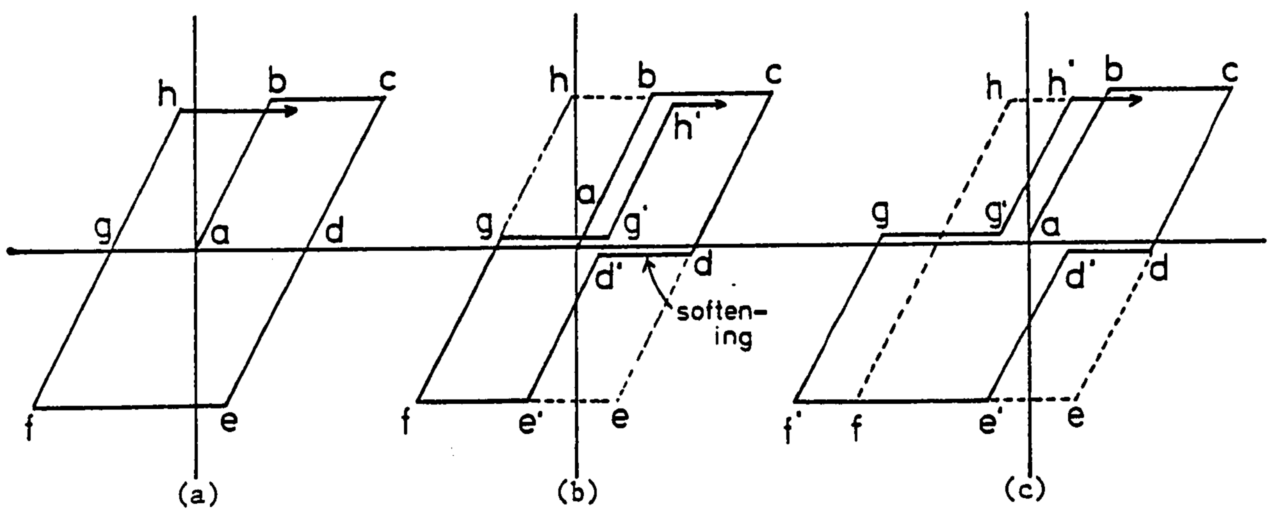

FIG. 4 SOFTENING EFFECT ON ELASTO-PLASTIC HYSTERESIS LOOP (a)elasto-plastic loop; (b)softening effect given constant deflection; (c)softening effect given constant energy

2.4 TOUGHNESS

An important factor in the resistance of a material to fracture is its toughness, the ability to absorb the energy. Any material can be loaded to the point of fracture, even the most brittle material can absorb some energy in the process of being strained to fracture. In Figure 5, at the instant preceding fracture the stress is σ_f and the total strain is ε_{ft}. When fracture occurs, the stress falls to zero and the strain falls to ε_f, the plastic strain after fracture. In this case, the recovered elastic strain upon fracture is equal to $\varepsilon_{ft} - \varepsilon_f$. The elastic strain energy, the area under linear portion of the stress-strain curve, is high in the case of a steep slope and high levels of stress. But even a high value of this energy cannot contribute to toughness, since all of it is recoverable energy. It is through plastic strain that energy is absorbed.

The above conclusion can also be achieved from the 'energy absorption capacity' approach.

2.5 WORK AND ENERGY

Equation 1. implies that the applied forces can be reduced by providing good ductility to the structure. Nevertheless, ductility alone is not adequate to assess the ability of the structure in withstanding the earthquake motion because there could be a large value of μ associated with a small force, and the area under the curve would be inadequate. For this reason the 'energy approach' gives a better estimation in rating the efficiency of the structure.

In general, it can be argued that in an earthquake, a structure has to do as much as work the net energy input to the structure from the ground. This includes, energy absorbed by the joint or work capacity(strain and/or damage), strain energy(elastic), energy losses(to heat etc.) without damage, and energy feedback or radiation from the structure to the ground.

Figure 6 illustrates two hypothetical cases, one for a very rigid story of a building and another for a more flexible and more ductile story. If it be assumed that the total energy requirement is the same for both cases, the necessary equal areas or stored energy U are shown in Figure 6.

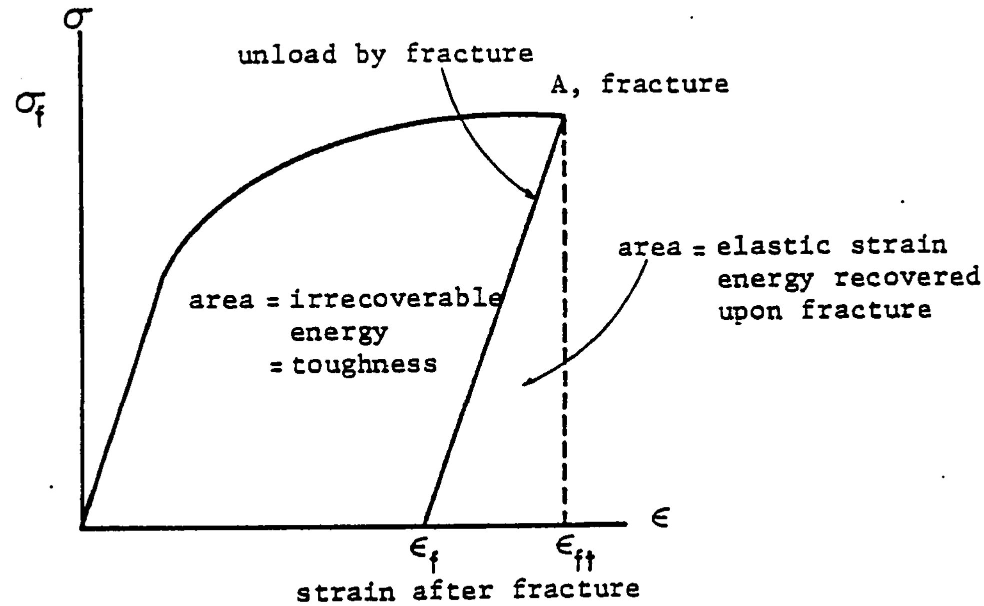

FIG. 5 STRAIN AFTER FRACTURE

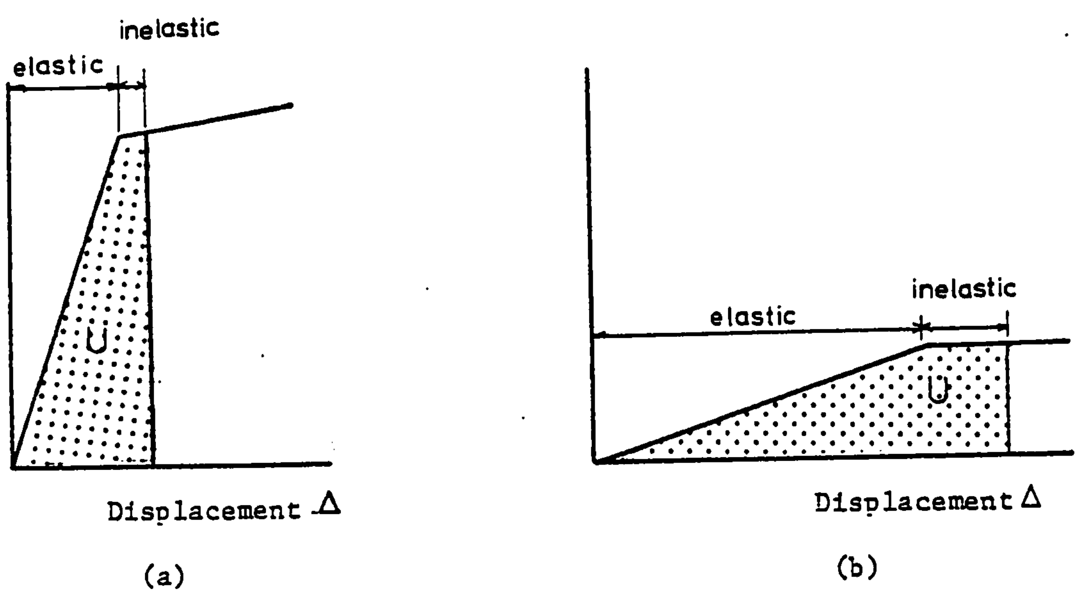

FIG. 6 IDEALIZED FORCE-DISPLACEMENT CURVES FOR TWO DIFFERENT DUCTILITY OF STRUCTURES

A flexible structure will absorb the same amount of energy as a rigid strucure but with less force. However, in order to develop the energy for the more flexible structure, considerably more displacement must occur. A designer has to provide sufficient strength and sufficient member ductility to satisfy the applied stimulus. The softening process (section 2.3) leads to a larger deflection without gaining an increase in energy.

2.6 THE NECESSARY BEHAVIOUR OF REINFORCED CONCRETE JOINT UNDER EARTHQUAKE LOADING

Reinforced concrete structures may be brittle or they may have great inelastic work capacity, depending on the amount and the disposition of the reinforcing steel in relation to the concrete sections.

An extensive study by Clough [3], on the effect of variation of strength of columns and girders on their lateral displacement and their ductility, has given earthquake engineers a better understanding of the desired behaviour for joint members under earthquake excitation.

The 20-story building, shown in Figure 8, subjected to the El-Centro (May 18, 1940) earthquake accelerogram shown in Figure 7 was analyzed with a dynamic frame analysis computer programe. Figure 9 shows that in an ordinary structure designed by the UBC design code (girder strength 2 times the design girder moments; column strength 6 times the design column moment) the yielding is confined to the girders. The columns remain essentially elastic; thus it may be concluded the yield energy absorbed by the girders has the effect of protecting the columns from overstress. By varying the strengths of the various elements, however, the yielding can be shifted from one portion of the structure to another.

To evaluate the effect of girder strength on the ductility requirements, two additional structures were analyzed and compared with the results from the standard building. The two new buildings had girder strength of 1.5 and 4 times the design girder moments, respectively. The results of these analyses are presented in Figure 10. The building with stronger girders shows less girder yielding, which tends to force more yielding into the columns and thus to increase the lateral displacements. Reducing the girder strengths produced the opposite effect.

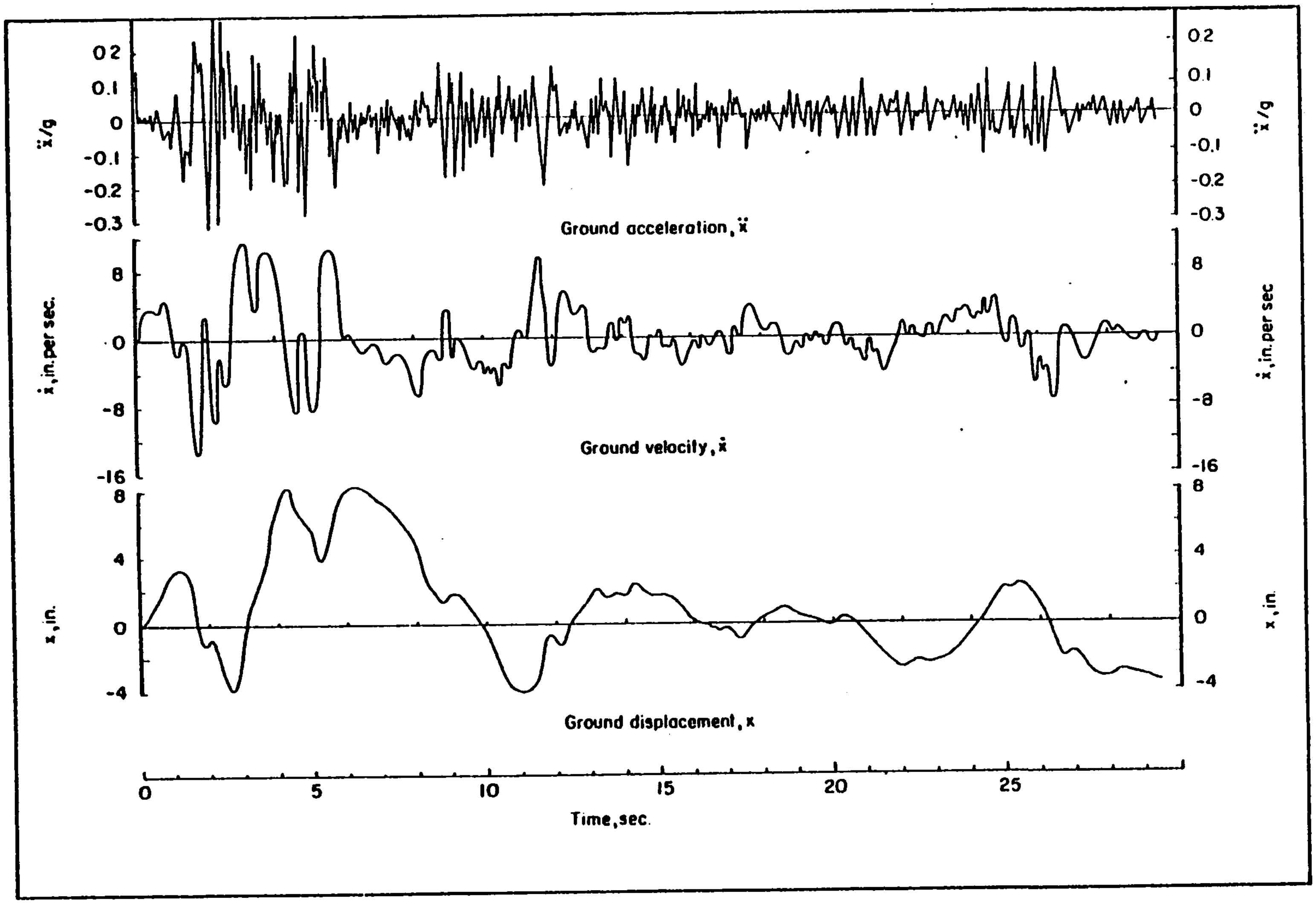

FIG. 7 GROUND ACCELERATION, VELOCITY, AND DISPLACEMENT, EL CENTRO, EARTHQUAKE OF MAY 18, 1940

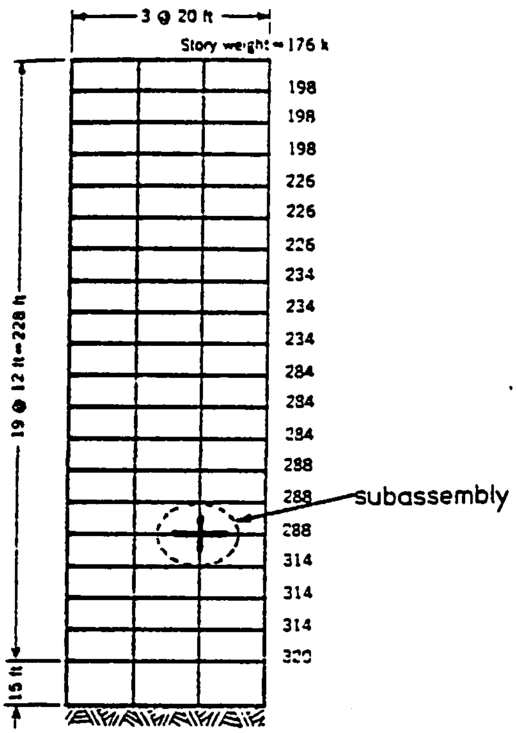

FIG. 8 20-STORY DUCTILE STRUCTURE

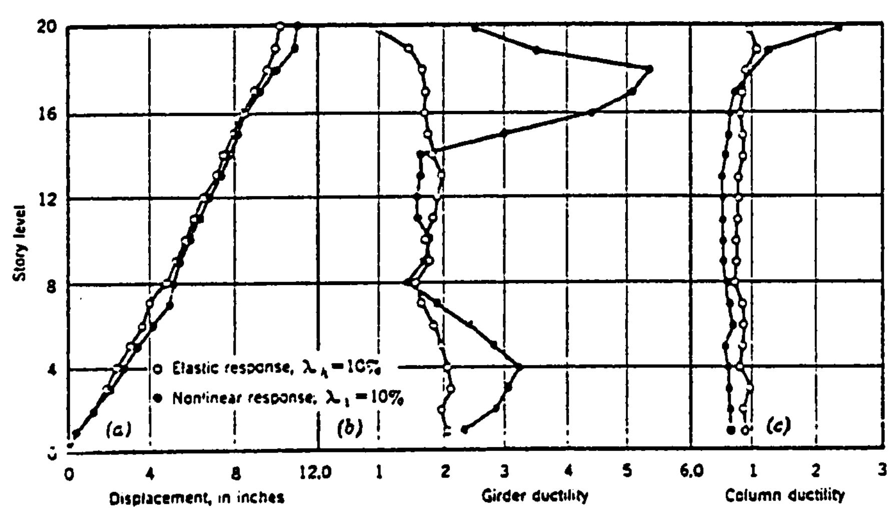

FIG. 9 COMPARISON OF ELASTIC AND NONLINEAR DYNAMIC EARTHQUAKE RESPONSE

Two other additional buildings were analyzed, having yield moments 2 and 10 times the design column moments, respectively. Their results are shown in Figure 11. These figures show that increasing the cclumn strength had little effect, which is not surprising in as much as the standard building showed very little column yieldng. However, the reduction of column strength caused a significant reduction in girder yield and corresponding increase in column yield. The question must then be asked, where would yielding occur when a beam-column subassembly has reached its ultimate capacity? Many research programs have been underway at some universities to study the behaviour of cast-in-place reinforced concrete beam-column joints. It is known that the most efficient design is a design of a balanced strength so that local yielding will be distributed evenly and no excessive damage will result at any point. Since such a balanced design is difficult to achieve, the design philosophy of a weak beam - strong column is adopted. This is because local yielding of the beams does not seriously affect the vertical lcad carrying capacity of the structure while local column yielding could lead to collapse.

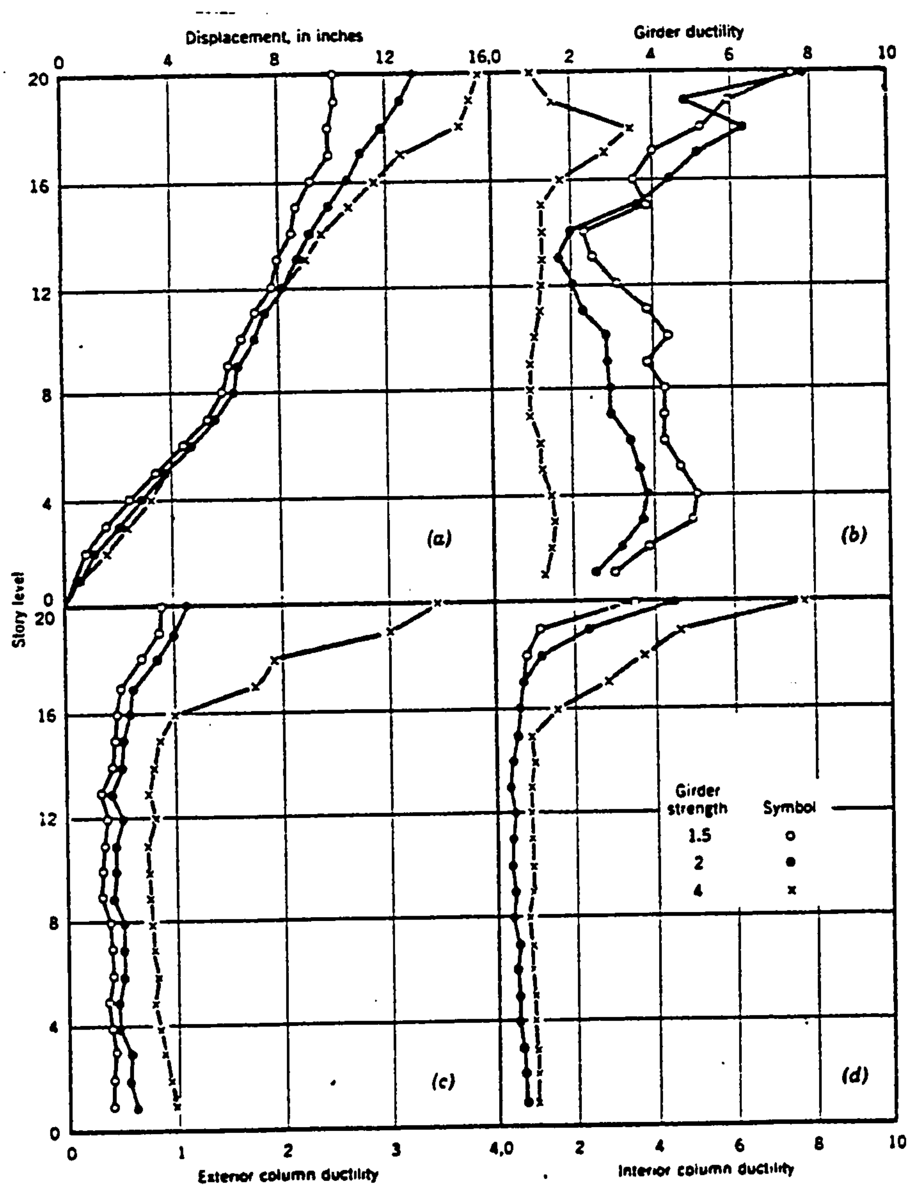

(From R.W.Clough, 1975)

FIG.10 EFFECT OF GIRDER STRENGTH ON NONLINEAR RESPONSE

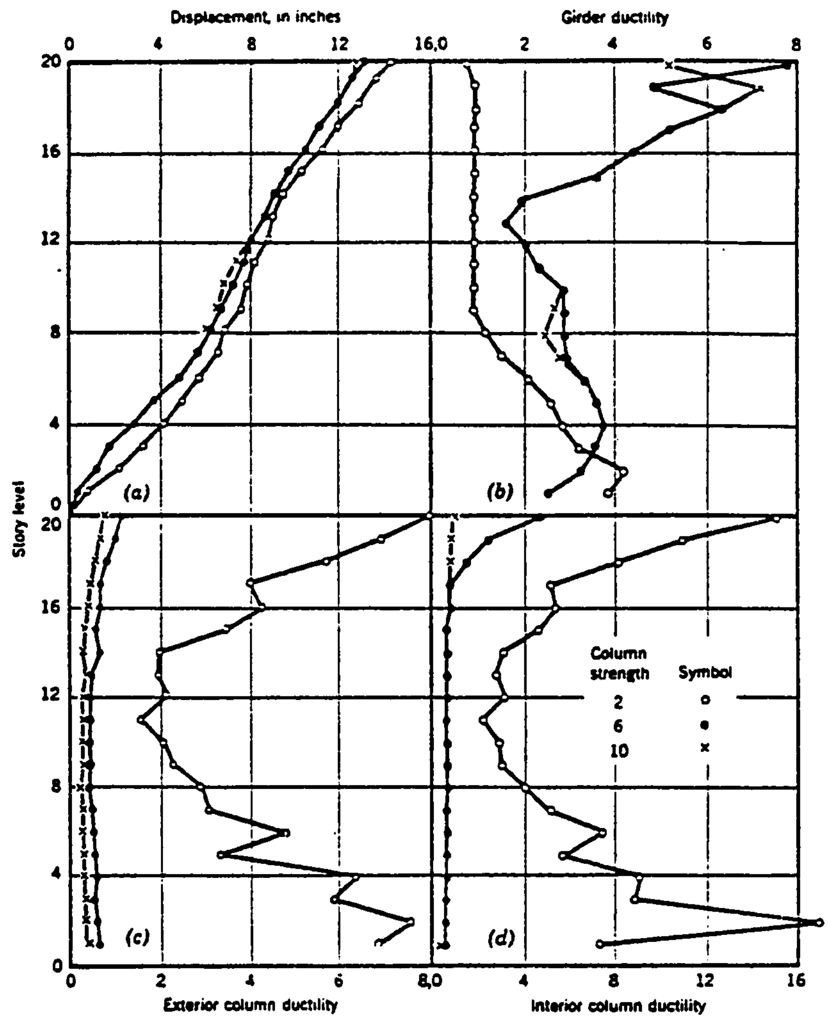

(From R.W.Clough, 1975)

FIG. 11 EFFECT OF COLUMN STRENGTH ON NONLINEAR RESPONSE

Concrete structures, because of their low ductility and relatively heavy weight, are particularly vulnerable to severe ground shaking. The sources of potential types of structural brittle failure should be eliminated. Thus it is necessary to prevent premature crushing and shear of concrete; sudden cracks (as in the case of members with extremely low reinforcement ratio); sudden loss of bond; premature crushing or splitting of the concrete cover accompanied by local buckling of the main reinforcement. Although some of the above potential sources for brittle failure can be controlled by satisfying the present code provisions, there are others that continue to give serious problems. Among those, as Bertero and Popov points out[4] bond failure, which leads to softening of the subassembly, is one of the most undesirable and has been the cause of damage to or failure of many structures in recent strong earthquakes. The shear and bond behaviour of reinforced concrete under monotonically increasing load is altogether different from the shear and bond behaviour observed under repeated reversed loading. The present shear and bond seismic code provisions which are based on the results obtained under increasing monotonic loading are inadequate.

Chapter III

EXPERIMENTAL PROGRAM

Although it would be ideal to test a real building under actual loading conditions to which it might be subjected during its service life, such tests are not feasible due to economic considerations. Therefore, experimental work on small scale isolated members subjected to generalized eathquake forces have been developed to simulate the actual field conditions.

3.1 LABORATORY SIMULATION SET-UP

The general deflected shape of selected subassemblage in Figure 12 due to earthquake forces may be represented as in Figure 13. Figure 14,15 respectively show joint forces and subassembly free body diagram of a typical interior beam-column connection. The joint assemblages were positioned in the testing frame as shown in Figures 16,17.

Applying a vertical force on one end of the beams and an equal but oppcsite vertical force on the other end of the beams permits simulation of lateral seismic forces. Loads were applied at 17.5-inch from the centre of the column (14-inch from the face of the cclumn) except for specimen 1

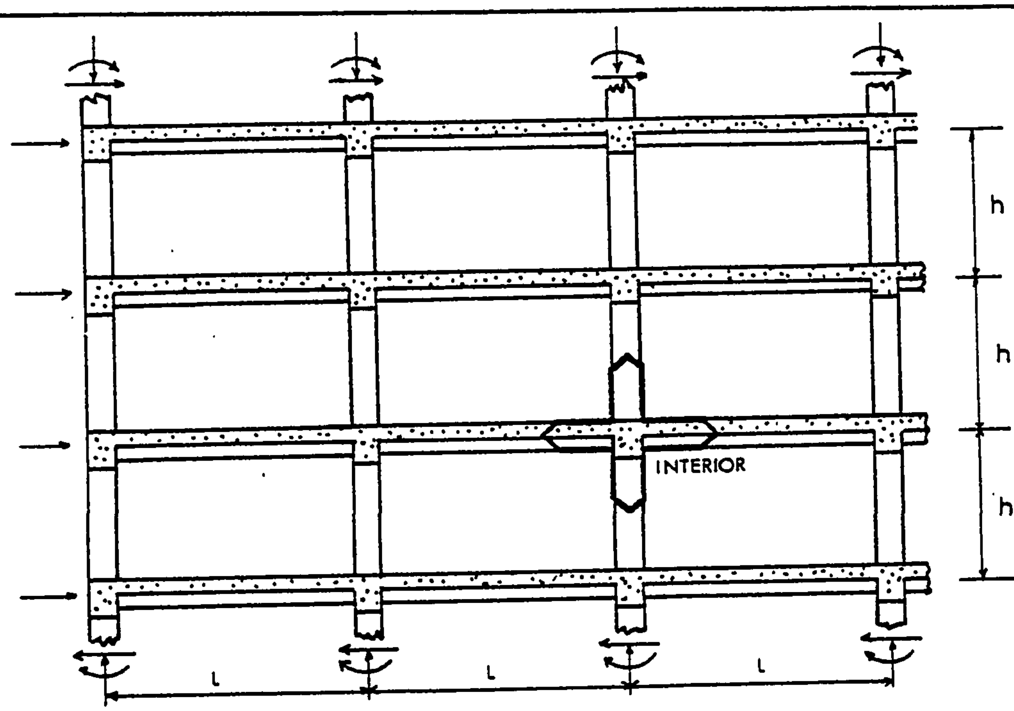

FIG. 12 BEAM-COLUMN SUB-ASSEMBLY

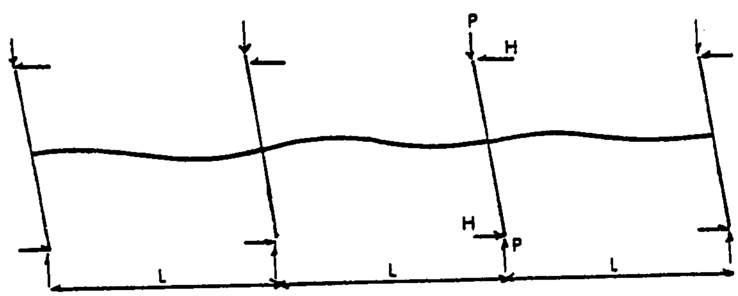

FIG. 13 DEFLECTED SHAPE

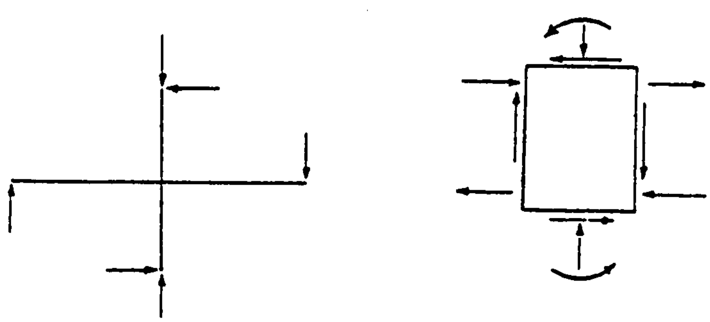

FIG. 14 FORCES IN THE JOINT

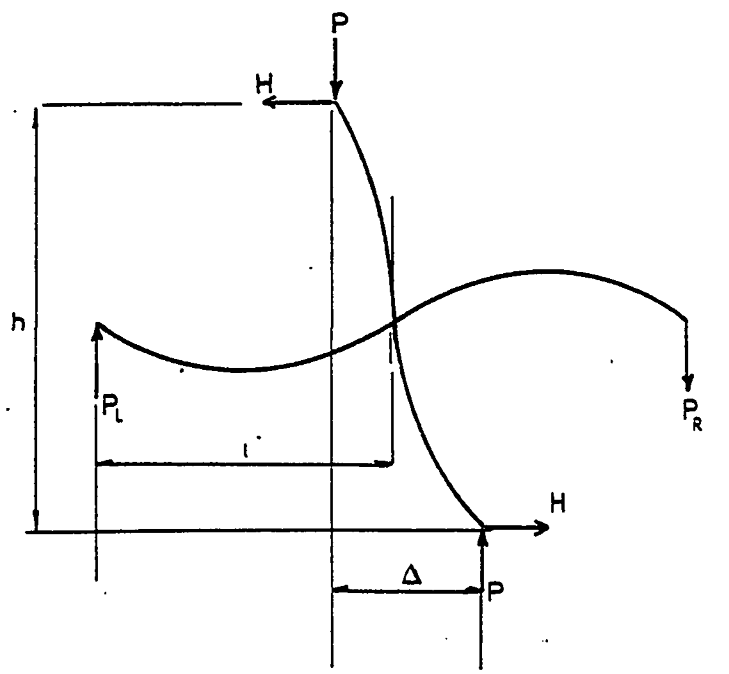

FIG.15a FREE BODY DIAGRAM OF SUB-ASSEMBLY

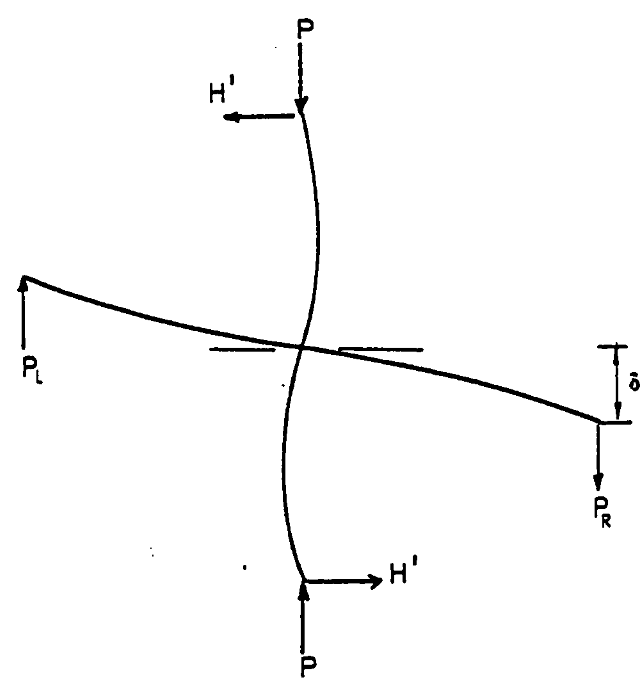

FIG.15b FREE BODY DIAGRAM OF TEST SUBASSEMBLY

for which the load was applied at 40-inch from the column centreline. The columns of specimen 1,3,4,5,6 were under a small constant axial compression load of 12-kip, however a larger column load of 140-kip was used for specimen 2. A small[2] column load leads to more conservative results.[3] The columns were hinged at the bottom (rotation allowed) and, the top was allowed to rotate as well as to move slightly laterally by installing pivot-rollers and horizontal jacks. The small column load and slight movement of the top of columns permit us to neglect entirely P-Δ effect. This assumption can be justified because of the moment contributed by the beam is much larger than of the column. The freebody diagram in Figure 15a therefore is replaced by Figure 15b. The effect of slab and cross beams on the behaviour of the joint is beyond the scope of this study.

---

[2]Column load can act as a confinement to the joint. A small column load gives less confinement to the joint and thus, weaken the joint. This is apply only to properly designed joint. A very weak joint, severe deterioration is expected even with a small load. In such circumstances, a large column load may have a adverse effect to the joint.

[3]It is also believed that the column may even undergo tensile stresses to vertical accelerations of the ground during an earthquake.

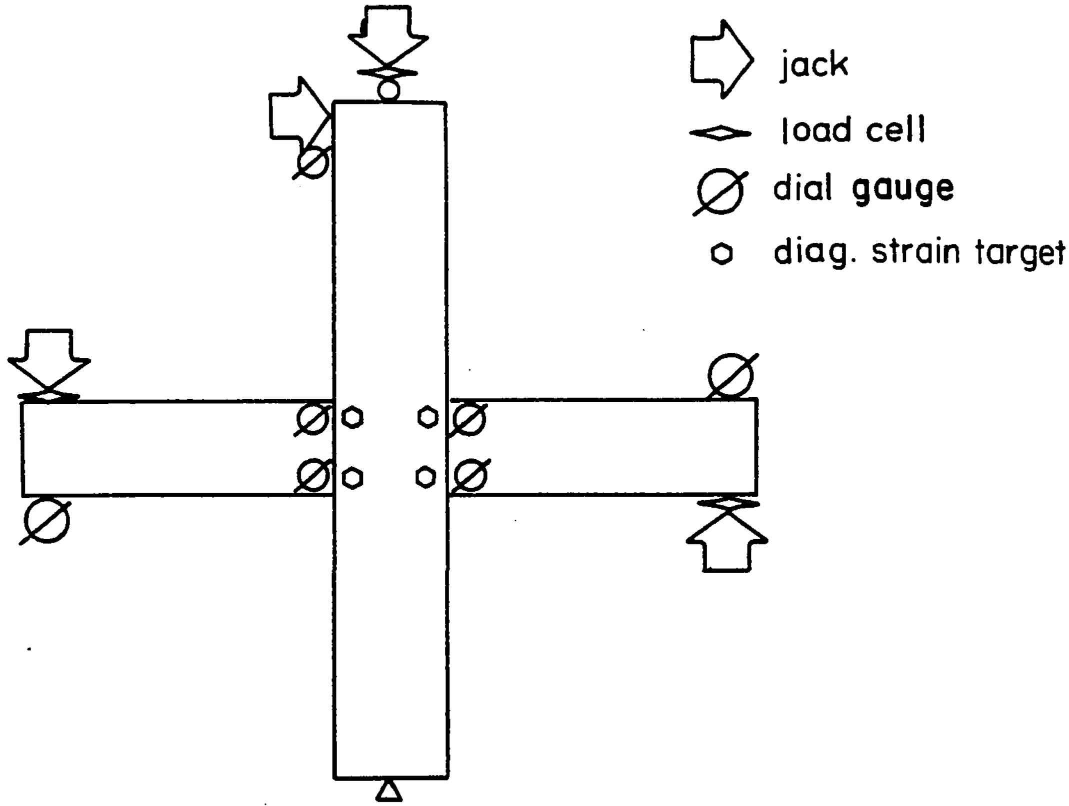

FIG. 16 INSTRUMENTS SETUP

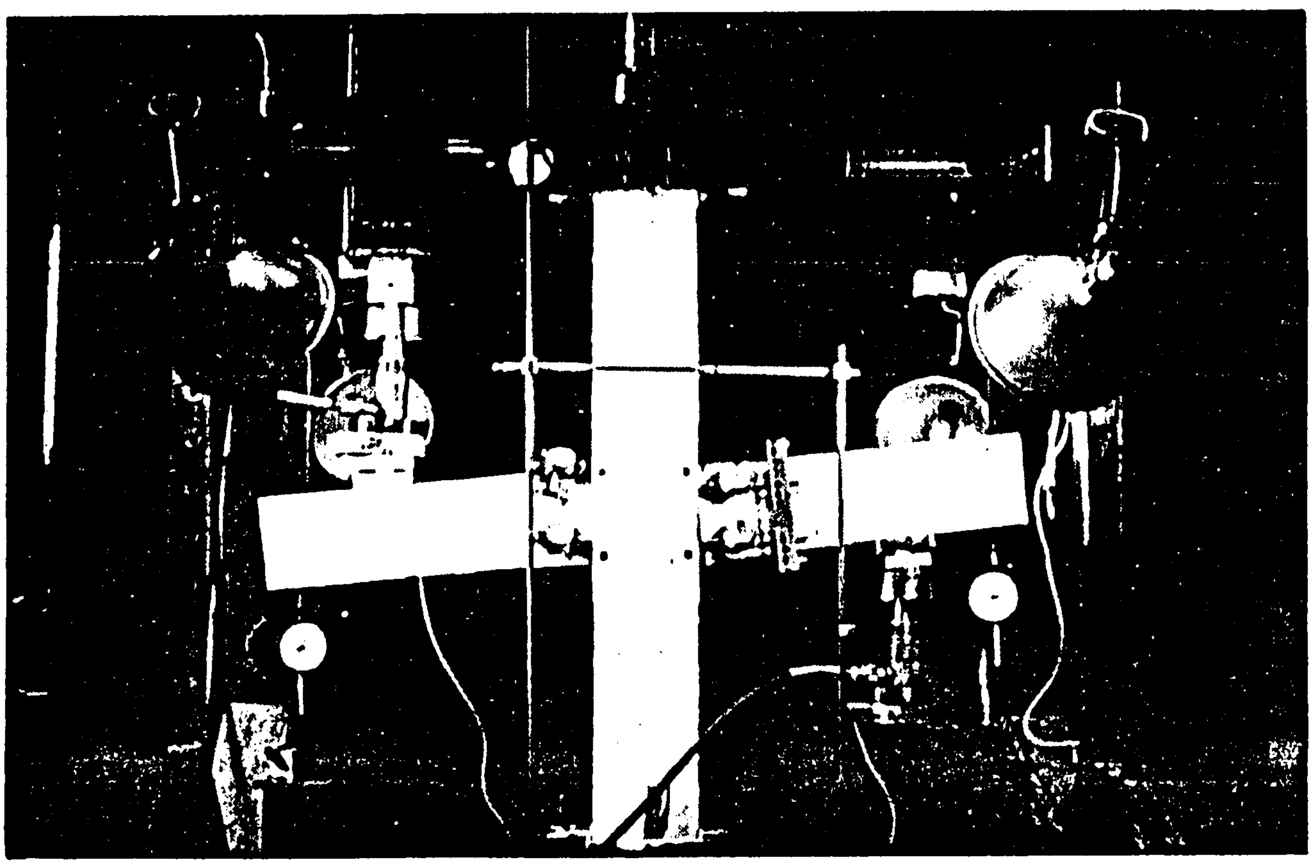

FIG. 17 TEST SETUP

3.2 DESCRIPTION OF SPECIMENS

The geometry of all the specimens were identical and is shown in Figure 18. Details of reinforcments are shown in Figure 19 and Table I. ACI 318-71 [5] design code with the improved reccmmendations prepared by ACI committee 352 [6] were adopted for the design of the 6.25x5.25 in. beams and the 8x7 in. columns. The details of the design is given in Appendix C. Commercially available #3 deformed bars and #2 plain bars were used as main joint reinforcements and stirrups respectively. Specimens 1 and 2 consisted of 3 top and 2 bottom bars for the beams and 10 bars for the columns. Specimens 3,4,5,6 consisted of equal 3 top and bottom bars for the beams and 6 bars for the columns; however, specimens 3,4,5 had reduced joint ties, in addition, they also had reduced joint bond or anchorage for each specimens. Details of the bond variations are given in Table I. The elimination of bond strength was easily made by simply wrapping the bars at the intended section with polyethylene sheet before pouring the concrete. This method was adopted after it has been tested and verified to be 100% effective. The variation of bond was controlled by the length of applied polyethylene around the bars. Normal-weight concrete with 4000psi., 28-day strength and Grade 60 steel were used in the experiments.

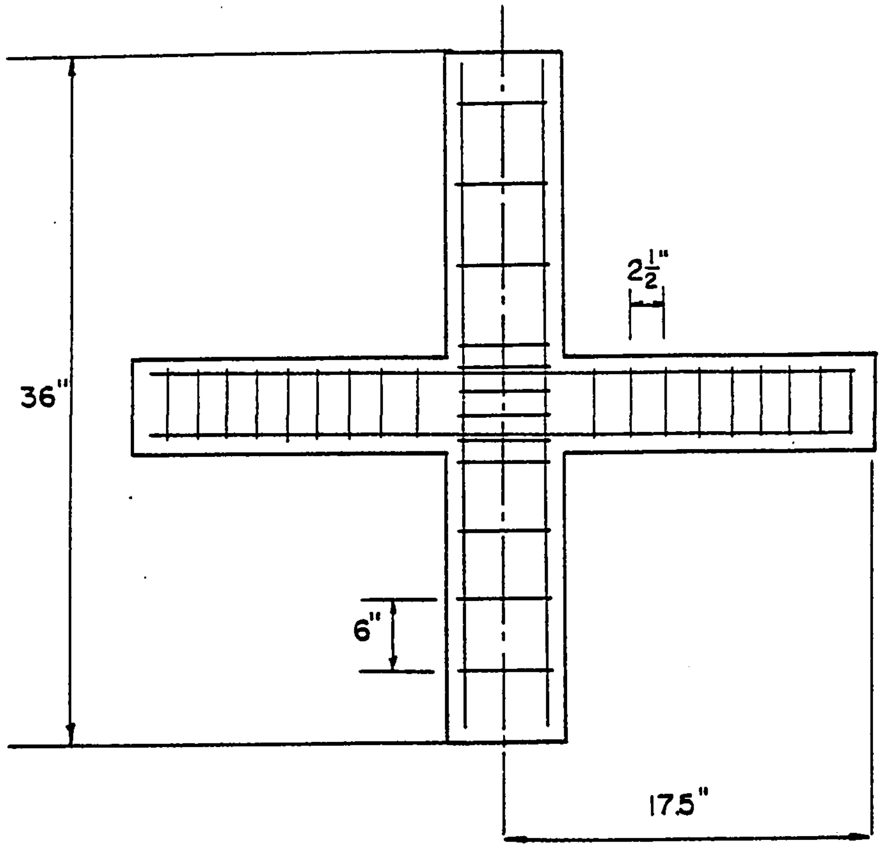

FIG. 18 ELEVATION OF BEAM-COLUMN SHOWING ITS REINFORCEMENT

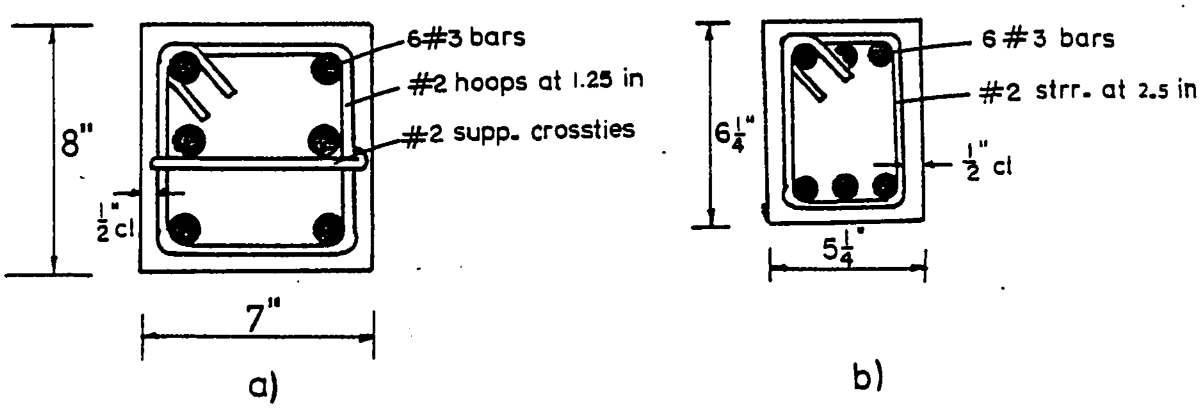

FIG. 19 CROSS SECTION AND REINFORCEMENT DETAILS FOR a)COLUMN; b)BEAM

3.3 INSTRUMENTATION

Both the beams and the joints were instrumented for deflection and rotation. Dial gauges of high sensitivity 0.001 in/div. were used for beam-tip deflection and beam-column rotation measurements. The joint face were also instrumented for diagonal strain readings. These readings simply disclosed the degree of damage due to cracks at the joint. A calibrated demec strain meter was used to measure the diagonal elongation or shortening of the joint face. The applied loads were measured by means of electronic strain meter which connected to load cells and a pressure gauge. Three Strain-Sert Universal Flat Load Cells (model FL25U-2SGKT) each having load capacity of 25,000 lb. were calibrated using an Tinius Olsen Testing Machine. One of the load cells was used to calibrate the pressure gauge. Inaccuracy caused by these devices was considered insignificant compared with the large load applied to the system. The locations of the instruments are shown in Figure 16.

3.4 LOADING PROGRAM

The selection of a definite loading program is an extremly difficult decision. The behaviour of a joint appears to be very sensitive to the previous history of loading. The joint performance will degrade considerably if it is loaded to/or near its ultimate resistance even during the first cycle. So the question must then be asked: how far should the deformation be incresed if the system has reached its ultimate resistance? In this study, the decision about the forces applied at the subsequent loading stage were made on the basis of the behavioural history of the joint. However, a similar loading scheme, though a very rough one, was adopted for all specimens.

Chapter IV

PRESENTATION OF EXPERIMENTAL RESULTS

A FORTRAN general program was developed and written to process the raw data and organize the result of each cycle into a set of systematic global coordinates. These coordinates then were plotted into a series of graphs by calling ten different plotting subroutines. These graphs are presented in Appendix A. The program was also equipped with a 'pointer' system to select the maximum value of all parameters every half cycle for the purpose of making comparisons and plotting loading program diagrams. The complete program together with the plotting subroutines is shown in Appendix B. The IBM 3031, AMDAHL 470/V611 computers and a CALCOMP1051 PLOTTER were used in the operation.

4.1 LOAD-DEFLECTION CURVES (FIGURE A1A-A6)

Load-Deflection Curves were obtained by measuring the loads exerted on the tip of the beams and plotted against their corresponding deflections.

i. Because of the unequal top and bottom beam reinforcements in specimens 1 and 2, both 'right' and 'left' beams were plotted and analyzed separately. This was done to give a better understanding of the behaviour as to

a) how did each beam react under the first cycle of loading? and,

b) how would these different reactions influence the foregoing behaviour of the system?

ii. But in analyzing specimens 3,4,5,6, which had equal top and bottom beam reinfocements the average deflection of the right and left beams as well as average of the applied loads were used in plotting the results. This was done to avoid unnecessary repetition, and can be justified because both deflections were approximately identical to each other everytime the load was applied.

iii. All deflection measurements were made from the initial undeflected position of the beams.

iv. At each load, measurements were made almost simultaneously, so that inacuracy caused by creep of the members could be avoided.

v. Each Load-Deflection Curve is accompanied by the appropriate loading program and its deflection.

vi. The corresponding moments produced at the joints were also shown on each graph.

4.2 MOMENT-CURVATURE CURVES (FIGURE A7-A12B)

i. Since the right-hand beam was the only beam instrumented for the rotation measurements, the curvature (measured in radians) represents the relative rotation of the right-hand beam relative to the column.

ii. All moments shown in the diagrams were taken and calculated with respect to the column centre line.

iii. Both Load-Deflection and Moment-Curvature Diagram can be used to evaluate the ductility and energy capacity of the joint.

4.3 MOMENT-DIAGONAL JOINT STRAIN CURVES (FIGURE A13A-A18B)

i. Diagonal-joint-strain measured the elongation or shortening of concrete face in the diagonal directions. These measurements were then plotted against their corresponding moments. The result of joint diagonal cracks, therefore, can be used to describe the degree of deterioration of the joint knowing 0.00013 unit strain is the ultimate strain in tension before the concrete starts cracking.

ii. The slope or inclination of the rebouncing curve when unloading can be used to indicate the condition of the effect of bond at the joint on that particular cycle. The bond is considered to be effective, resulting good recovery of cracks, if the curve tends to rebound back to the original location when unloading.

iii. Because all specimen have two different diagonal directions (Left top - right bottom and Right top - left bottom directions) it was appropriate to present the results of each direction separately in order to get a closer and better understanding of their behaviour.

4.4 DEFLECTION-DIAGONAL JOINT STRAIN CURVES (FIGURE A19A-A22B)

These curves were drawn to establish the relationship between beam deflection and joint deterioration in various types of joint bond and reinforcement ----- how these differences would affect the relationship of the beam deflection and its joint deterioration.

4.5 CURVATURE-DIAGONAL JOINT STRAIN CURVES (FIGURE A23A-A28B)

i. When a large crack occurred at the joint interfaces, the beams will rotate significantly with respect to the column with a resulting increase in curvature. Therefore, beside representing the ductility of the joint, the curvature, which measures the rotation of the beam with respect to the column, can also be used to describe the damage of beam-column interface. From observation the relative rotation of the beam-column, in many instances, is due mainly to the cracks occurred in the interfaces.

ii. The object of establishing this relationship is to see the development of damage at the beam-column interface in relation with the joint diagonal cracks.

4.6 DEFLECTION-CURVATURE CURVES (FIGURE A29-A32)

Though apparently the two are compatible, their relationship in the Deflection-Curvature Curves can be used to confirm the weakening of the connections and/or the beam. In the early stage of loadings, the beam took a bent shape. This was because the beam-column connection still gave considerable amount of resistance to the deflected beams. But in the later stage of loading when yielding had occured in the beam or in the beam-column interfaces, the beams were no longer bent but followed a straight path as illustrated in Figure 20 the yielding points now became rotation pivots. Because of this weakening process, non-linear relationship in the later part of the loading program was anticipated.

4.7 ENERGY CAPACITY (FIGURE 33-34)

In this experiment, input energy is defined as the maximum work done by the load on the beam which can be represented by the maximum area covered in the Load-Deflection or Moment-Curvature Curves before the unloading process. Energy absorbed is defined as input energy that has been absorbed, some by inelastic strain, and some by inflicting damage to the system. Energy absorbed can be estimated by measuring the area within a loop in the Load-Deflection and Moment-Curvature Curves.

Elastic strain energy is defined as the remaining energy from input energy minus absorbed energy assuming small energy losses.

The cumulative (of every half cycle) of input and absorbed energy of specimens 3,4,5,6 were plotted against their corresponding number of half cycle. The average of absorbed energy per-cycle were also computed and tabulated in Table I.

The input and absorbed energy is obtained by measuring the areas with planimeter as it was defined in section 2.5. The energy estimated from moment-curvature refers to joint energy whereas obtained from load-deflection refers to 'overall' energy.

This crude estimation of input and absorbed energy* provides a useful tool in comparing the absorption capacity of each specimen.

----

*These energy measurements should not be regarded as true energy. More specific energies, say the amount of absorbed energy that would cause damage and non-damage work can be estimated by Resrve Energy technique [7].

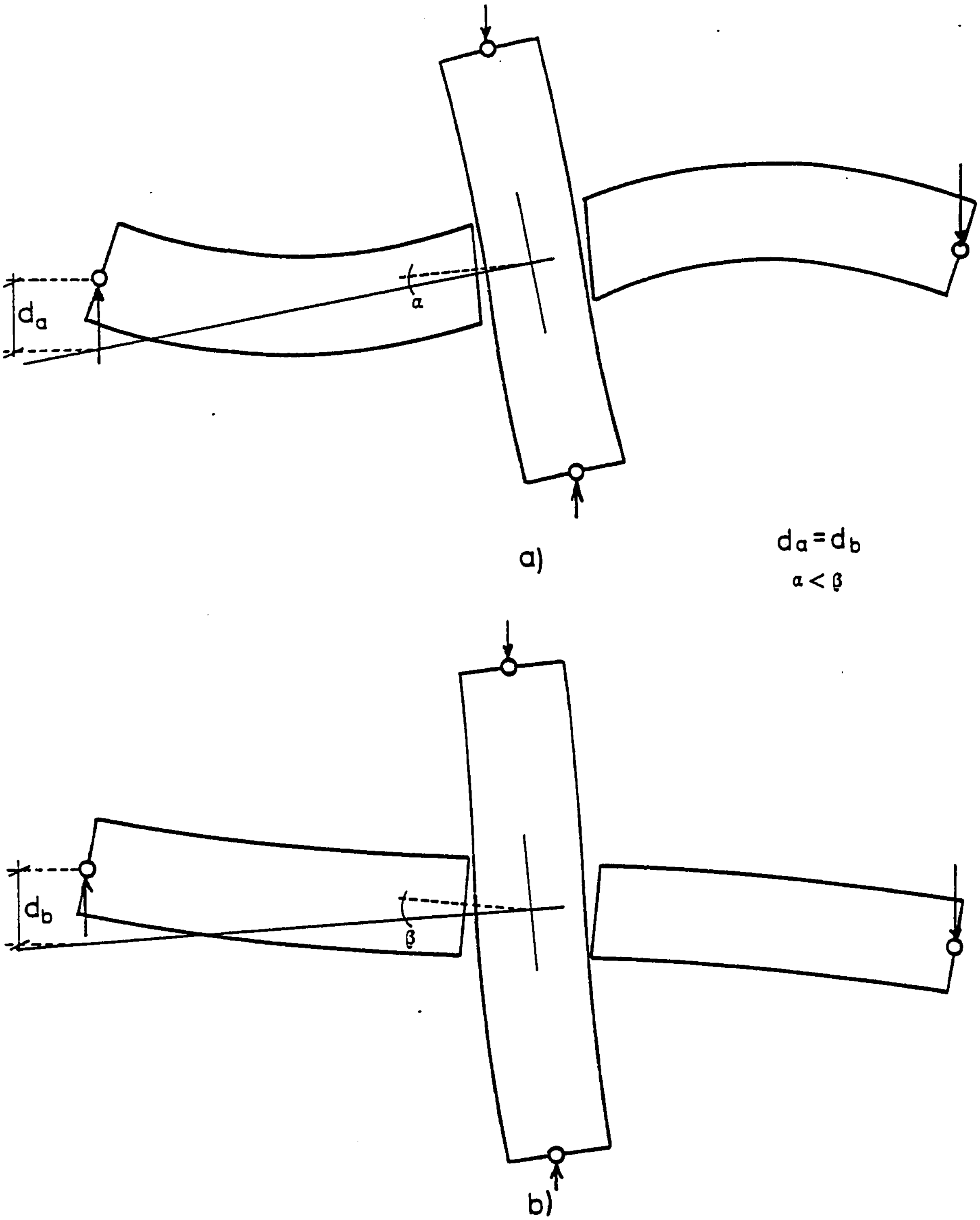

FIG. 20 (a).High resistance at beam-column interface, resulting a significant bending at the beams;
(b).Deterioration of the beam-column interface, resulting a larger beam rotation for the same deflection given in (a)

Chapter V

DISCUSSION OF EXPERIMENT RESULTS

Specimens 1 and 2 were identical and designed according to the design criteria prepared by ACI Committee 352. However, the magnitude of the axial loads acting on the columns were different as well as the location of the applied loads acting on the beams (see Table I). Since the quantity of upper and lower beam reinforcements were different, the Load Deflection Curves (right and left hand side) of both specimens were analyzed and presented separately. For the purpose of this study, specimens 3,4,5 which had equal top and bottom beam reinforcing bars were designed and made such that they had 40% less column reinforcement as well as 67% reduction of their joint ties as compared to specimens 1 and 2. Further more, specimens 3,4,5 differed in the amount of bond between the main beam steel and the concrete in the joint. These different variations, 'full', 'half' and 'no' bond respectively apply to bond forces generated by beam reinforcements only (bond forces generated by column were excluded). Specimen 6 was built to satisfy the joint design requirement recommended by ACI Committee 352, that is no attempt was made to reduce joint-bond as well as joint-tie.

Each of the above specimens was discussed individually in the fcllowing sectios.

5.1 GENERAL

i. The first 'visible' crack was noticed at about 2.5-kip at beam column left-top and right-bottom interfaces and immediately followed by beam flexural cracks at about 3 kips. Except for specimen 1, these flexural cracks proceeded to shear cracks and some bond cracks as the load increased.

ii. The joint diagonal cracks for some specimens were noticed as early as the first load cycle at 4.5-kip. These cracks usually started horizontally at the diagonal corners where the joint meet the beams. This was because of the joint shear stresses which caused diagonal cracks had not yet fully developed and the horizontal cracks were mainly due to the stresses occurred in the beam reinforcement. As the load increased to the point where joint shear stress were fully developed, large diagonal cracks occurred at the centre of the joint followed by new secondary cracks parallel to the main crack, and/or extension of the old cracks.

Load reversal resulted in the same phenomena but in the opposite direction. Eventually all of these diagonal cracks extended into the column out of the joint region.

iii. Bond cracks occurred in the beam near the beam-column interfaces indicating maximum bond stresses in this region.

iv. Small column flexural cracks were also noticed in specimen 3,4,5,6 after 7 kips. This was because of the reduction of column reinforcements in these specimens.

5.2 SPECIMEN 1

The joint of this specimen was designed to meet the criteria prepared by ACI Committee 352. The column reinforcement consist of 10#3 main bars distributed 5 on each side of the column faces where the beam was going to be extended. 6#2 closed lateral joint ties 1.25-inch apart were made at the joint (Figure 21) ; 6#2 lateral ties 6-inch apart occupied the rest of the column. The beam had 3#3 top bars and 2#3 bottom bars passing through the joint; beam stirrup spacing was 2.5-inch (Figure 22). A constant axial force of 14-kip was applied to the column throughout the testing. The load application on the beam was positioned at 40-inch from the column centre line.

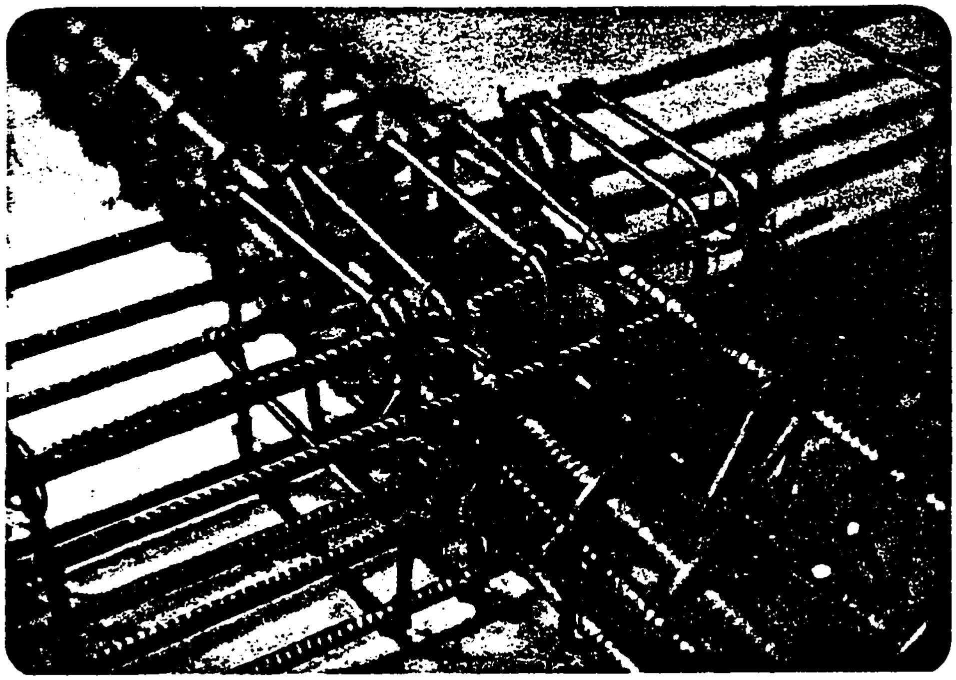

FIG. 21 JOINT REINFORCEMENT, SPECIMENS 1,2

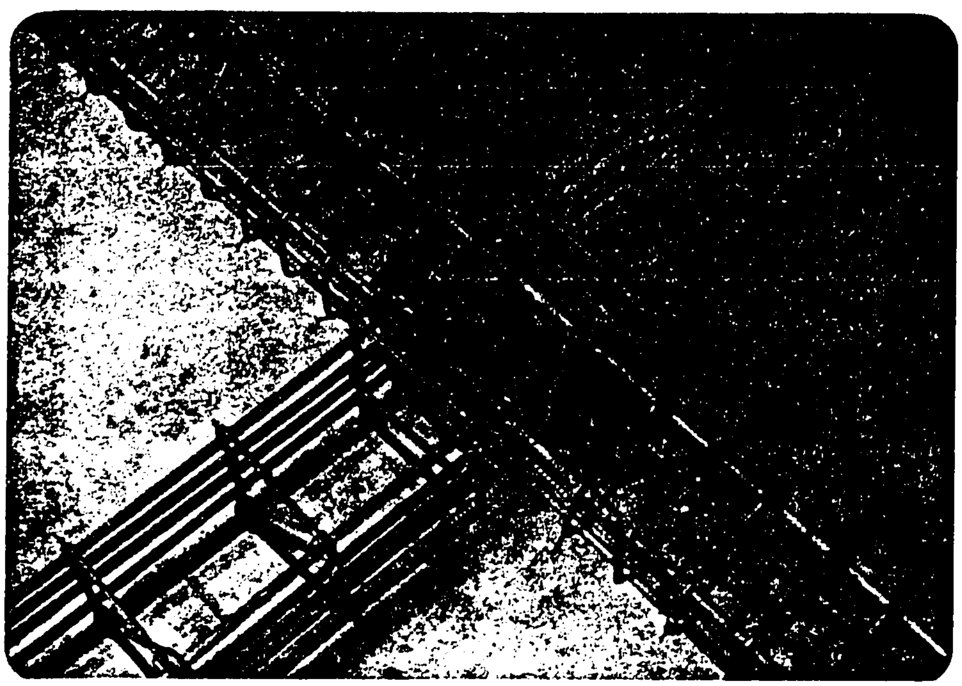

FIG. 22 SUB-ASSEMBLY REINFORCEMENT, SPECIMENS 1,2

All the other specimens, namely 2,3,4,5,6 were tested with the beam loads located at 17.5-inch from the column centre line. To compare the results from this specimen with the other specimens an equivalent load was used giving the same beam moment at a lever arm of 17.5-inch.

The equivalent load was obtained as follows,

$$M = P \cdot X1$$

$$Pe = \frac{M}{X2}$$

$$Pe = P\frac{X1}{X2}$$

where P=load; Pe=load equivalent; M=moment; X1,X2=original and specified moment-arm that is 40-inch and 17.5-inch respectively.

Its corresponding deflection,

$$DELe = DEL\ \frac{X2}{X1}$$

where DEL=deflection; DELe=deflection equivalent.

Due to some technical difficulty, the unloading measurements of rotation and diagonal joint strain of specimens 1 and 2 were abandoned. The unloading paths then were approximated by straight line as shown in the diagrams.

i. Under flexural tension, the right hand beam which has less tension steel reached its yielding point first before the left hand beam. As a result, an overall larger deflection (20%) of the beam was observed in the sucessive load cycles (Figures A2a,b). This is due to the loss of bond caused by the flexural cracks or bond failure.

ii. Figures 23,24 show that very little damage was done at the joint, and the diagonal cracks tend to incline horizontally. The former was because of high concrete strength; the presence of joint lateral ties as well as adequate column reinforcement. The latter presumably because higher bond stresses occurred at the beam as a result of the smaller amount of steel in comparison with the column reinforcement.

iii. Considerable damage occurred at beam-column interfaces (Figure 25).

iv. Fluxural cracks were the prominent features on the beam; some bond cracks were also found but their locality was limited to near the column only. This proved that the largest bond stresses occurred at the beam-column interfaces (Figure 26).

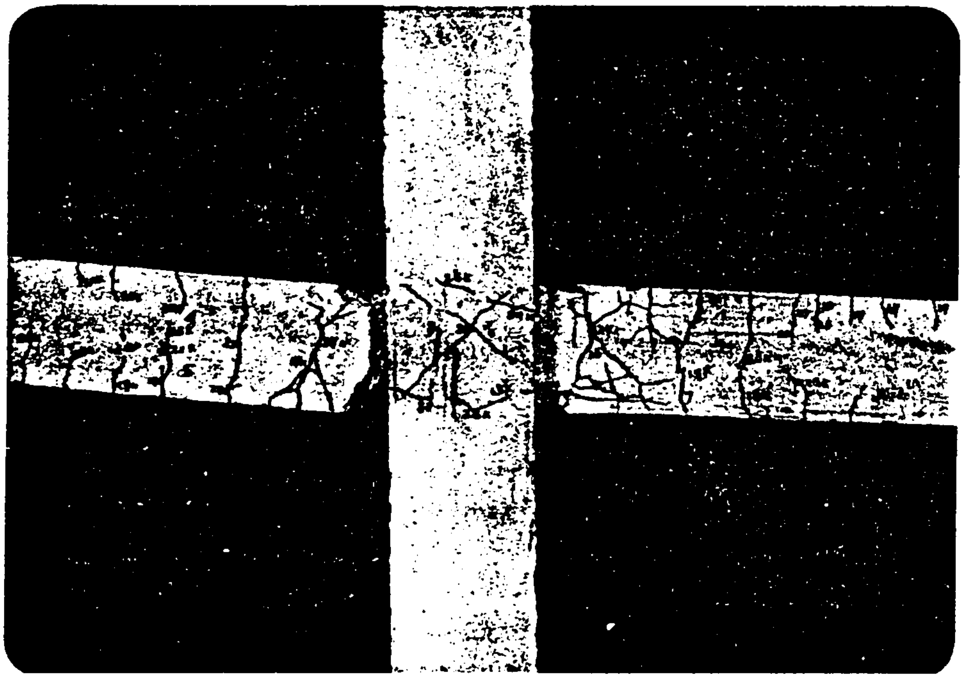

FIG. 23 SPECIMEN 1 WHEN TEST WAS TERMINATED

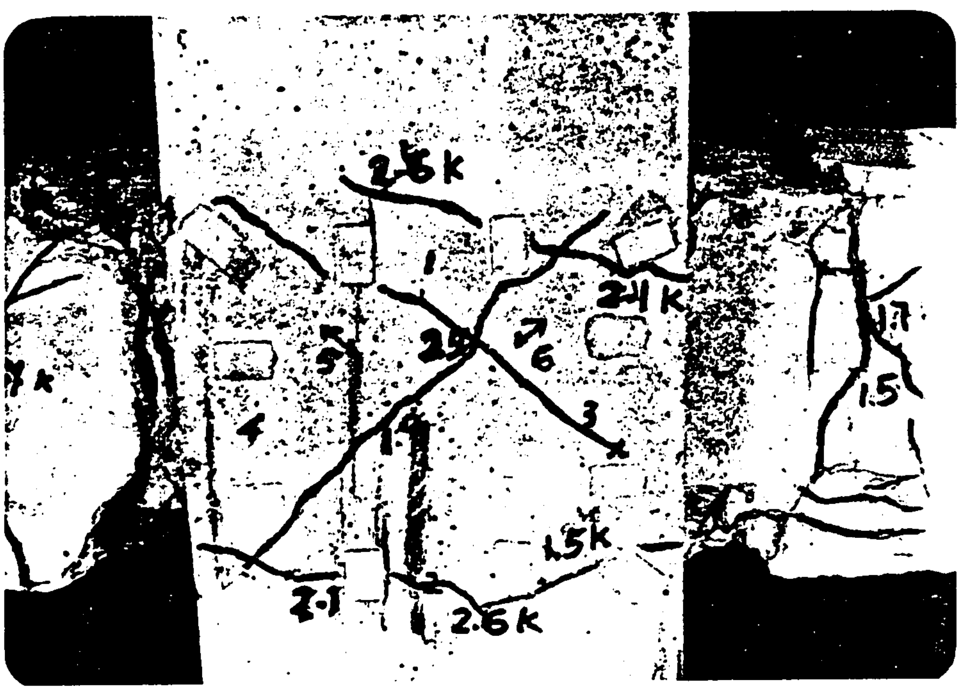

FIG. 24 JOINT CONDITION OF SPECIMEN 1 WHEN TEST WAS TERMINATED

FIG. 25 BEAM-COLUMN INTERFACE OF SPECIMEN 1
WHEN TEST WAS TERMINATED

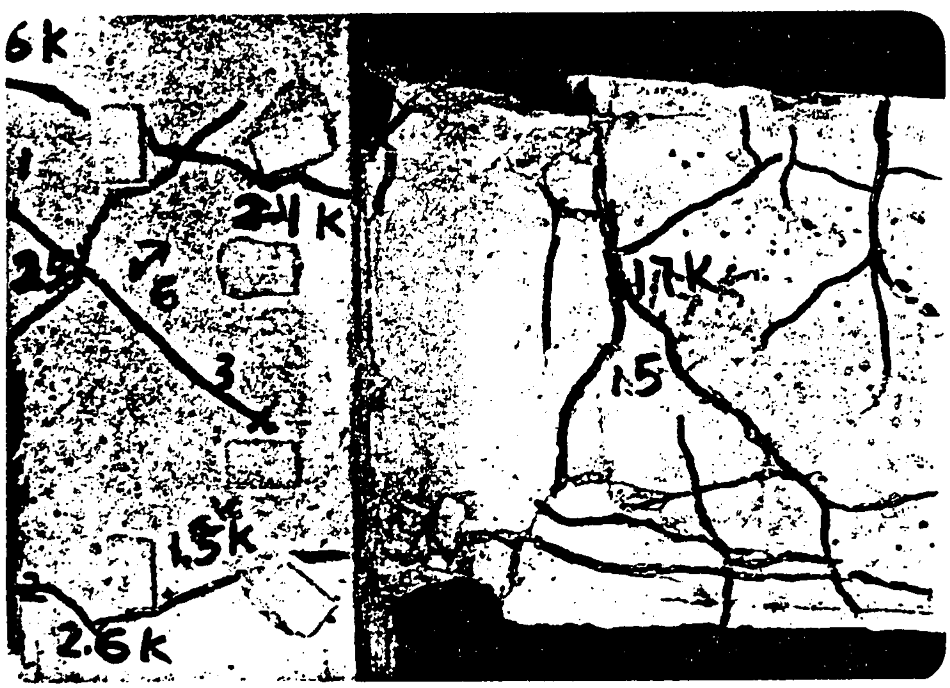

FIG. 26 BOND CRACKS OF SPECIMEN 1 AT FAILURE

5.3 SPECIMEN 2

This specimen was made identical with specimen 1 except the location of the applied load on the beam was moved towards the column from 40-inch to 17.5-inch(measured from column centre line), and the axial load applied to the column was increased from 12-kip to 140-kip. No diagonal cracks occurred at the joint (Figure 27) because of higher concrete strength (see Table I) and higher axial load that gives an substantial increase in joint confinement; Hinges were formed at the beam-column interfaces (Figures 27,28). Shear cracks (Figure 28) due to higher beam loading was also noticed.

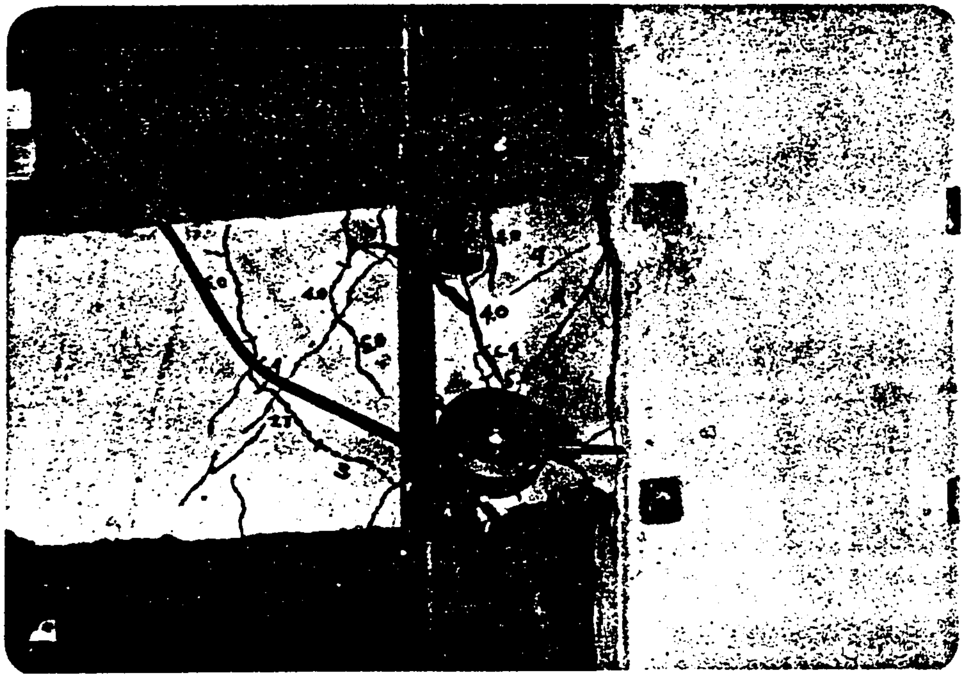

FIG. 27   JOINT CONDITION (FRONT) WHEN TEST WAS TERMINATED

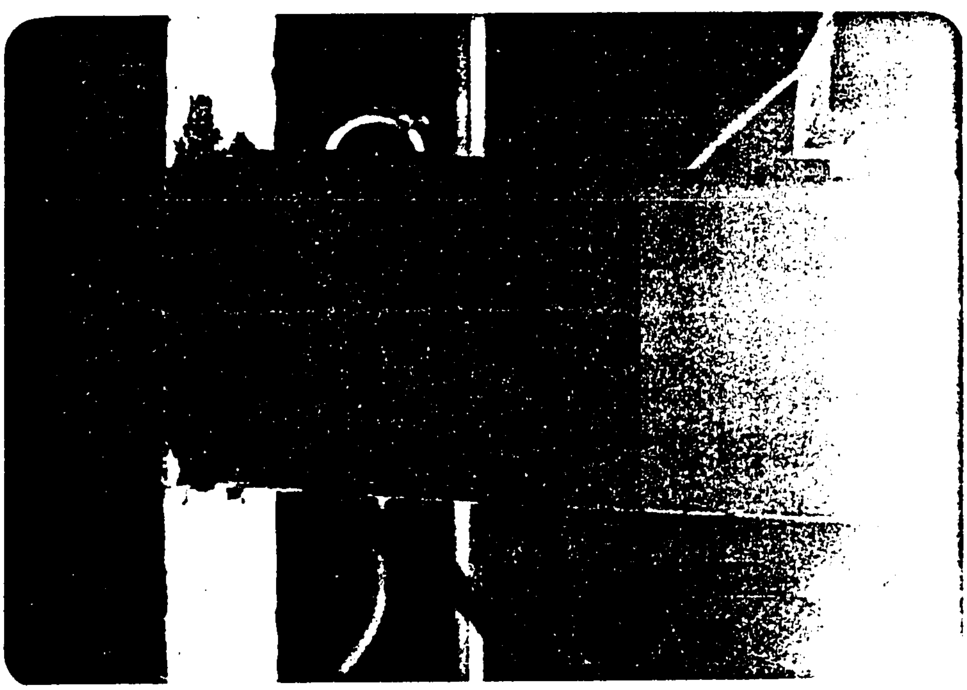

FIG. 28   JOINT CONDITION (BACK) WHEN TEST WAS TERMINATED

5.4 SPECIMEN 3

This joint assembly had equal 3#3bars at top and bottom beam, 6#3 bars column reinforcement (reduction of 40%) and two joint lateral ties with no supplement ties (reduction of 77%) (Figure 29).

i. After the first cycle, large diagonal cracks occurred at the joint and extended rapidly in the second cycle (Figure 30). These diagonal cracks later extended deep into the column (Figure 31).

ii. Slow recovery of the cracks at the joint when load reversed its direction (Figures A15a,b).

iii. The cracks became larger each cycle and finally extensive damage at the joint resulted in the concrete cover spalling off as the load increased. This spalling activity reduces the cross section of the column and under a large column axial load buckling of the main bars at the joint is likely to happen. The bending of the column main bars, as shown in Figure 32, was due to the coupling action of the beams on the column bars. This initial 'local' bending action will invite the total buckling of the whole column under large axial loads.

iv. The system resulted in large damage to the joint but little damage the beam. It can be observed that the beam and beam-column interface show no signs of yielding (Figure 31).

v. The system has a good joint energy absorption efficiency but low energy capacity (Figure A33a).

The lack of confinment given by joint ties and the reduction of column reinforcements presumably are the cause of the above behaviour.

FIG. 29 JOINT REINFORCEMENT, SPECIMEN 3

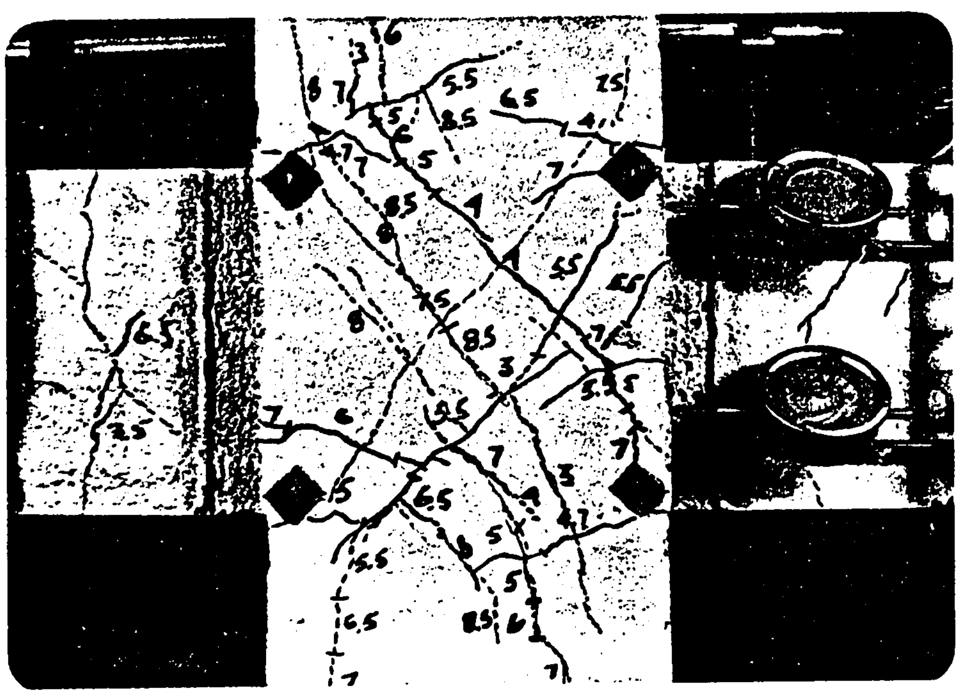

FIG. 30 JOINT CONDITION OF SPECIMEN 3 AT SECOND CYCLE

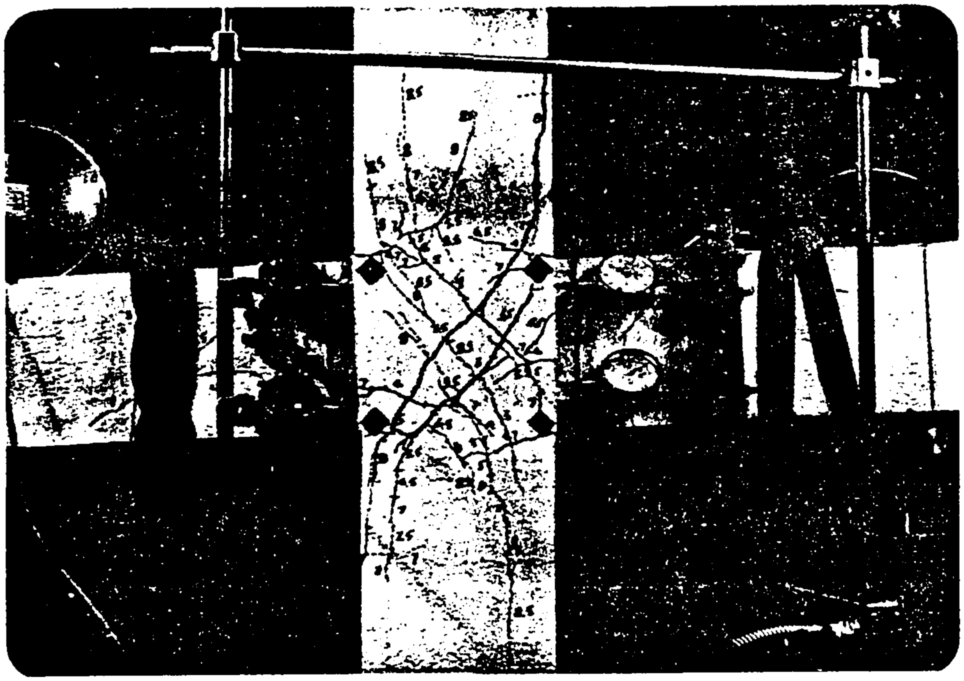

FIG. 31   SPECIMEN 3 AT THIRD CYCLE

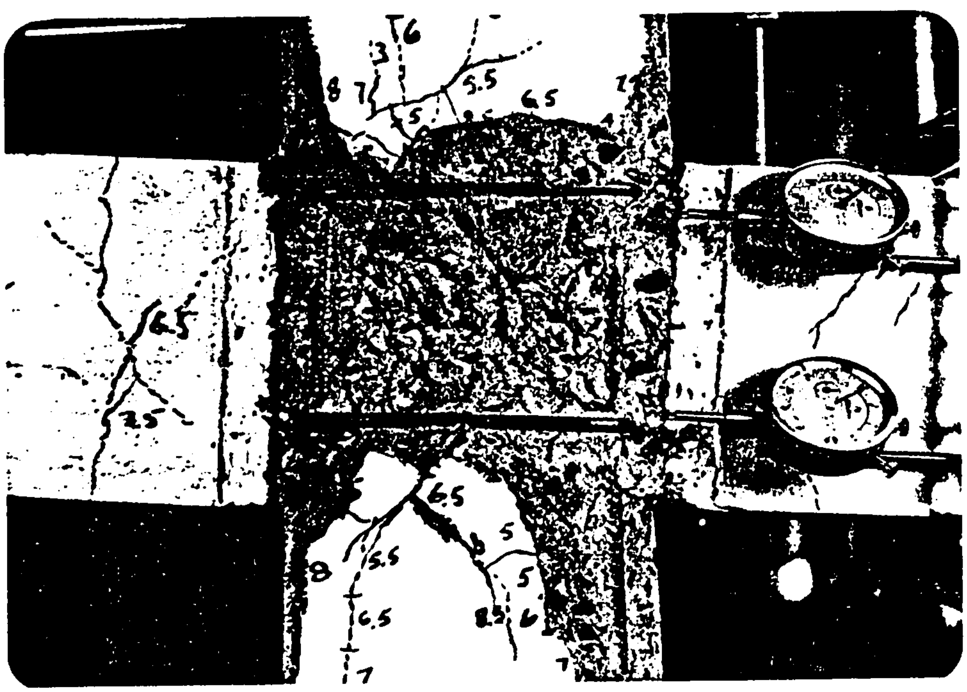

FIG. 32   SPECIMEN 3 WHEN TEST WAS TERMINATED

5.5 SPECIMEN 5

This specimen had the same properties as of specimen 3 except the bond of the beam reinforcement at the joint was eliminated. The following behaviour was observed.

i. Yielding occurred at the beam column interface causing extensive damage at this region and slip or 'pull out' of the beam main steel with respect to the column.

ii. The 'softening' behaviour of the system especially at the start of a new load cycle is clearly shown in Figure A5. The softening effect causes either a relatively low energy absorbtion capacity or an excessive deflection, which is not desirable in earthquake resistant structures (see section 2.3).

iii. Figure A5 shows that the ultimate load was reduced by 12% compared with specimen 3.

iv. A significant decrease in subsequent loadings indicates a degradation of the system as the number of load cycles increased (Figure A5).

v. The first diagonal crack appeared at about 7-kip (compared with 3-kip in other specimens) showing that no load is being transferred from the beams into the joint. Few small diagonal cracks were found at the completion of the test when the subassembly failed, proved again that the adverse effect to the system caused by the lack of joint confinement has been suppressed by not reducing beam bond effect at the joint.

vi. The presence of bond cracks at the beam-column interface indicates high bond stresses at the region (Figure 33).

vii. Extensive crushing damage was observed when beams adjacent to column were under flexural compression action (Figure 33).

viii. Joint and beam showed little damage. All damage being concentrated at beam column interfaces (Figure 34).

ix. The system has a low joint energy absorption efficiency but high absorption of the input energy (Figure A33b).

All of the behaviour described above were interelated and as a consequence of one another. The elimination of anchorage force or bond force helped to preserve the joint from deterioration, The elimination of bond forces resulted in the formation of a plastic hinges which damages at the beam-column interfaces. The presence of bond cracks(vi) plus the crushing action under compression (vii) caused the beam concrete cover to spall-off in the vicinity of the joint.

FIG. 33 SPECIMEN 5 AT THE END OF CYCLE 2

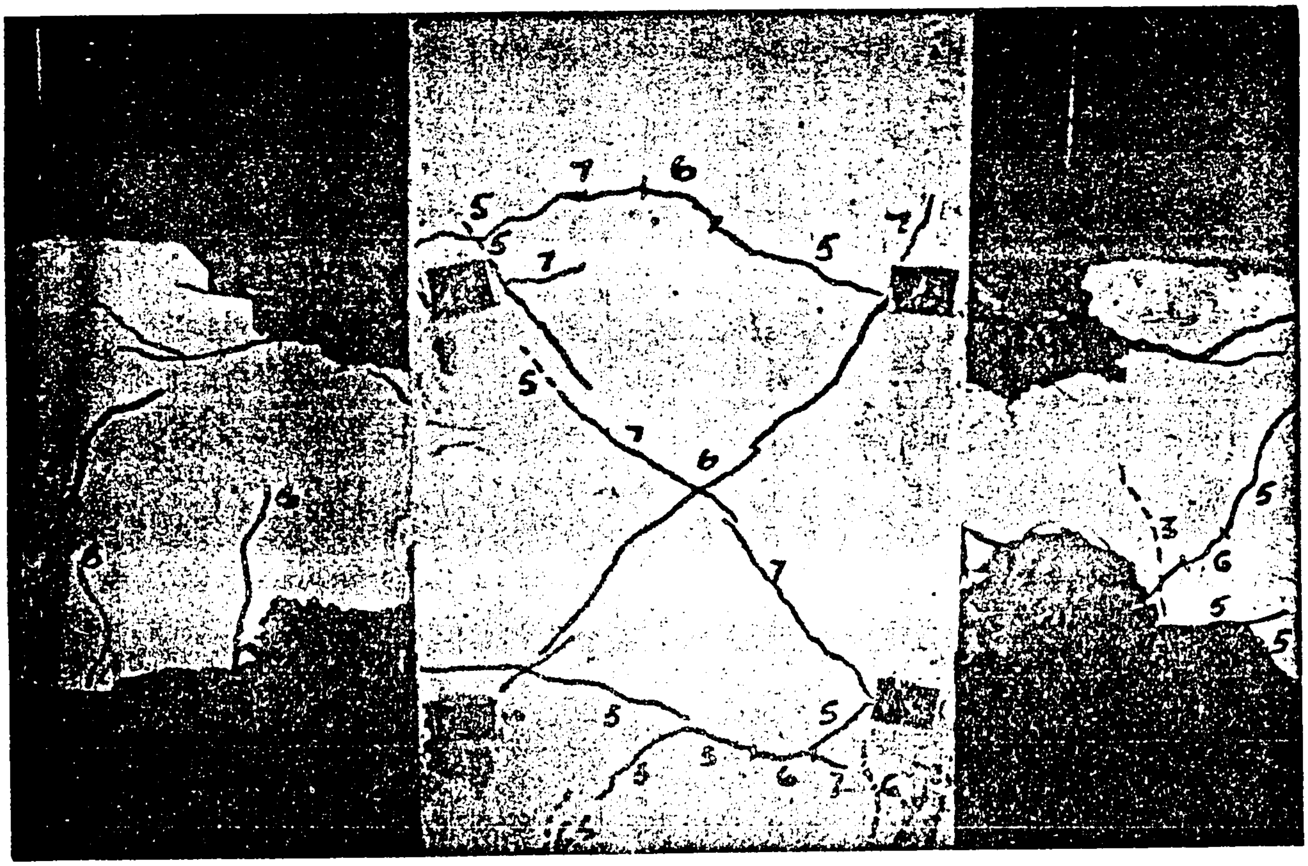

FIG. 34 SPECIMEN 5 WHEN TEST WAS TERMINATED

5.6 SPECIMEN 4

A reduction of 50% of the bond forces of specimen 3 by wrapping the bars in the middle-half section were introduced in this specimen. The performance of the subassembly, as predicted, lay moderately in between the previous two specimens.

i. Medium sized diagonal cracks were observed and yet nearly no damage on the beam-column interfaces (Figures 35,36 and Table I). The plastic hinges were formed in the beams away from the column.

ii. Due to the fact that it could arrive successively at the ultimate load of 800-kip or higher without losing its load capacity and only inflict little damage at the joint under such loading, this system was the most efficient one compared with the previous two subassemblies.

iii. The lack of joint diagonal cracks until the load reached 6.5-kip also proved the high performance of this subassembly.

iv. High energy capacity (Figure A34a).

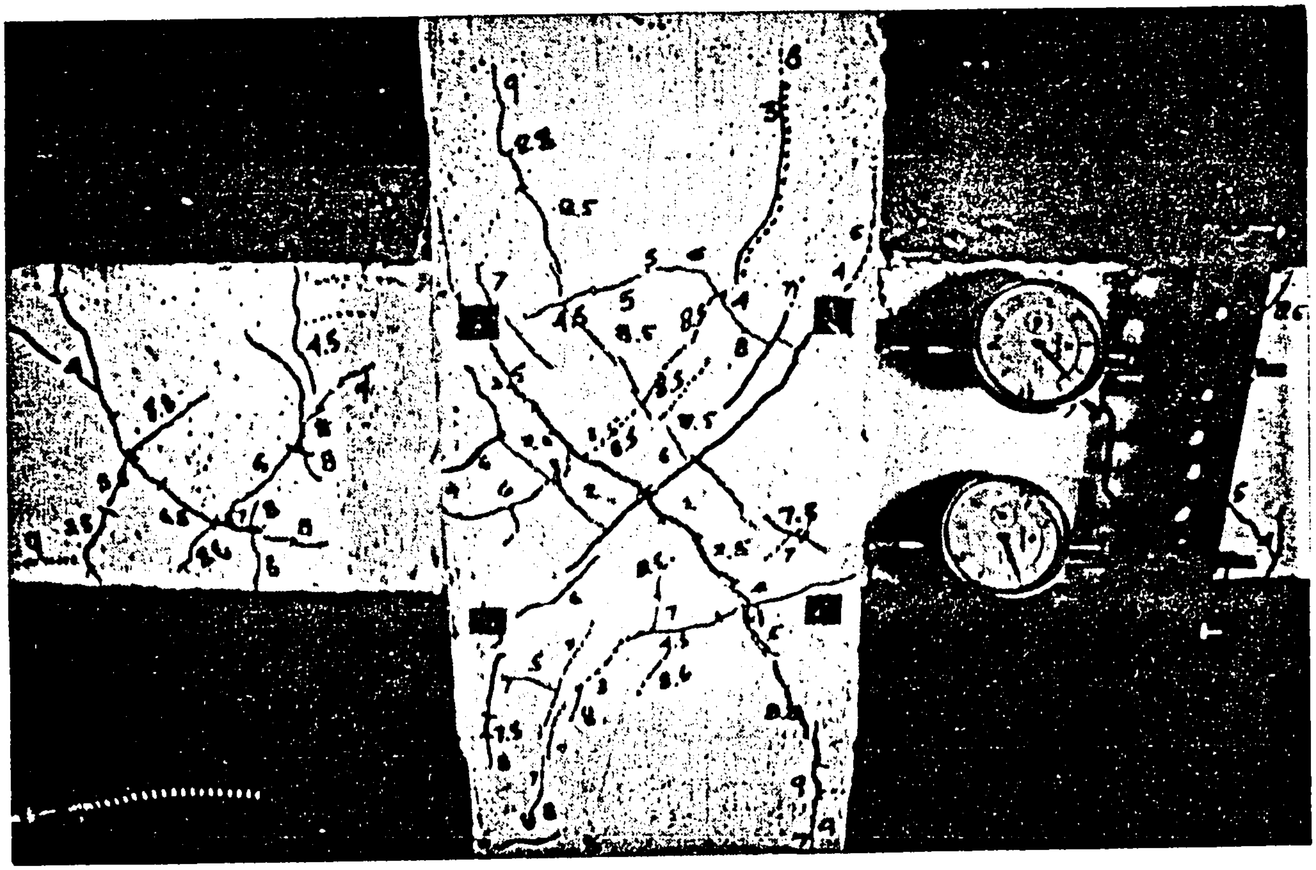

FIG. 35 SPECIMEN 4 WHEN TEST WAS TERMINATED (FRONT)

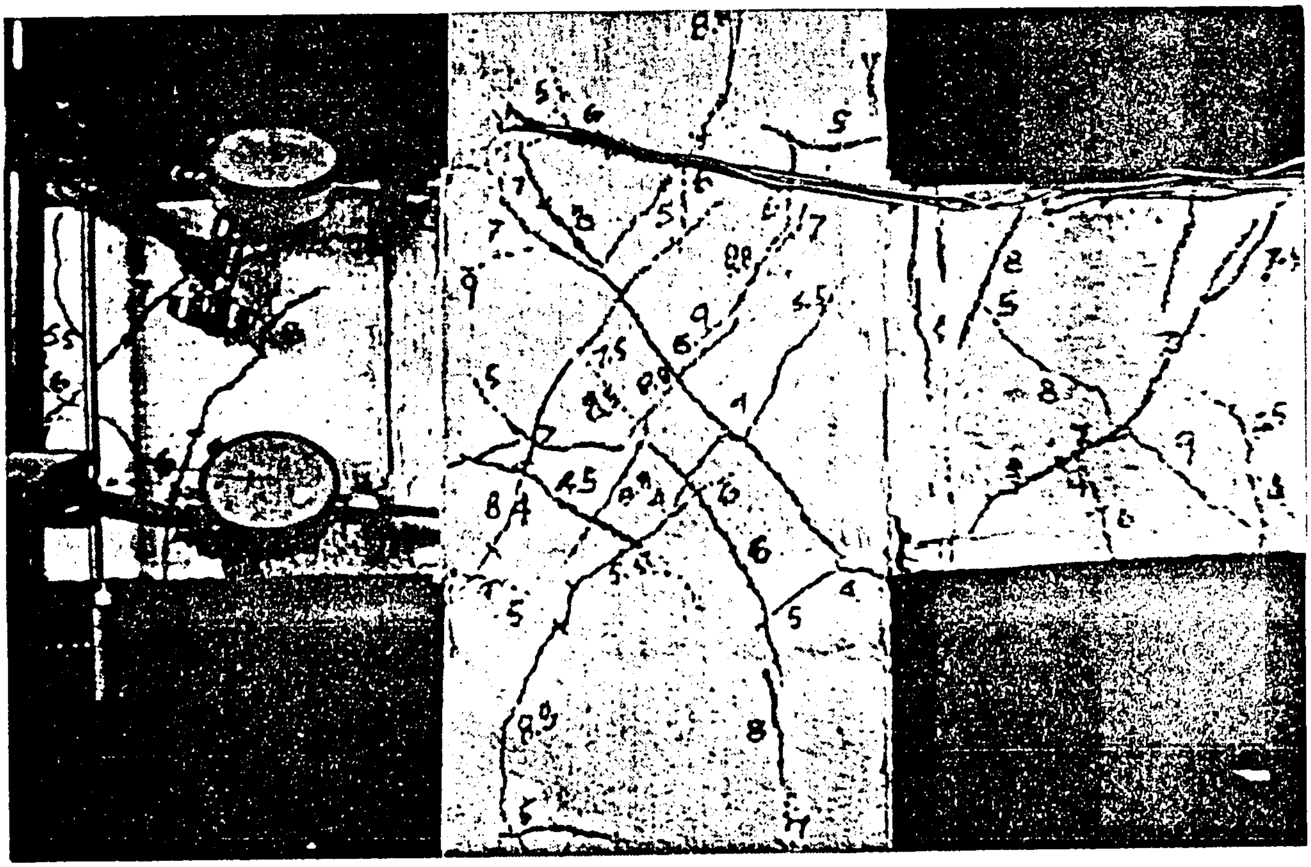

FIG. 36 SPECIMEN 4 WHEN TEST WAS TERMINATED (BACK)

5.7 SPECIMEN 6

With the presence of lateral ties at the joint as recommended by ACI Committee 352, the performance of the subassembly was greatly improved.

i. Moment-Curvature Curve shown in Figures A6,A12 shows that the system has good ductility.

ii. With the same member-geometry and reinforcement as in specimen 3 except the joint area now has lateral ties, the ultimate load of the joint increased by 7%.

iii. Good recovery on diagonal cracks when the load was reversed, indicating a good and lasting bond effect (Figure A18a,b).

iv. The first diagonal cracks occurred at 6.5-kip in the second half of the first cycle, although 7-kip has been reached in the first half of the cycle. Medium diagonal cracks of the same magnitude as in specimen 4 were observed after testing showed that the adverse effect caused by bond to the joint was negated by the presence of joint lateral ties.

v. The yield region of the beams occurred quite a distance from the column and well distributed over a reasonable length of the beams.

vi. This system has the highest energy capacity of those tested. This include 'total' or 'average'; 'input' or 'absorbed' energy of the joint or the beam-column subassembly (see Table I).

5.8 ENERGY ABSORPTION CAPACITY

The fundamental requirements of multistory structures to survive in any severe earthquake motion is as follows. First, the individual members and joints must have a large energy aborption capacity; Second, a large part of this absorbed energy must be returned or radiated back to the soil so that it causes as little damage as possible to the structures. Specimen 6 is the best system. This conclusion is based not only on the energy absorption capacity point of view as shown in Figure A33-A34 nor the joint absorption efficiency (Table I) but also from the nature of damage done to the specimen (Figures 37,38). The latter, requires more detail and analytical analyses of how much of this energy would inflict damage to the system and how much is being radiated back to the soil.

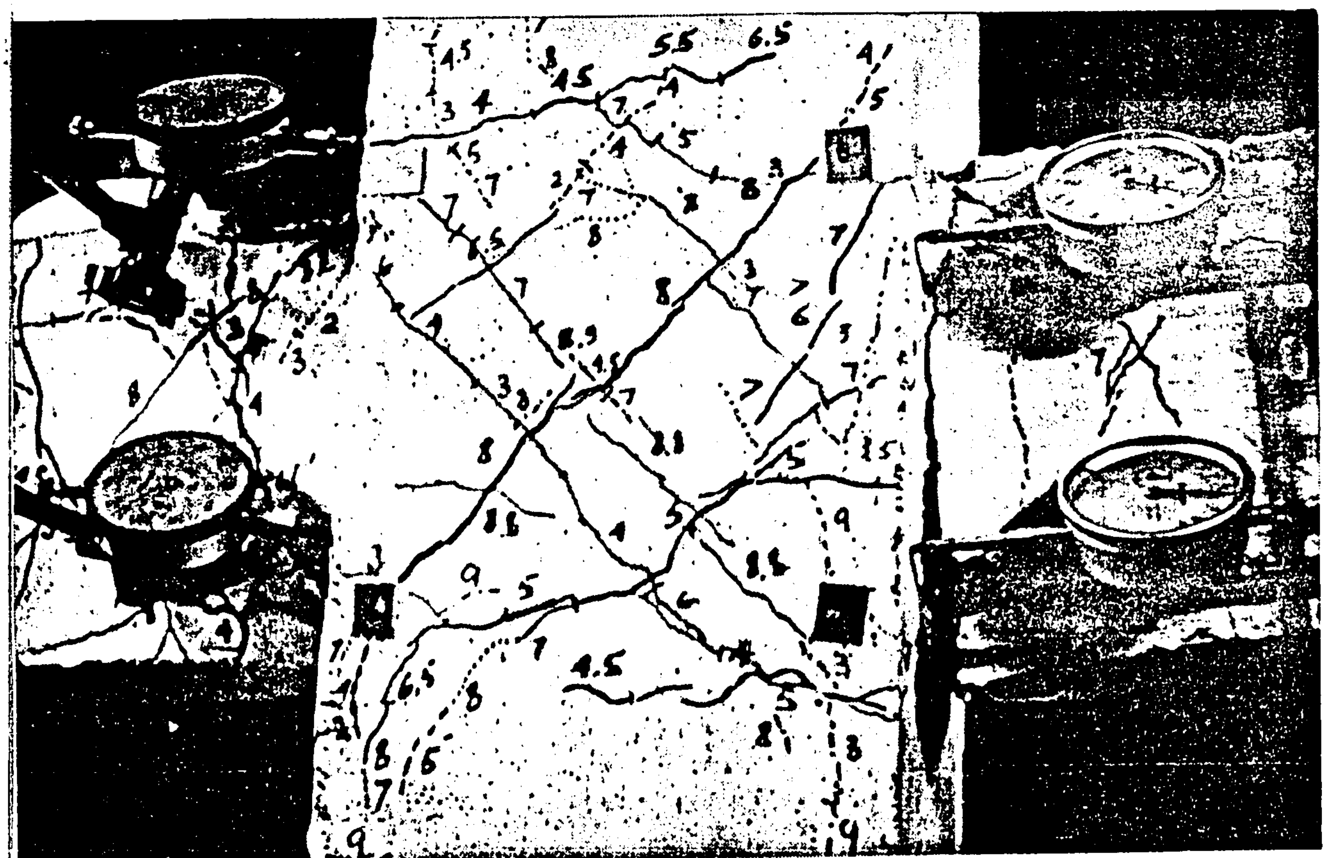

FIG. 37 SPECIMEN 6 WHEN TEST WAS TERMINATED (FRONT)

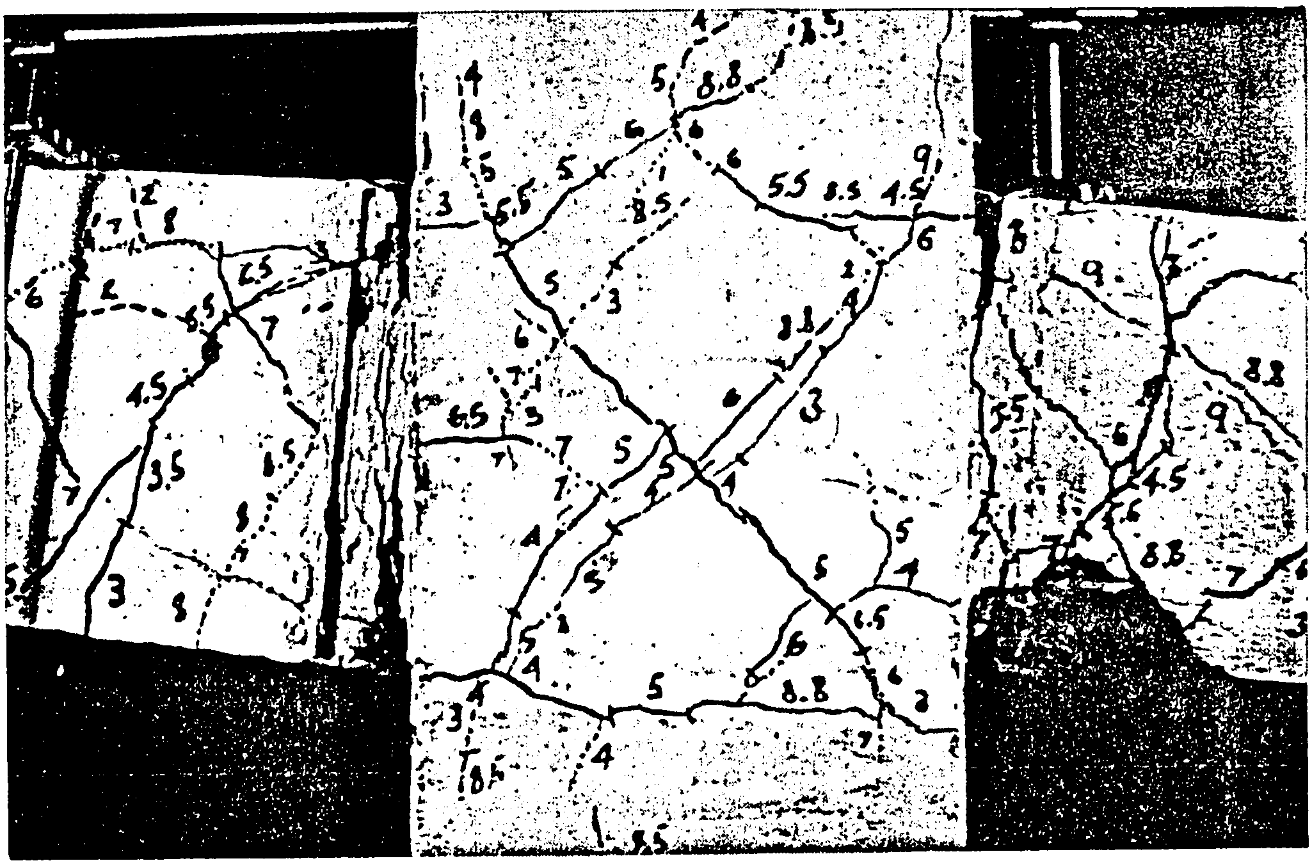

FIG. 38 SPECIMEN 6 WHEN TEST WAS TERMINATED (BACK)

TABLE I

	SP. 1	SP. 2	SP. 3	SP. 4	SP. 5	SP. 6
No. of column reinforcement (#3 bars*)	10	10	6	6	6	6
ρ_{col}	0.023	0.023	0.014	0.014	0.014	0.014
No. of beam reinforcement (#3 bars*) top	3	3	3	3	3	3
bottom	2	2	3	3	3	3
ρ_{bt}	0.012	0.012	0.012	0.012	0.012	0.012
ρ_{bb}	0.008	0.008	0.012	0.012	0.012	0.012
No. of joint lateral ties (#2 bars**)	6†	6†	2	2	2	6†
Condition of Bond	full	full	full	half(50%)	nil(0)	full
Column axial compression (kips)	12	140	12	12	12	12
f'_c (psi)	4400	5100	3500	3300	3700	4100
No. of cycle	2.0	1.5	2.5	3.5	3.0	3.5
P_{max} positive direction (kips)	7.91††	7.57	7.90	7.86	7.52	7.13
negative direction (kips)	7.22††	8.32	7.82	8.28	6.89	8.35
M_{max} positive direction (kip-in)	255	268	276	275	263	250
negative direction (kip-in)	216	295	274	290	241	292
$Deflection_{max}$ positive direction (in)	0.920†††	0.398	1.352	1.146	2.111	2.153
negative direction (in)	0.580†††	1.457	1.462	1.923	1.711	2.021
ϕ_{max} positive direction (rad)	0.0241	0.0122	0.016	0.042	0.025	0.064
negative direction (rad)	0.0259	0.0481	0.034	0.030	0.069	0.034
Max joint diagonal tensile strain (micro in/in) LT-RB	133.65	32.40	13972.50	12700.80	6998.40	8691.3
RT-LB	311.85	170.18	14758.20	11988.00	3944.70	10700.1
Total joint input energy (kip-in-rad)			9.43	20.60	12.48	24.42
Average joint input energy per cycle (kip-in-rad/cycle)			3.77	5.88	4.16	6.98
Total joint absorbed energy (kip-in-rad)			7.65	17.17	9.38	22.10
Average joint absorbed energy per cycle (kip-in-rad/cycle)			3.06	4.91	3.13	6.32
The absorption efficiency of the joint			81%	83%	75%	90%
Total sub-assembly input energy (kip-in)			26.47	42.01	28.49	44.95
Average sub-assembly input energy per cycle (kip-in/cycle)			10.59	12.00	9.50	12.84
Total sub-assembly absorbed energy (kip-in)			14.82	23.94	17.80	28.97
Average sub-assembly absorbed energy per cycle (kip-in/cycle)			5.93	3.42	5.93	8.27

* deformed bar

** plain bar

† supplement ties

†† load equivalent

††† deflection equivalent

Chapter VI

CONCLUSION

On the basis of the results in the previous chapters the following conclusion can be made:

i. The behaviour of the joint is mainly dependent on the strength of the concrete, the amount of the main reinforcements, the amount of confinement in the joint core, the distribution of bond stresses at the joint core, the axial compression load exerted at the column, and the loading history.

ii. By increasing the strength of the concrete, the axial compression load and column steel ratio, the damage on the joint can be reduced considerably; however vertical accelerations in an earthquake could reduce the column load to zero or even tension and the compression help could not be relied upon.

iii. The absence of bond stresses in the joint core improves the performance of the joint at the expense of the beam-column interface.

iv. The maximum bond stresses which lead to local bond failure and finally weaken the member occurred in the transition region of 'bond' and 'nobond'.

v. The presence of lateral ties in many ways helps the performance of the joint in terms of higher ultimate load, better ductility, durable bonding, energy absorption capacity.

vi. Ductility alone is not the best means to describe the efficiency of energy absorption of the structure in resisting earthquake motion. The energy method gives a better estimation and more reliable answer because it takes the adverse effect caused by 'softening' into consideration.

Chapter VII

RECOMMENDATIONS

The following recommendations are based on previous observations and conclusion. Furthur varification through experiments or analytical approaches are needed to confirm each of the follcwing points.

i. In the case of joints having low confinement due to the absence of heavy lateral ties, the bond on the beam steel should be reduced and at the same time closer beam stirrups provided near the column. This arragement assures that the yielding will occur in the beam and reduce the damage occuring at the joint.

ii. In the case of using the design recommendations of ACI Committee 352, the performance of the joint can be improved by suppressing joint bond stresses in the middle-half region and consequently reduce the load transmitted into the joint.

iii. In order to have better joint confinement, the main column reinforcements should be distributed all around the column.

BIBLIOGRAPHY

1. Blume, J.A., "Structural Dynamics in Earthquake Resistant Design," Trans. A.S.C.E., 125, 1960, pp.1088-1139.

2. Clough, R.W. and Penzien, J., "Dynamics of Structures," McGraw-Hill, 1975, pp.594-604.

3. Clough, R.W., "Earthquake Response of Structures," Earthquake Engineering, Prentice-Hall, 1970, pp. 307-334.

4. Bertero, V.V. and Popov, E.P., "Seismic Behaviour of Ductile Moment-Resisting Reinforced Concrete Frames" A.C.I., Publication SP-53-11, 1977, pp.247-291

5. A.C.I. Committee 318, "Building Code Requirements for Reinforced Concrete--(ACI 318-71)," American Concrete Institute, Detroit, 1971.

6. A.C.I.-A.S.C.E. Committee 352, "Recommendations for Design of Beam-Column Joints in Monolithic Reinforced Concrete Structures," A.C.I. Journal, Proceedings V.73, No.7, July 1976, pp.375-393.

7. Blume, J.A., Newmark, N.M. and Corning, L.H., "Design of Multistory Reinforced Concrete Buildings for Earthquake Motions," Chicago, 1961, Portland Cement Association, 1961, pp.250-285.

8. Uzumeri, S.M., "Strength and Ductility of Cast-In-Place Beam-Cclumn Jcints" A.C.I., Publication SP-53-12, 1977, pp.293-350.

9. Park, R. and Paulay, T., "Reinforced Concrete Structures," John Wiley and Sons, New York, 1975, pp.716-758.

10. Sandor, B.I., "Cyclic Stress and Strain," The University of Wisconsin Press, Madison, 1972.

11. Dowrick, D.J., "Earthquake Resistant Design," John Wiley and Sons, London, 1977.

12. Fintel, M., "Resistance to Earthquake----Philosophy, Ductility and Details," Response of Multistory Concrete Structures to Lateral Forces, A.C.I.-Publication SP36-5, 1973, pp.75-96.

13. Warner, R.F., Rangan, B.V. and Hall, A.S., "Reinforced Concrete," Pitman Australia, 1977, pp.435-445.

14. Soleimani, D., Popov, E.P. and Bertero, V.V., "Hysteretic Behaviour of Reinforced Concrete Beam-Column Subassemblages," A.C.I. Journal, Proceedings V.76, No.11, Nov.1979, pp.1179-1195.

15. Hawkins, N.M. and Lin, I.J., "Bond Characteristics of Reinforcing Bars for Seismic Loadings," Third Canadian Conference, June 1979, vol.2, pp.1225-1252.

16. Uzumeri, S.M. and Seckin, M., "Behaviour of reinforced Concrete Beam-Column Joints Subjected to Slow Load Reversals," Publication No.74-05, Department of Civil Engineering, University of Toronto, March 1974, 85pp.

Appendix A

PLOTTING RESULTS

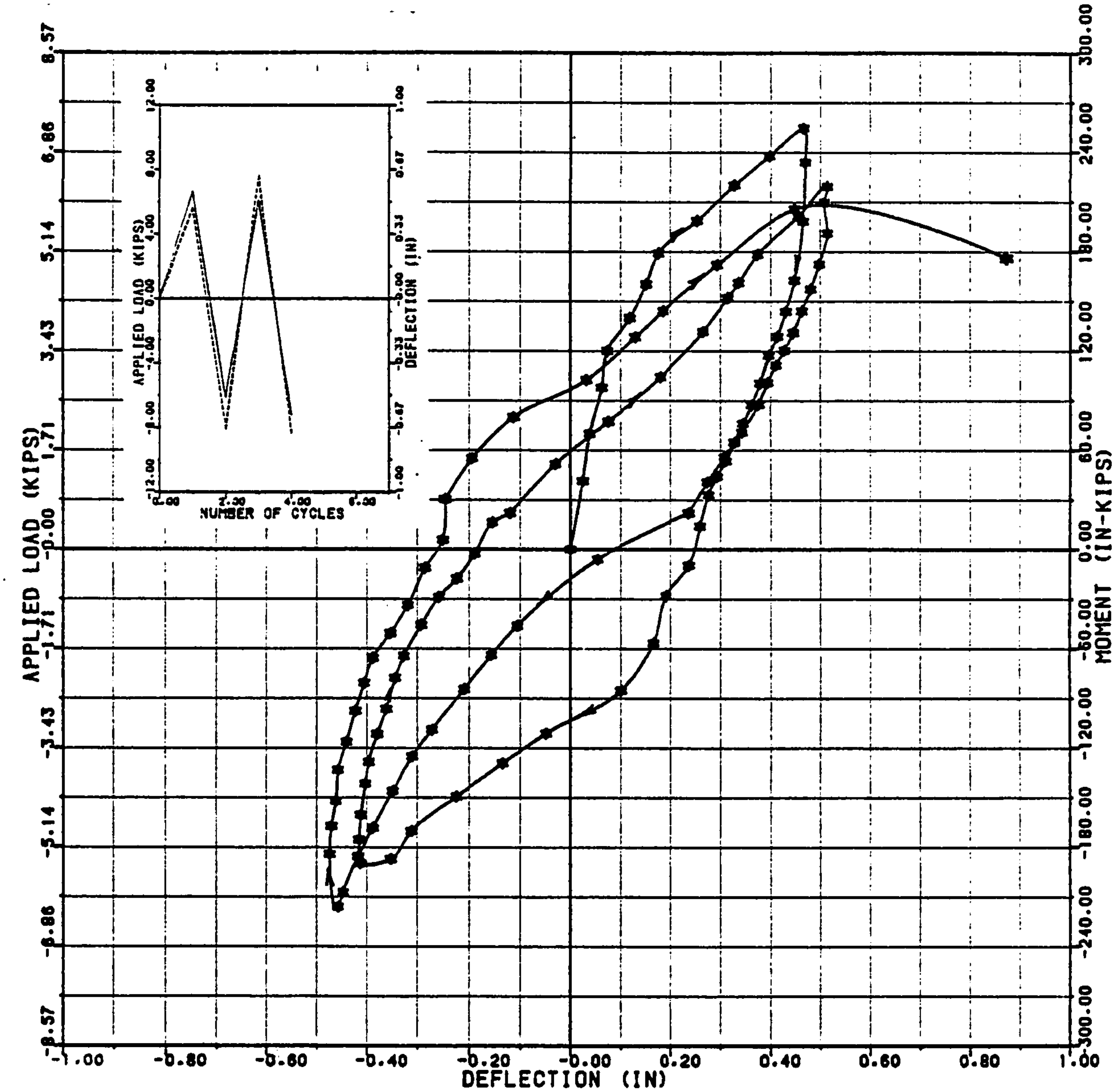

FIG. A1a BEAM TIP LOAD VERSUS BEAM TIP DEFLECTION (LEFT), SPECIMEN 1

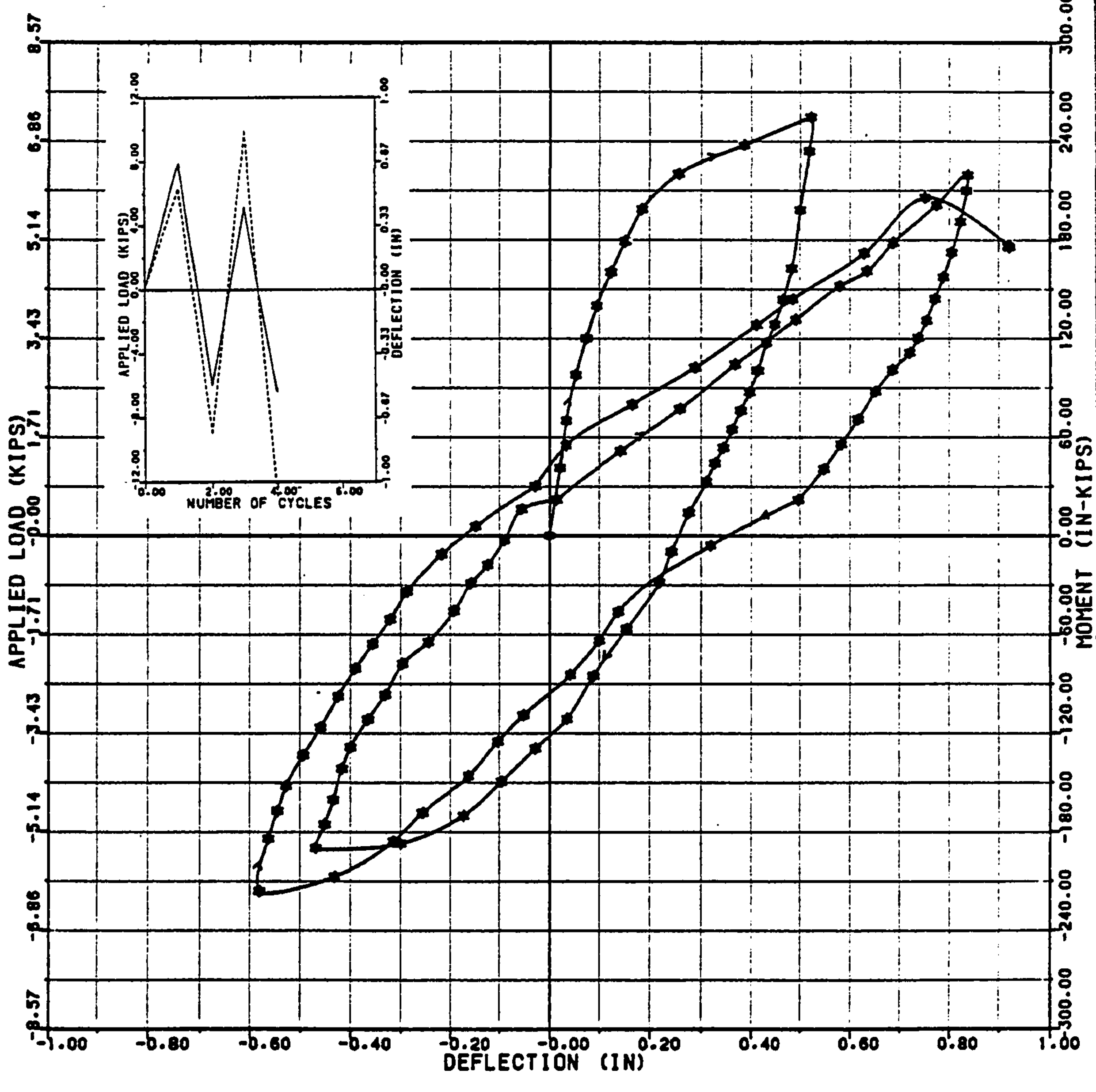

FIG. A1b BEAM TIP LOAD VERSUS BEAM TIP DEFLECTION (RIGHT), SPECIMEN 1

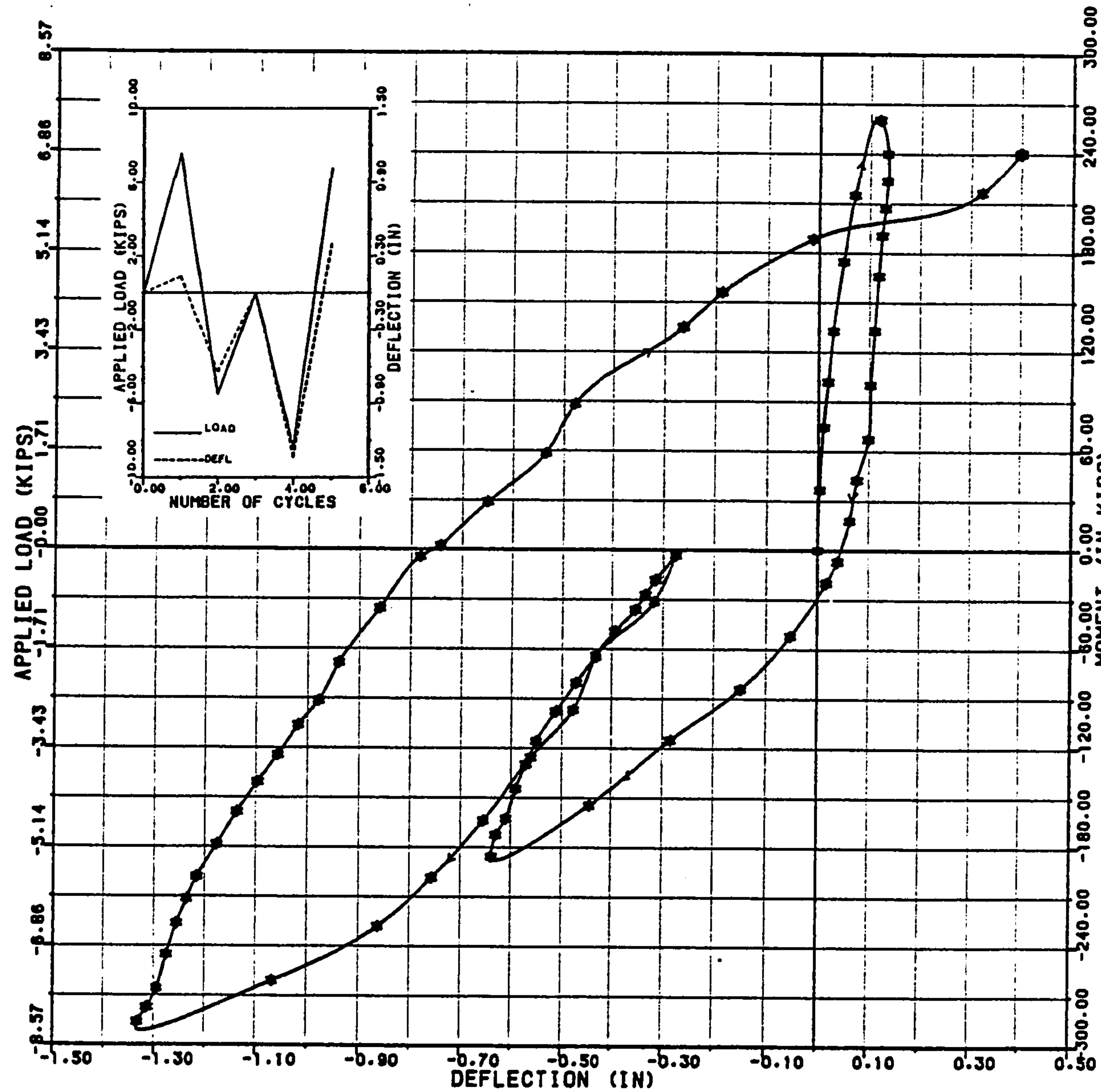

FIG. A2a BEAM TIP LOAD VERSUS BEAM TIP DEFLECTION (LEFT), SPECIMEN 2

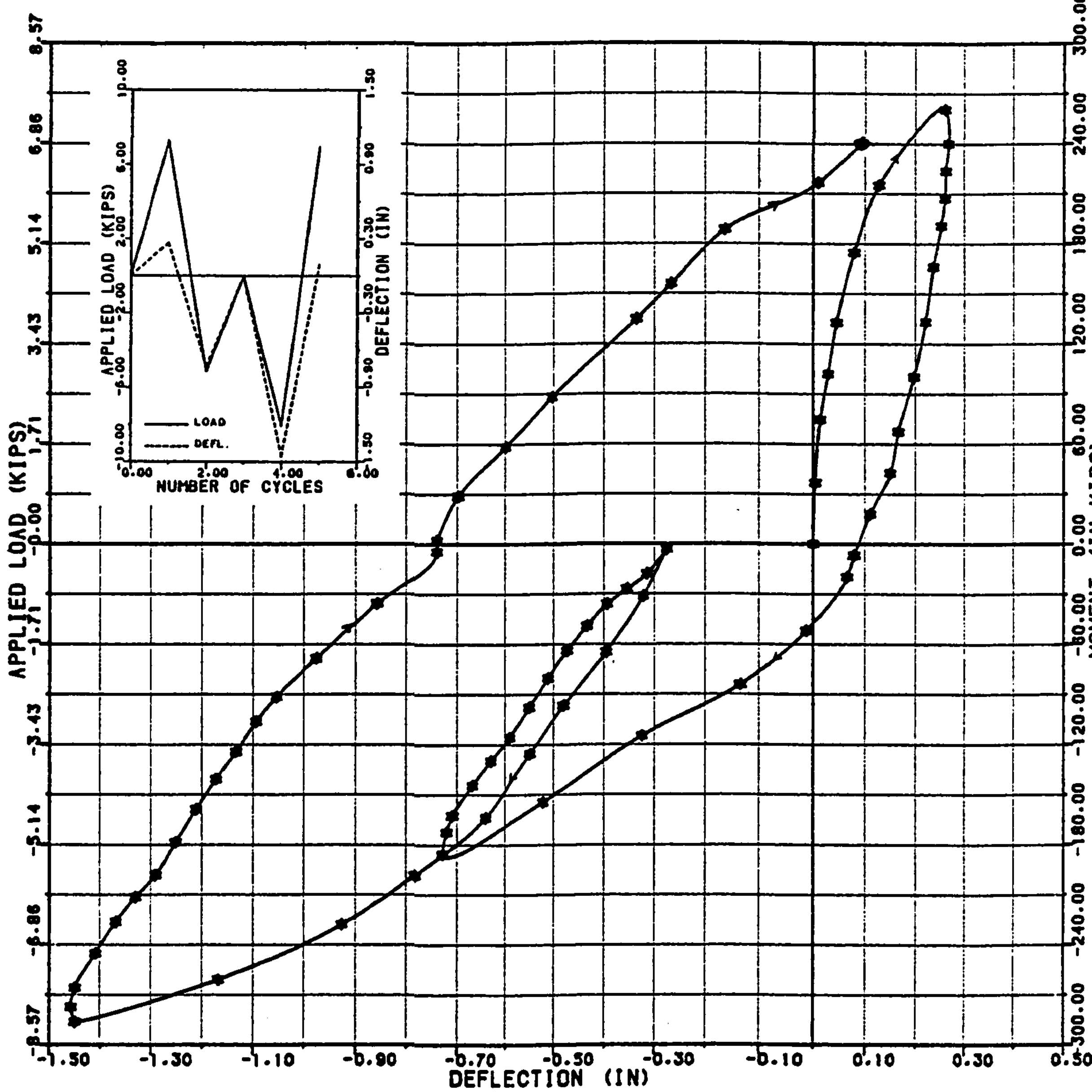

FIG. A2b BEAM TIP LOAD VERSUS BEAM TIP DEFLECTION (RIGHT), SPECIMEN 2

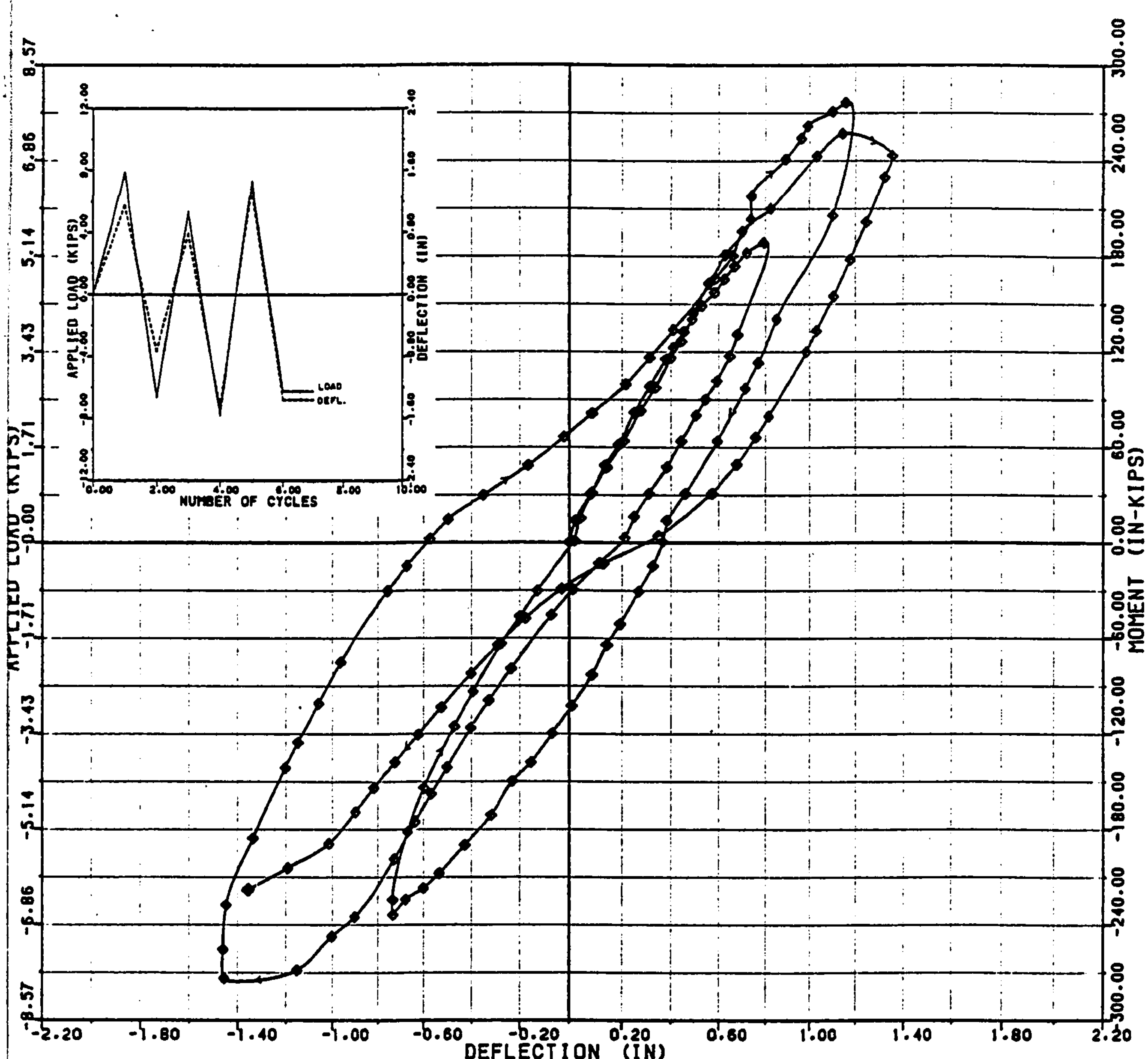

FIG. A3 BEAM TIP LOAD VERSUS BEAM TIP DEFLECTION, SPECIMEN 3

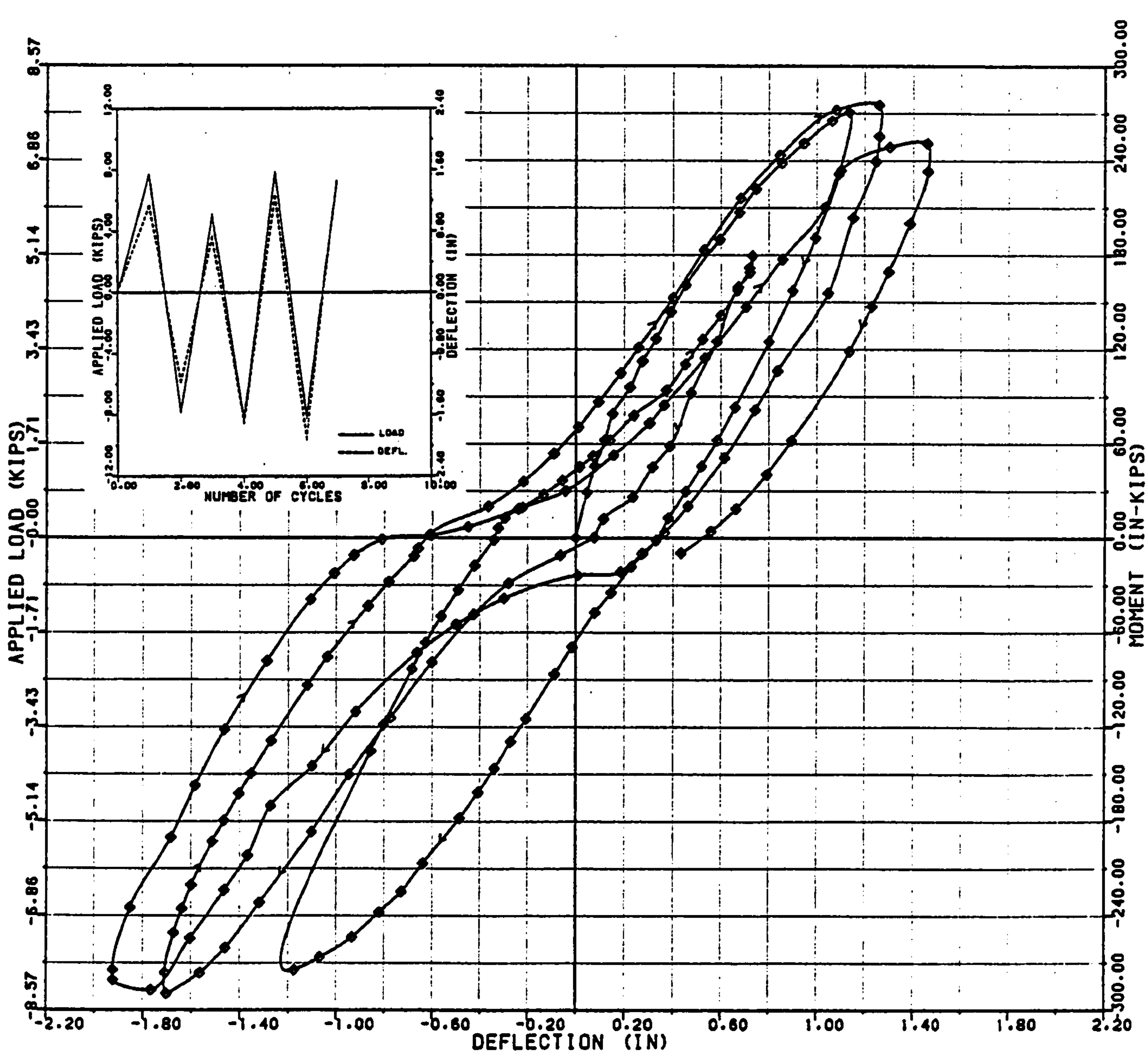

FIG. A4 BEAM TIP LOAD VERSUS BEAM TIP DEFLECTION ,
SPECIMEN 4

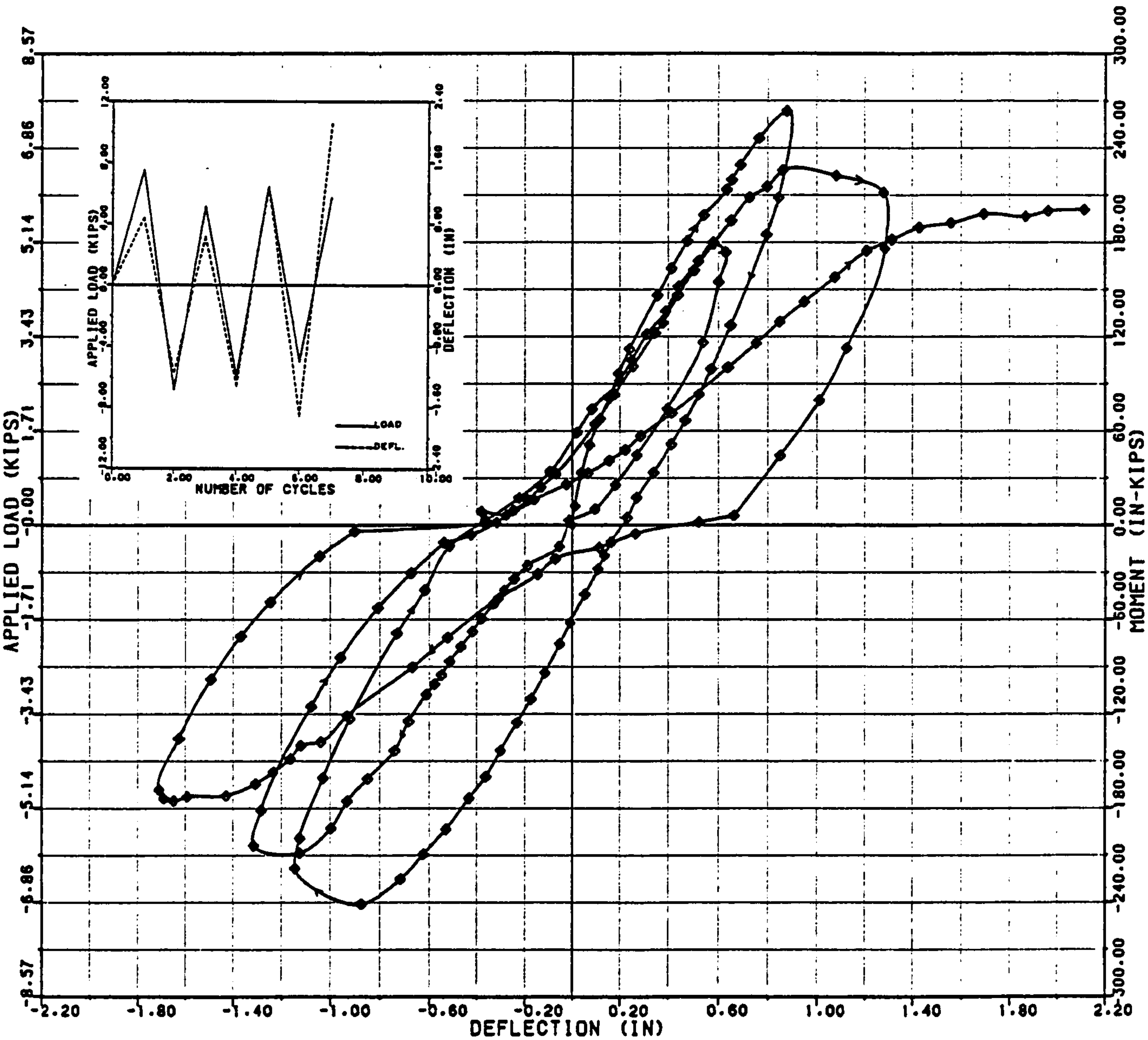

FIG. A5 BEAM TIP LOAD VERSUS BEAM TIP DEFLECTION, SPECIMEN 5

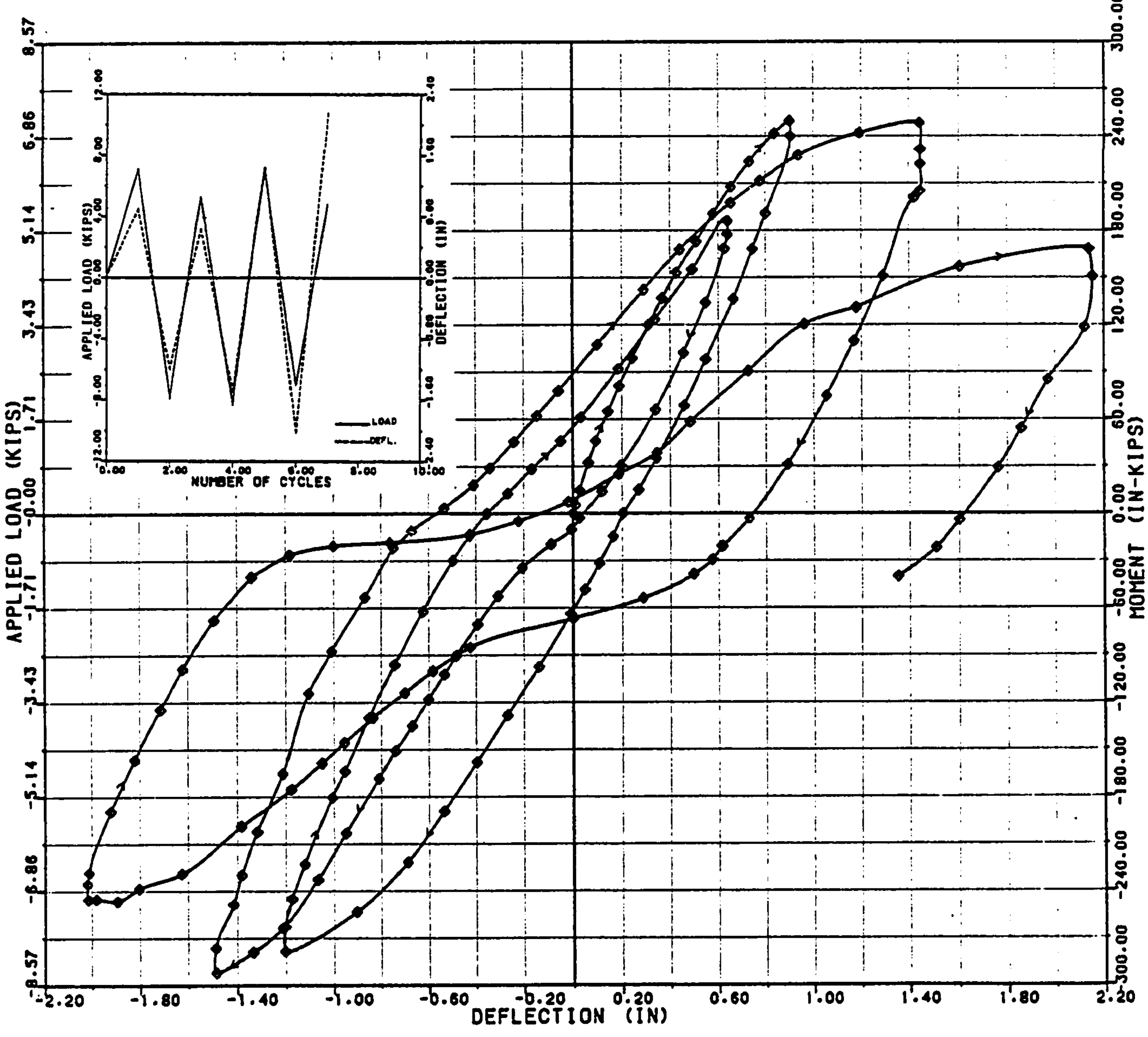

FIG. A6 BEAM TIP LOAD VERSUS BEAM TIP DEFLECTION, SPECIMEN 6

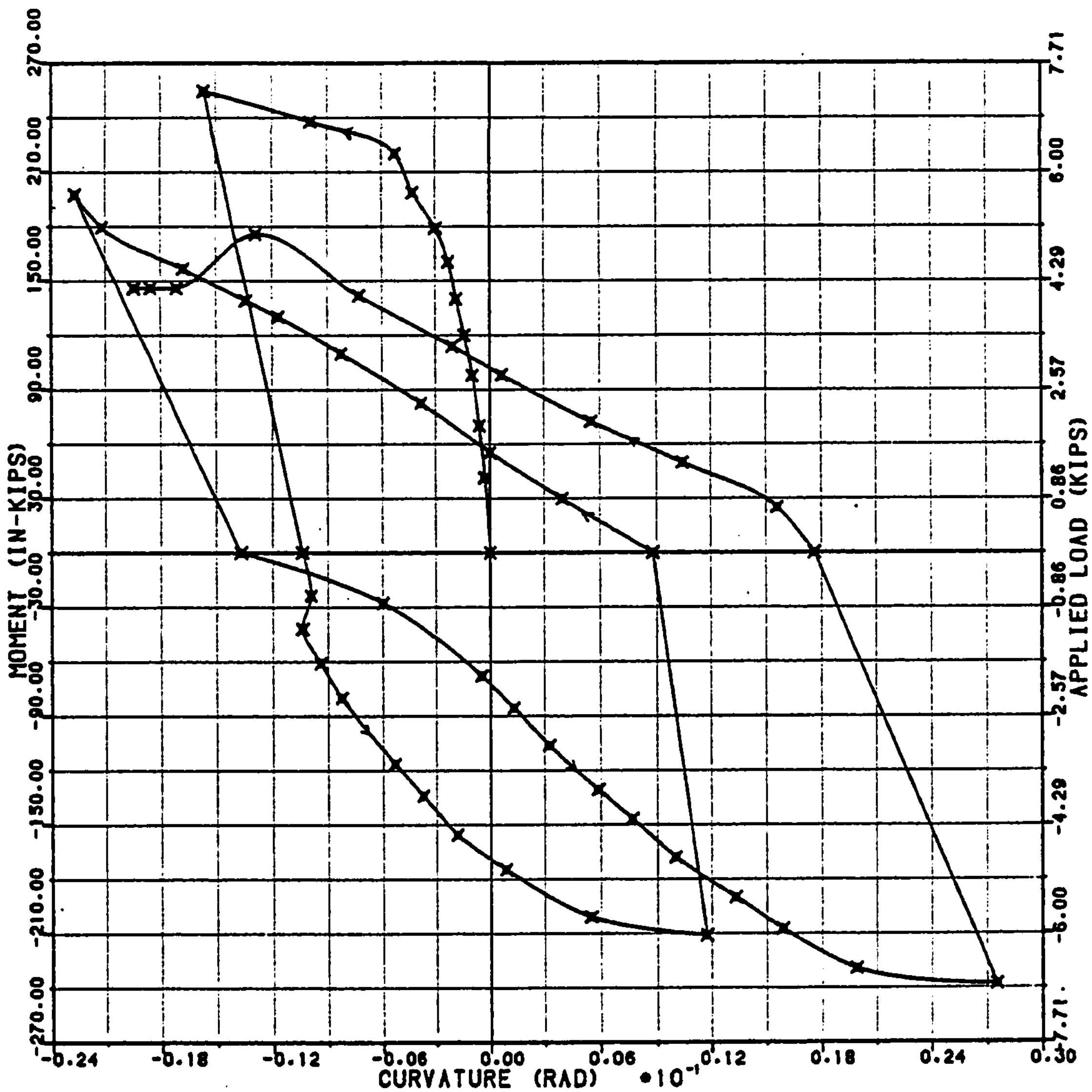

FIG. A7 BEAM CURVATURE VERSUS JOINT MOMENT, SPECIMEN 1

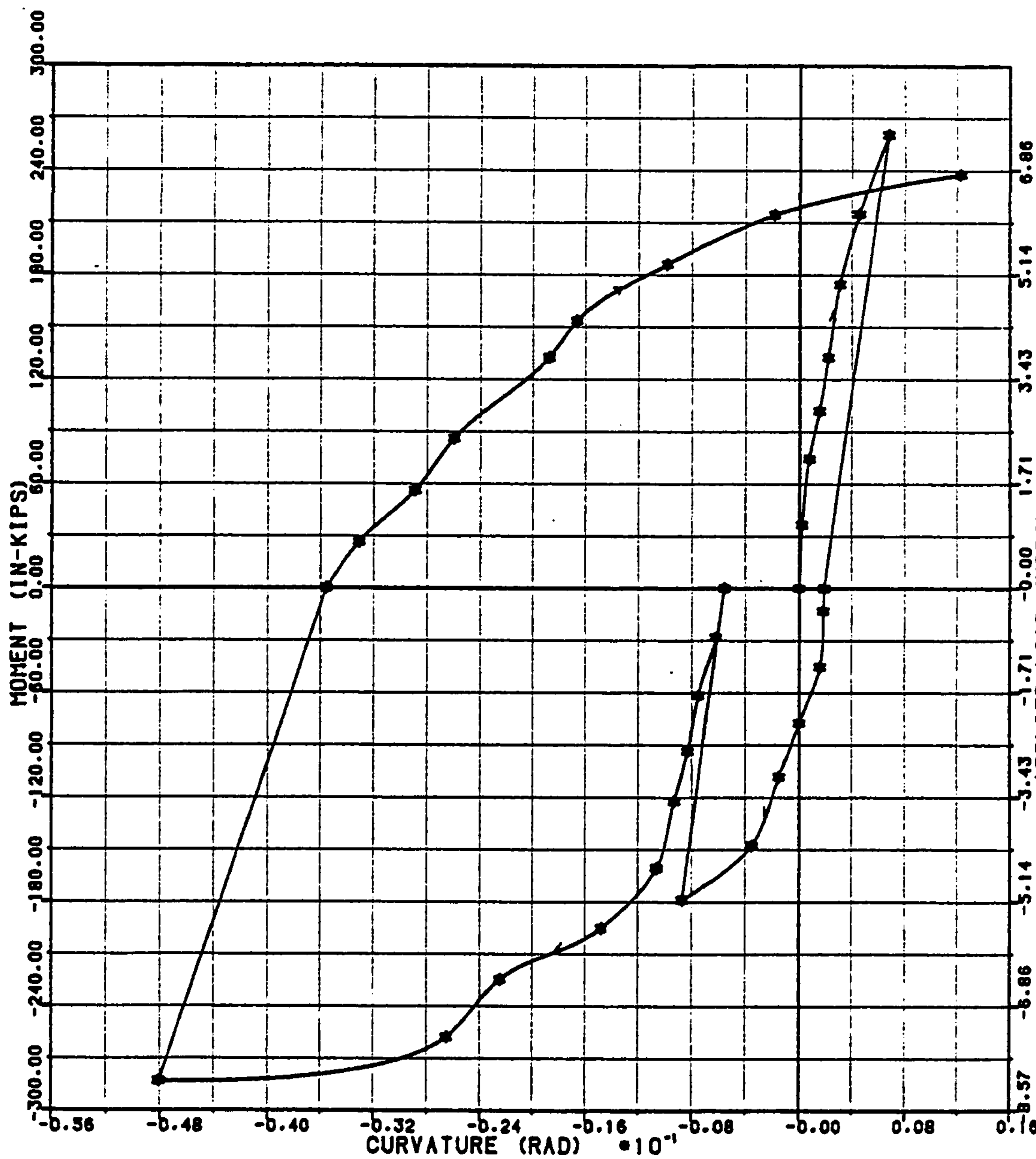

FIG. A8 BEAM CURVATURE VERSUS JOINT MOMENT, SPECIMEN 2

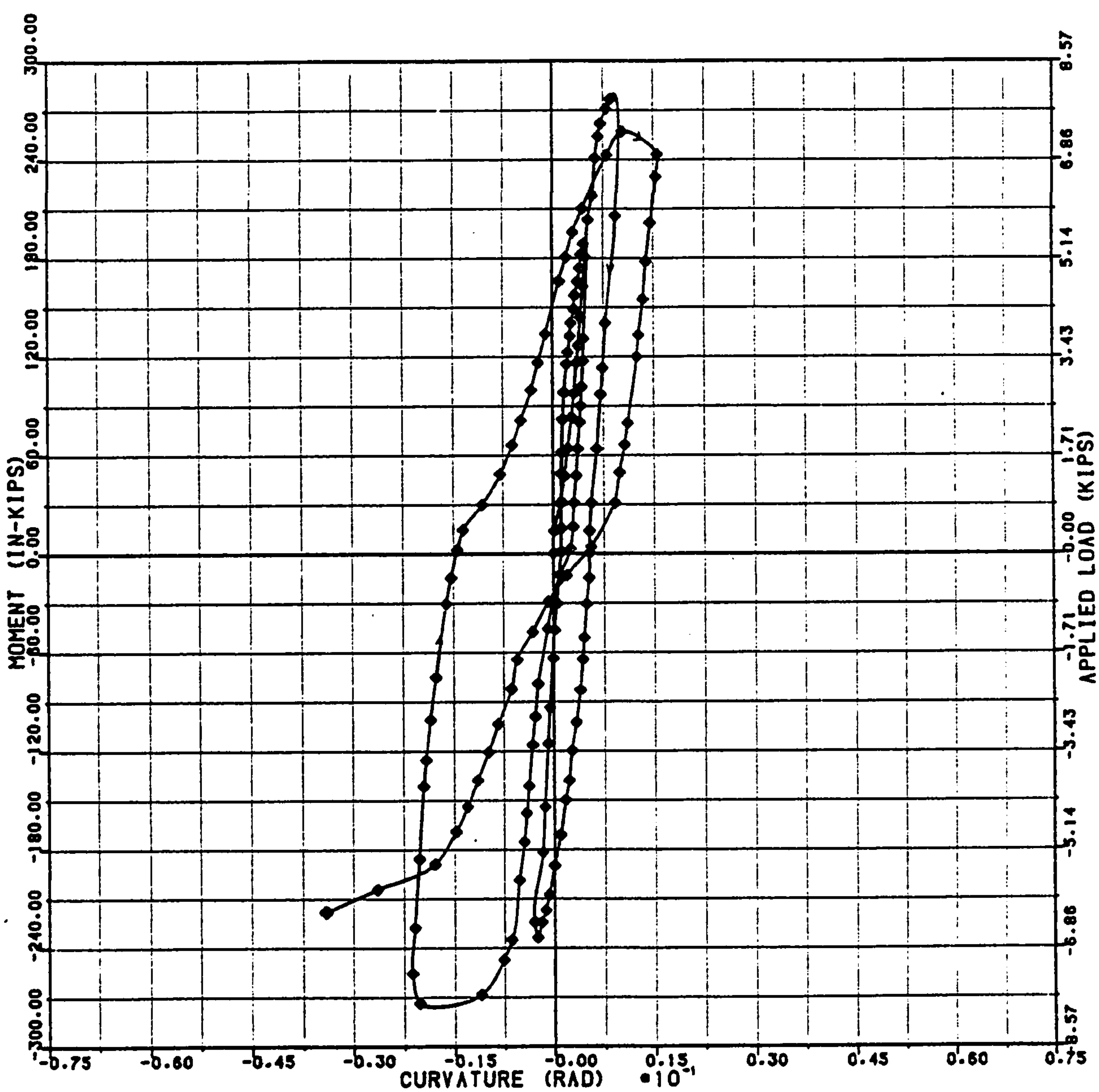

FIG. A9 BEAM CURVATURE VERSUS JOINT MOMENT, SPECIMEN 3

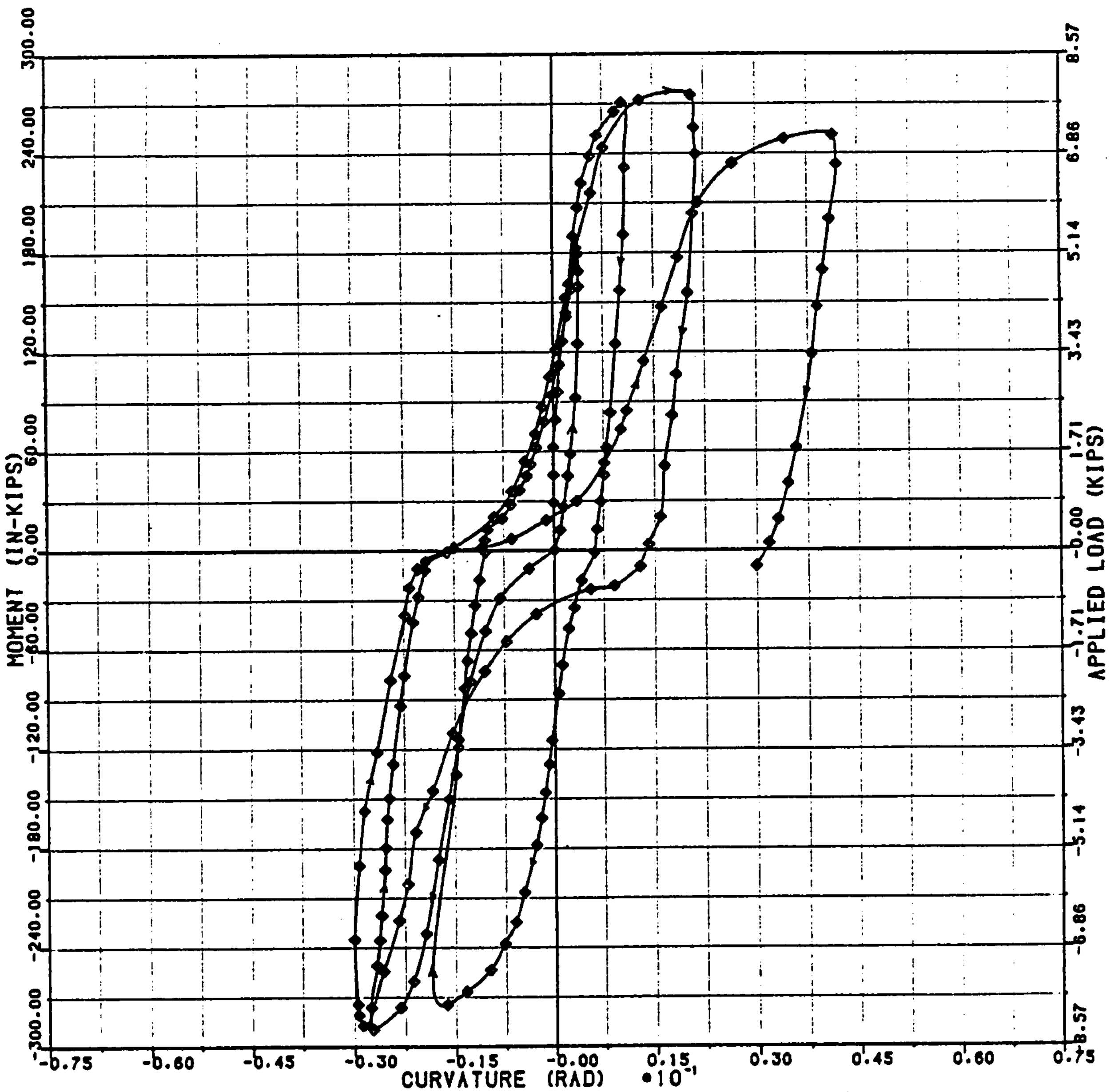

FIG. A10 BEAM CURVATURE VERSUS JOINT MOMENT, SPECIMEN 4

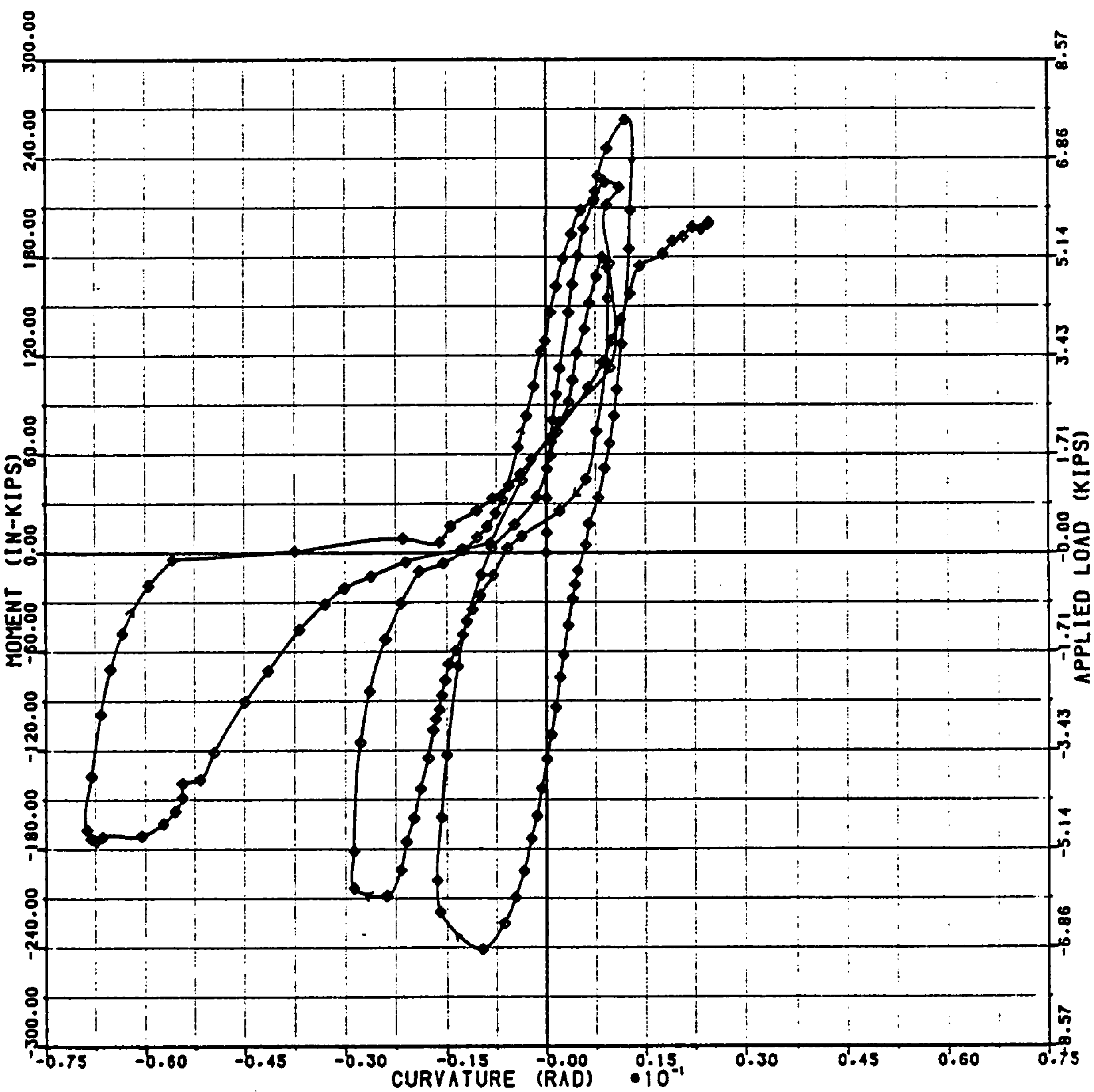

FIG. A11 BEAM CURVATURE VERSUS JOINT MOMENT, SPECIMEN 5

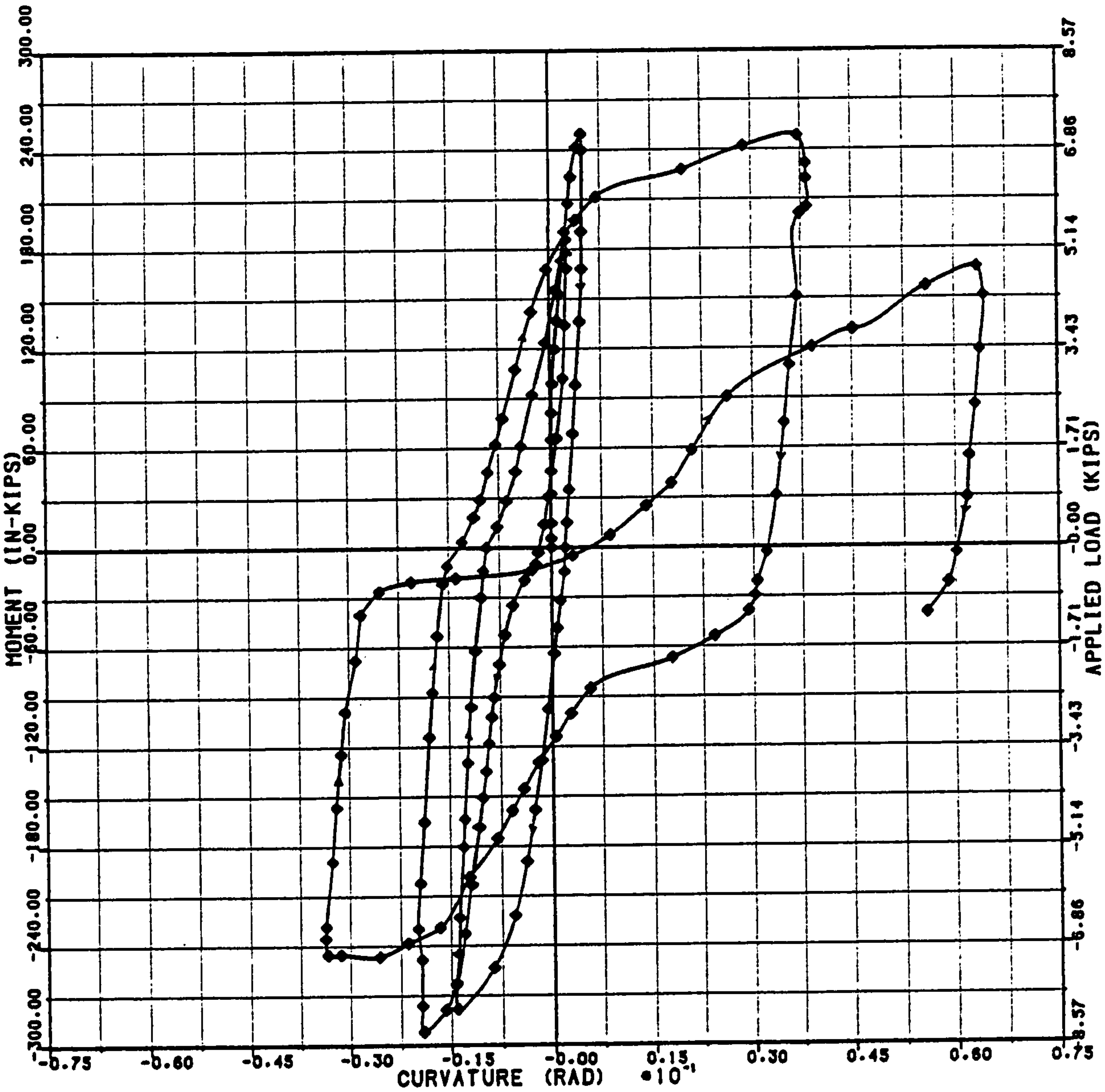

FIG. A12 BEAM CURVATURE VERSUS JOINT MOMENT, SPECIMEN 6

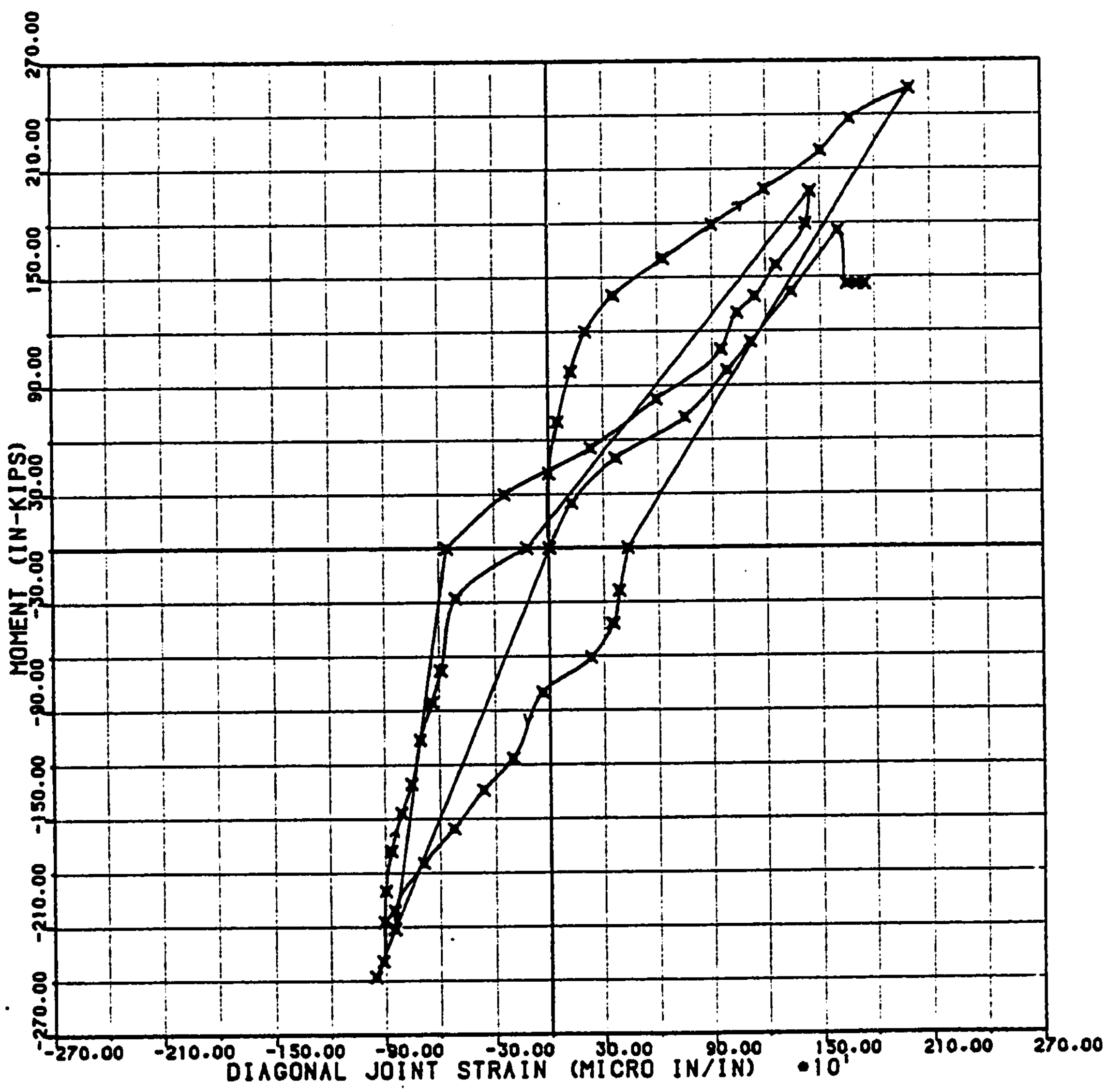

FIG. A13a DIAGONAL JOINT STRAIN (LT-RB) VERSUS JOINT MOMENT, SPECIMEN 1

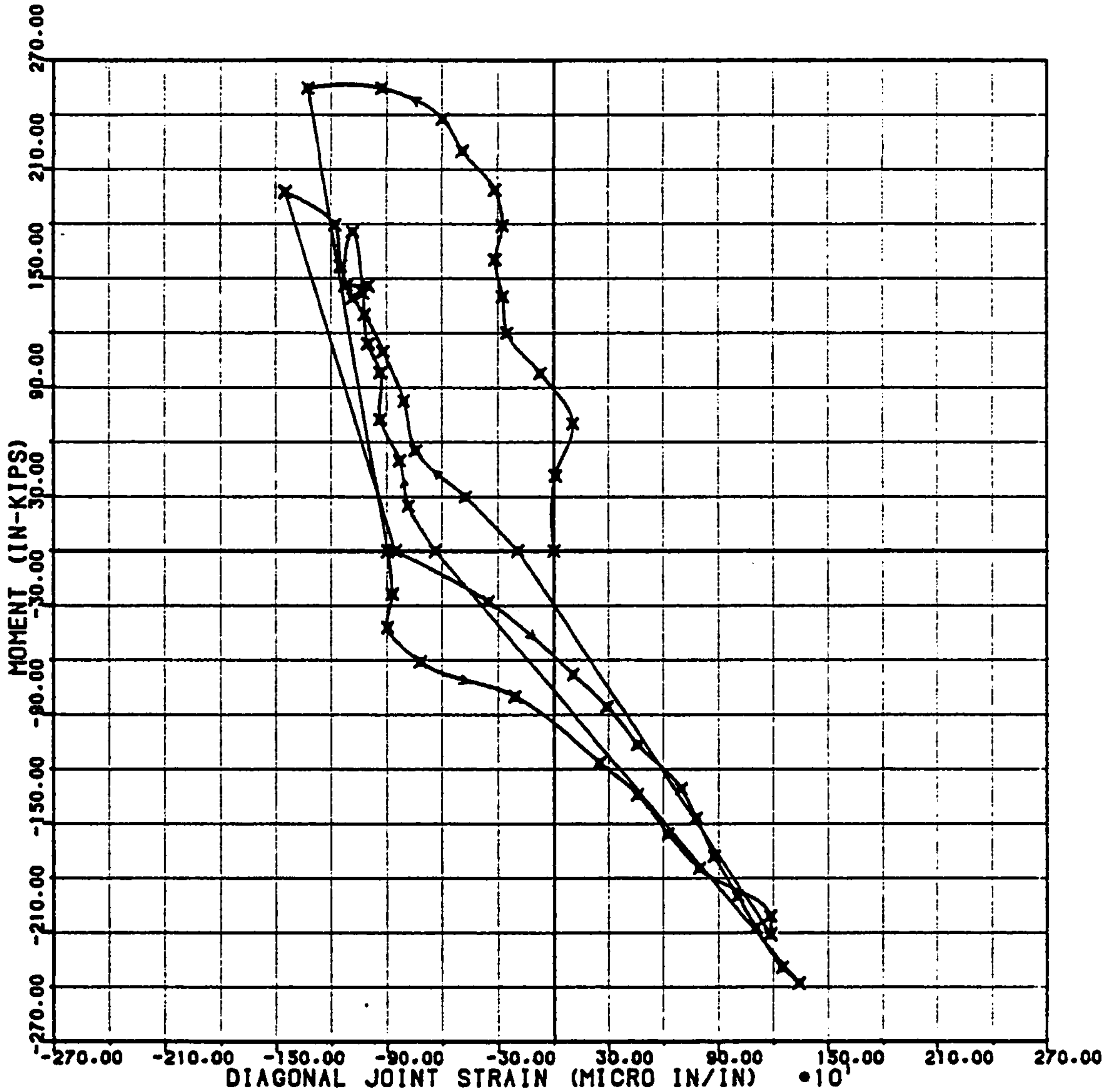

FIG. A13b DIAGONAL JOINT STRAIN (RT-LB) VERSUS JOINT MOMENT, SPECIMEN 1

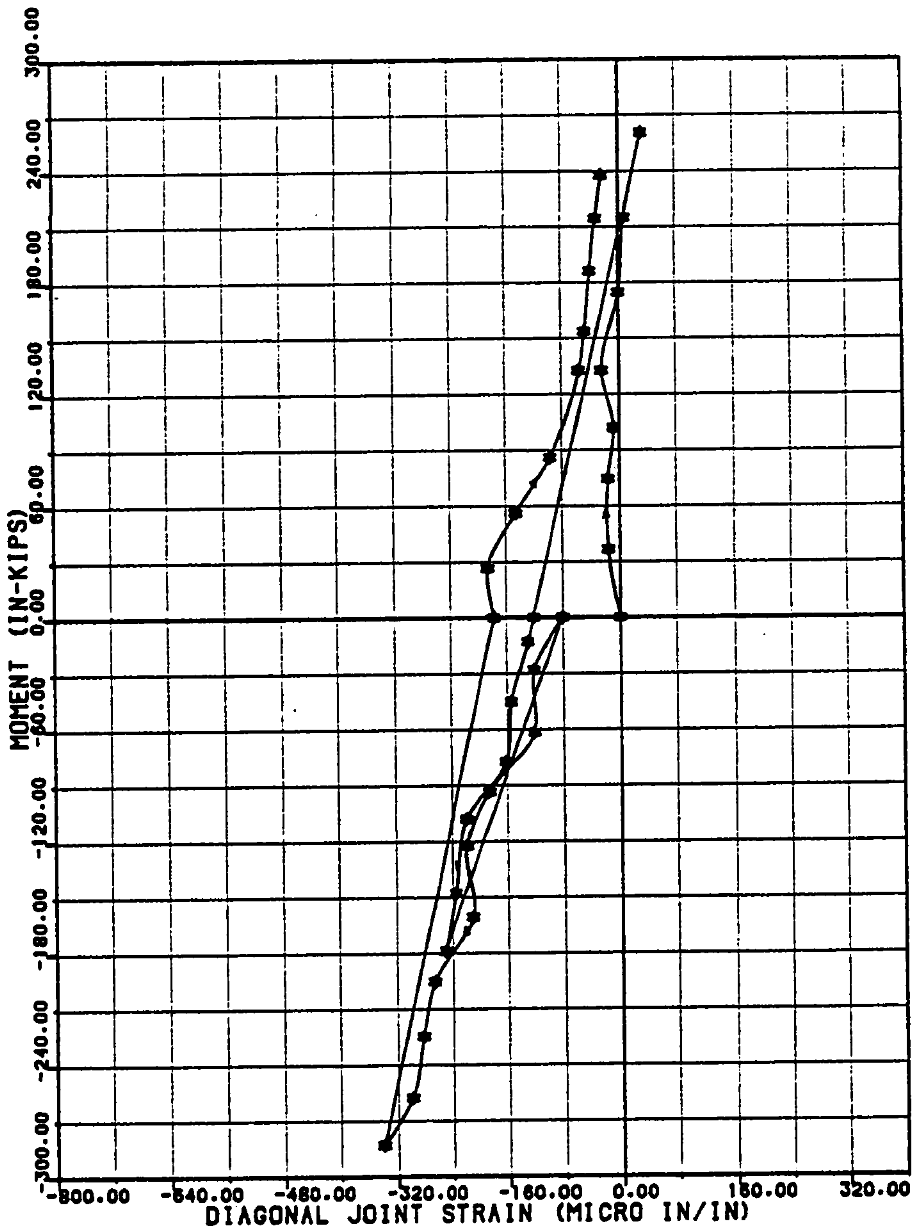

FIG. A14a DIAGONAL JOINT STRAIN (LT-RB) VERSUS JOINT MOMENT, SPECIMEN 2

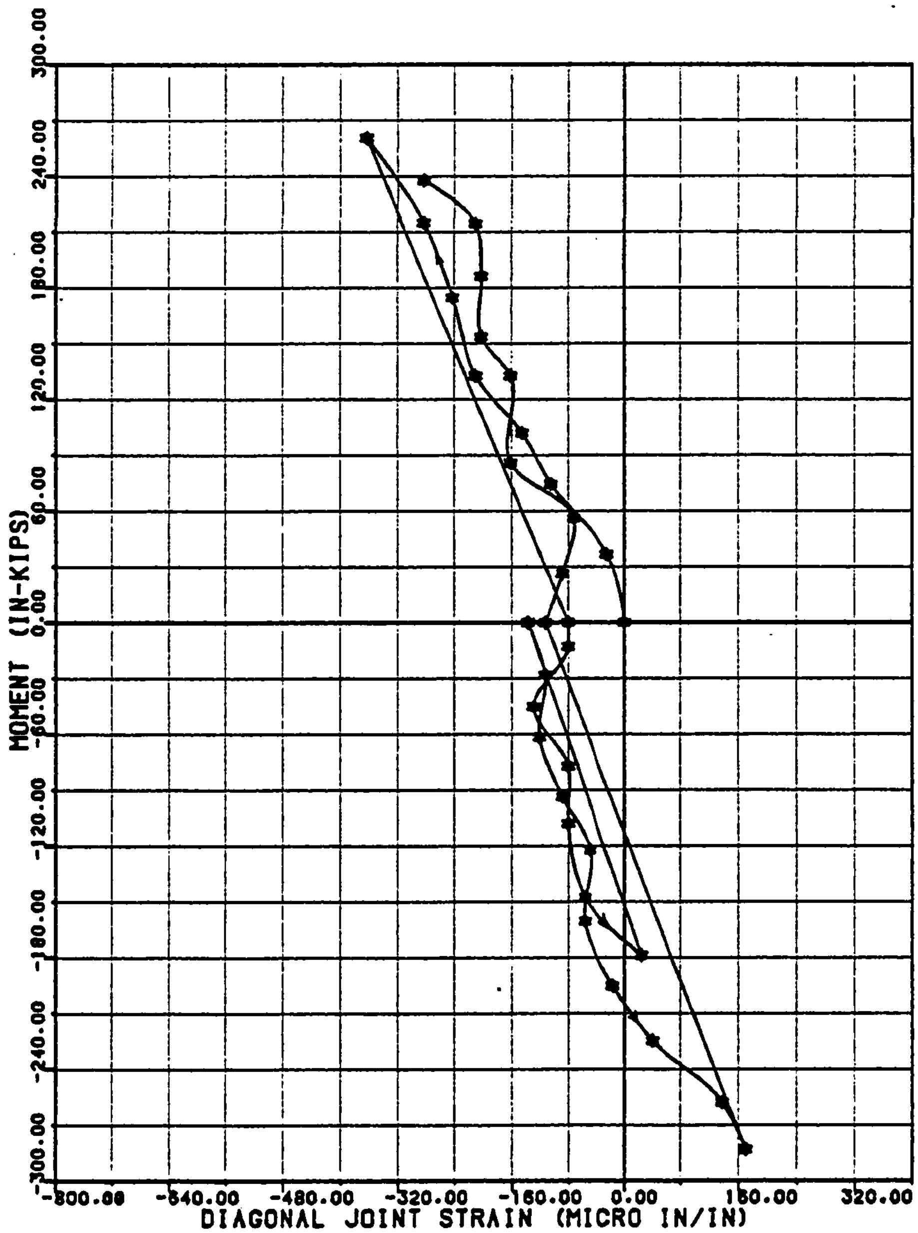

FIG. A14b DIAGONAL JOINT STRAIN (RT-LB) VERSUS JOINT MOMENT, SPECIMEN 2

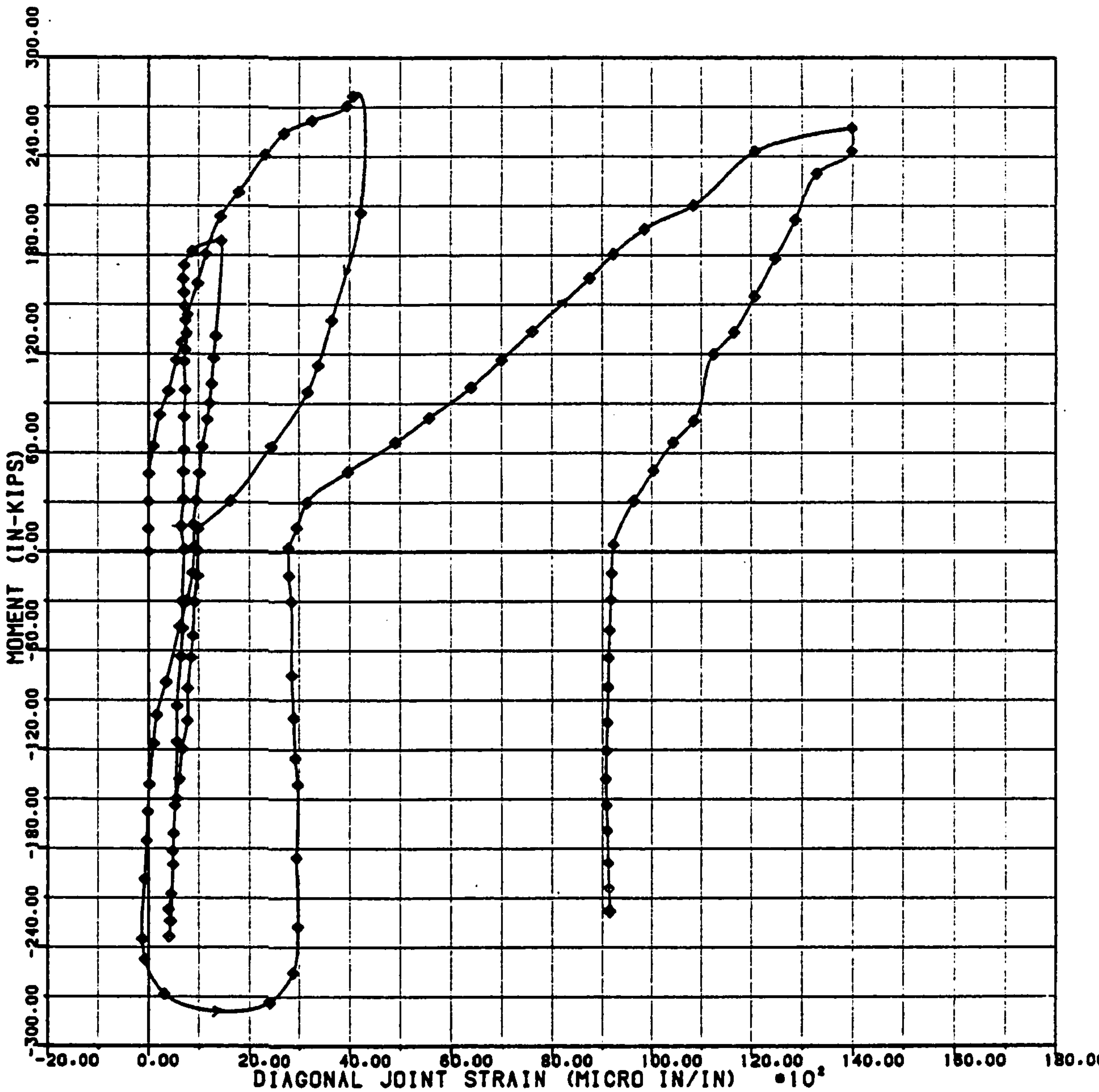

FIG. A15a DIAGONAL JOINT STRAIN (LT-RB) VERSUS JOINT MOMENT, SPECIMEN 3

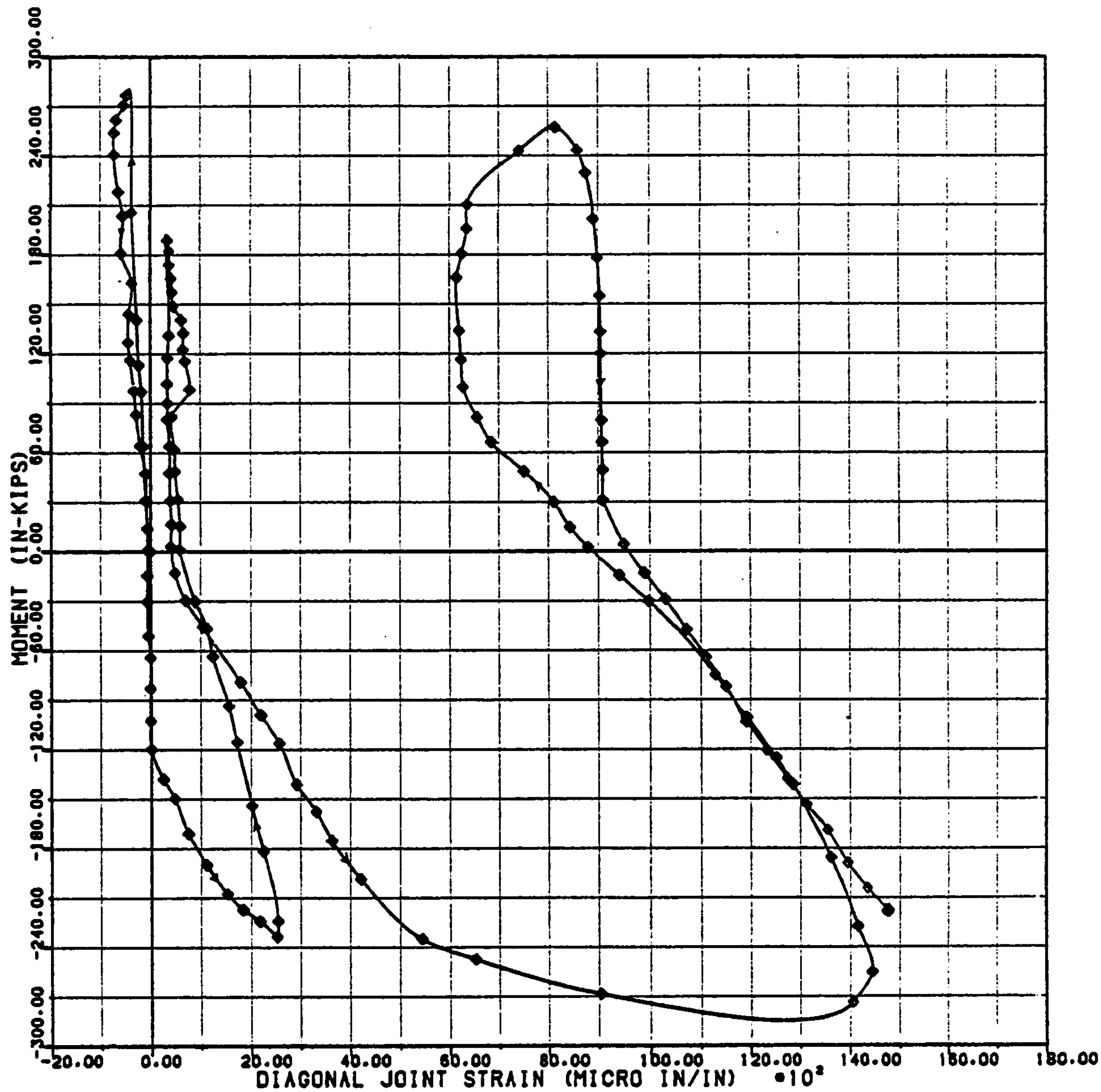

FIG. A15b DIAGONAL JOINT STRAIN (RT-LB) VERSUS JOINT MOMENT, SPECIMEN 3

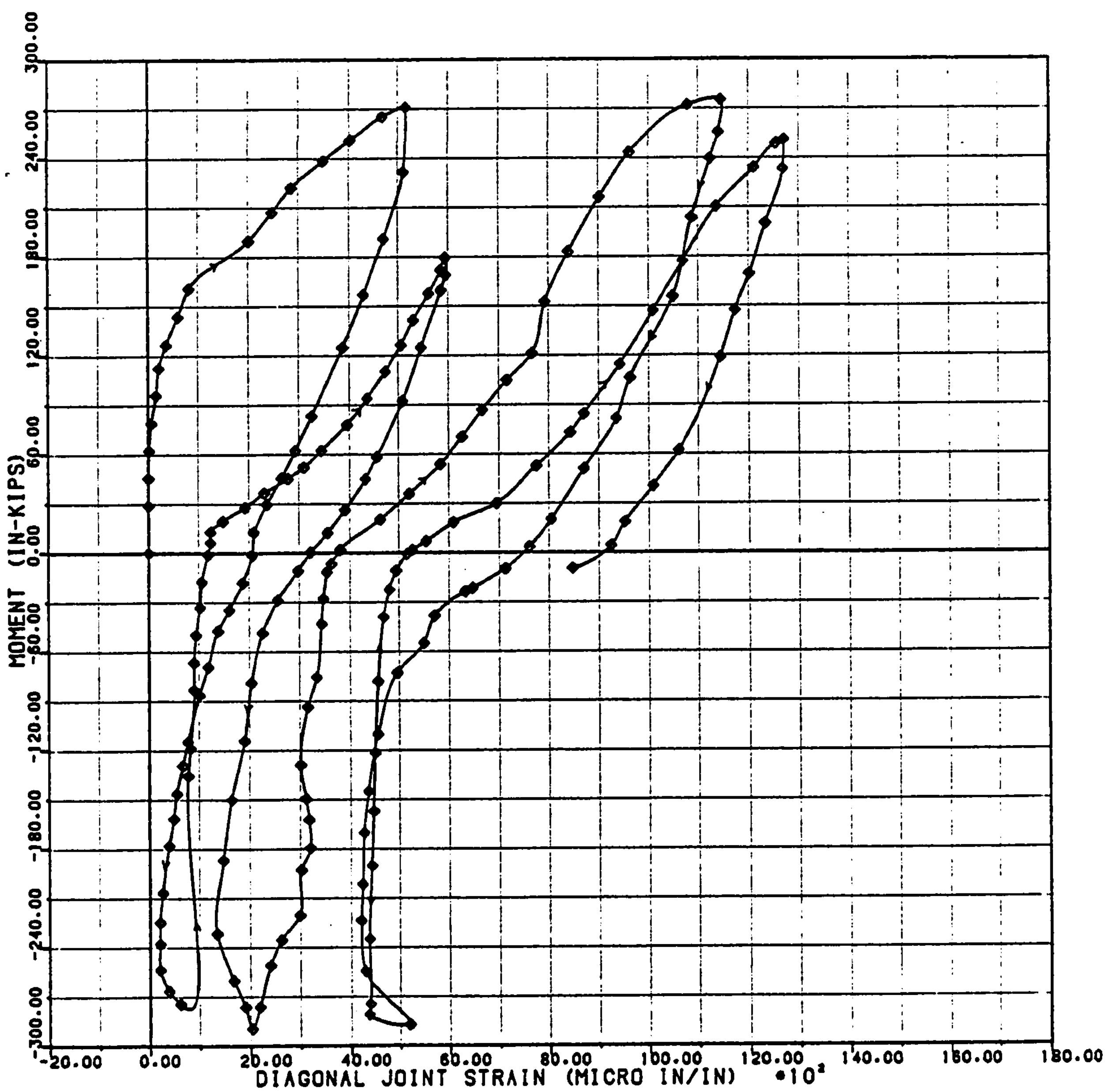

FIG. A16a DIAGONAL JOINT STRAIN(LT-RB) VERSUS JOINT MOMENT, SPECIMEN 4

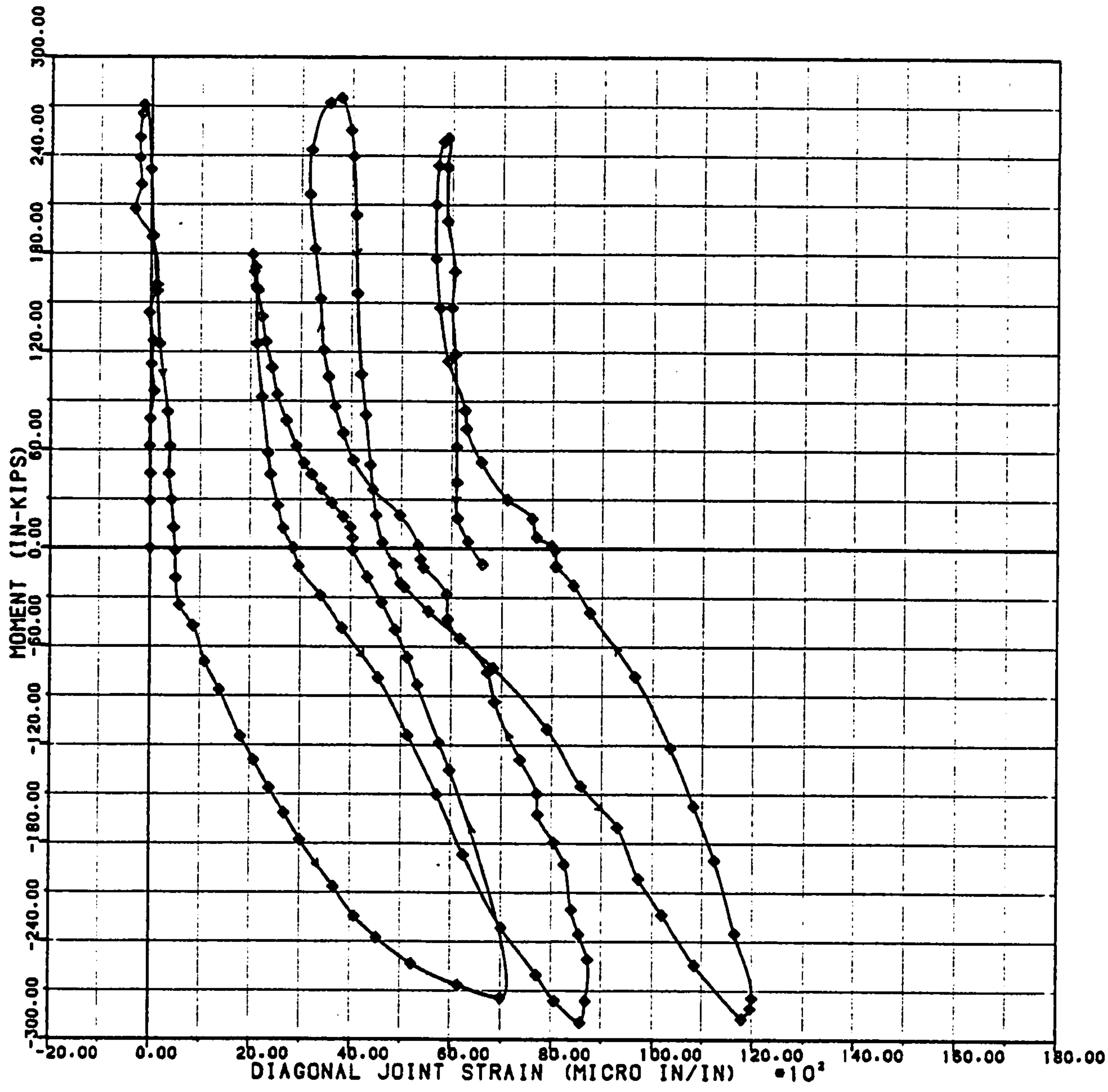

FIG. A16b DIAGONAL JOINT STRAIN(RT-LB) VERSUS JOINT MOMENT, SPECIMEN 4

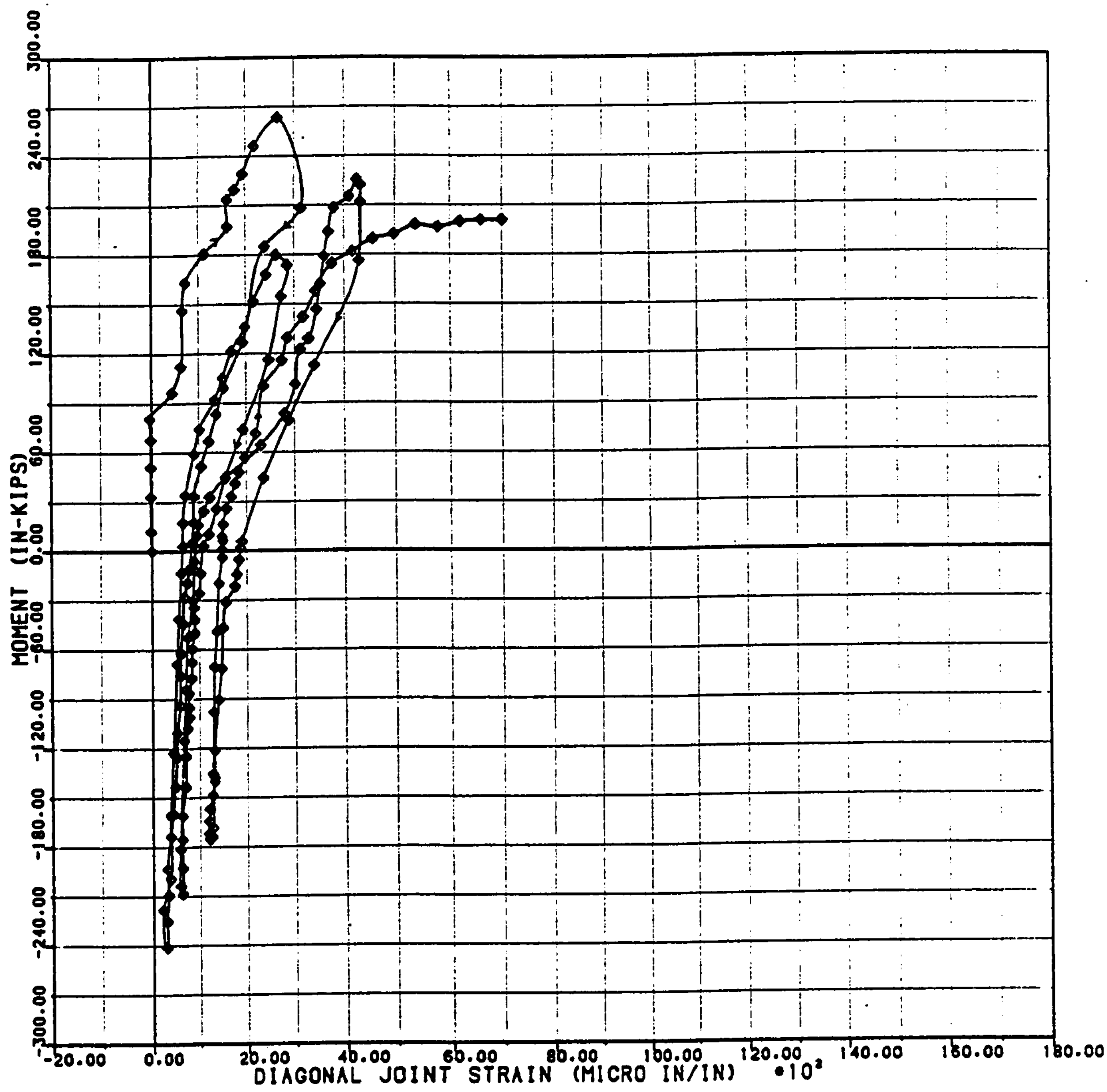

FIG. A17a DIAGONAL JOINT STRAIN(LT-RB) VERSUS JOINT MOMENT, SPECIMEN 5

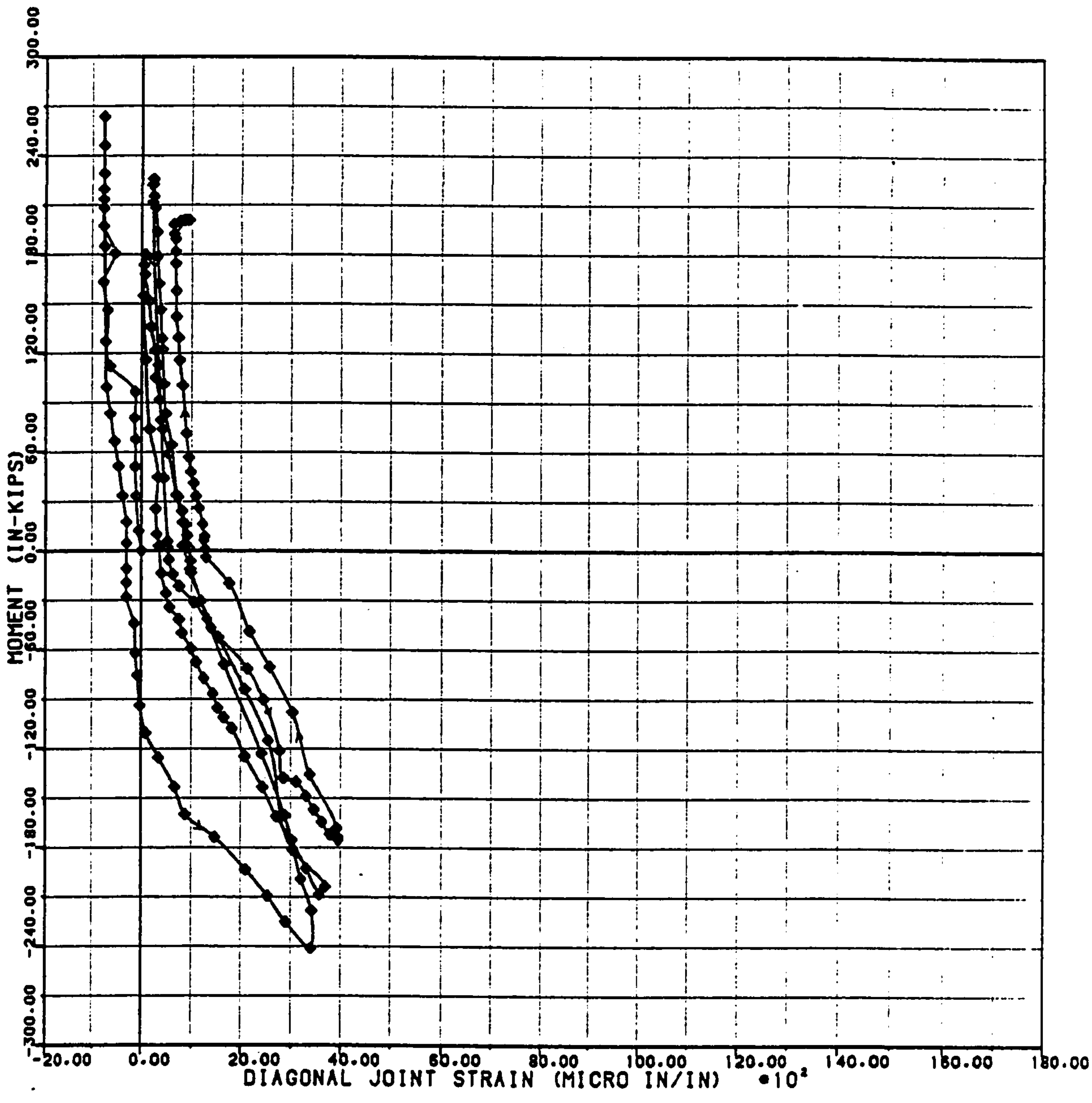

FIG. A17b DIAGONAL JOINT STRAIN(RT-LB) VERSUS JOINT MOMENT, SPECIMEN 5

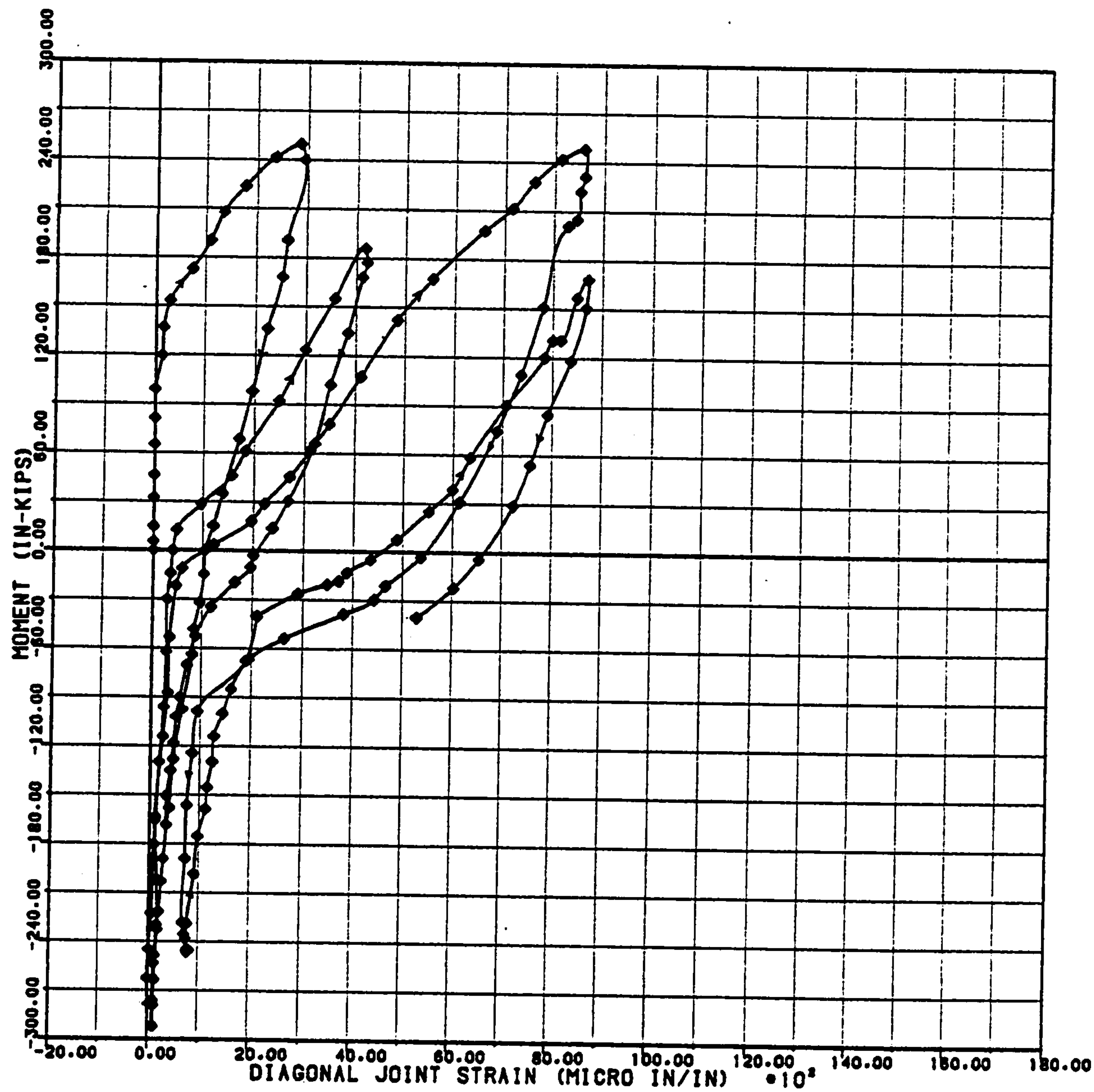

FIG. A18a DIAGONAL JOINT STRAIN (LT-RB) VERSUS JOINT MOMENT, SPECIMEN 6

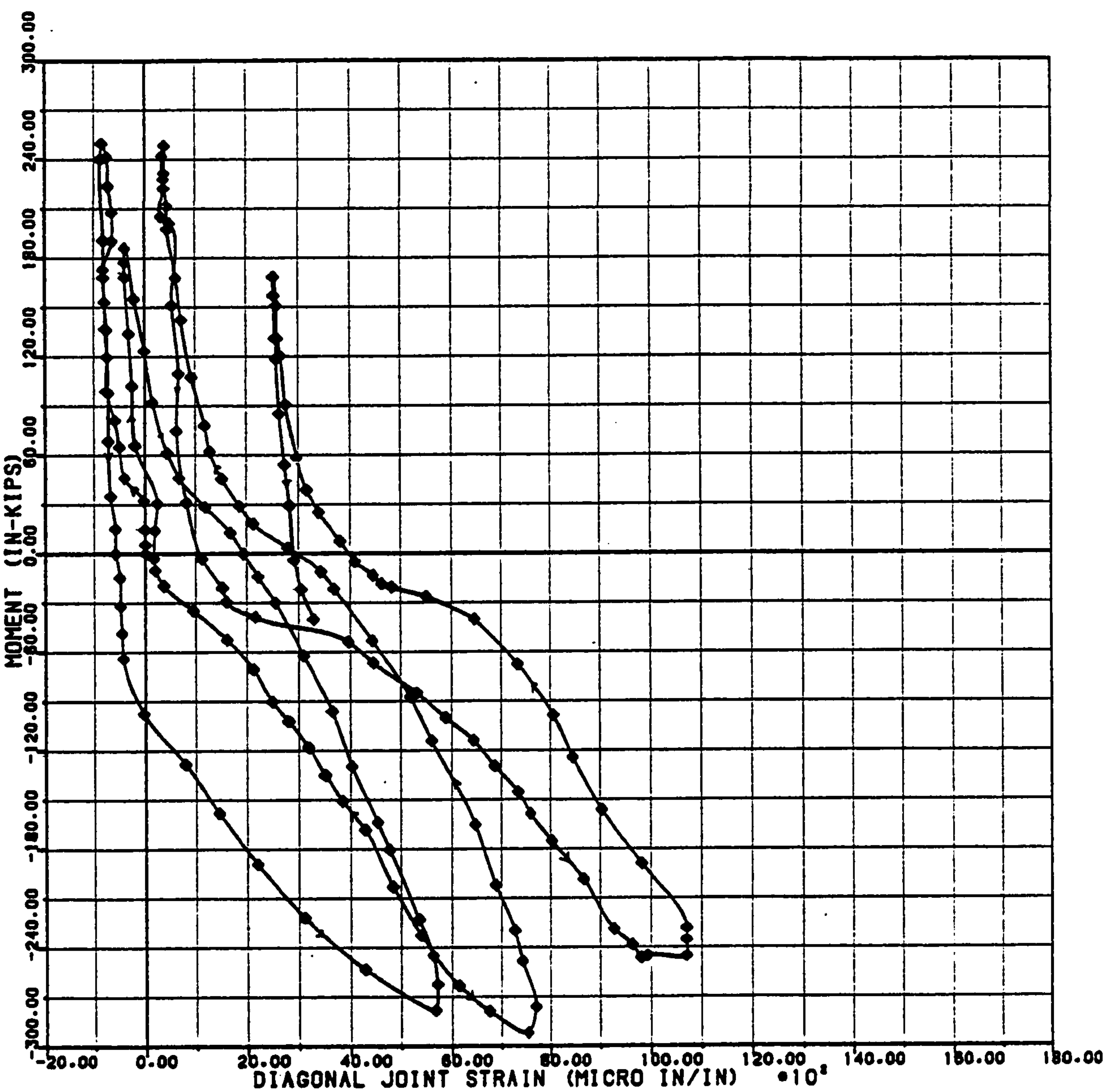

FIG. A18b DIAGONAL JOINT STRAIN (RT-LB) VERSUS JOINT MOMENT, SPECIMEN 6

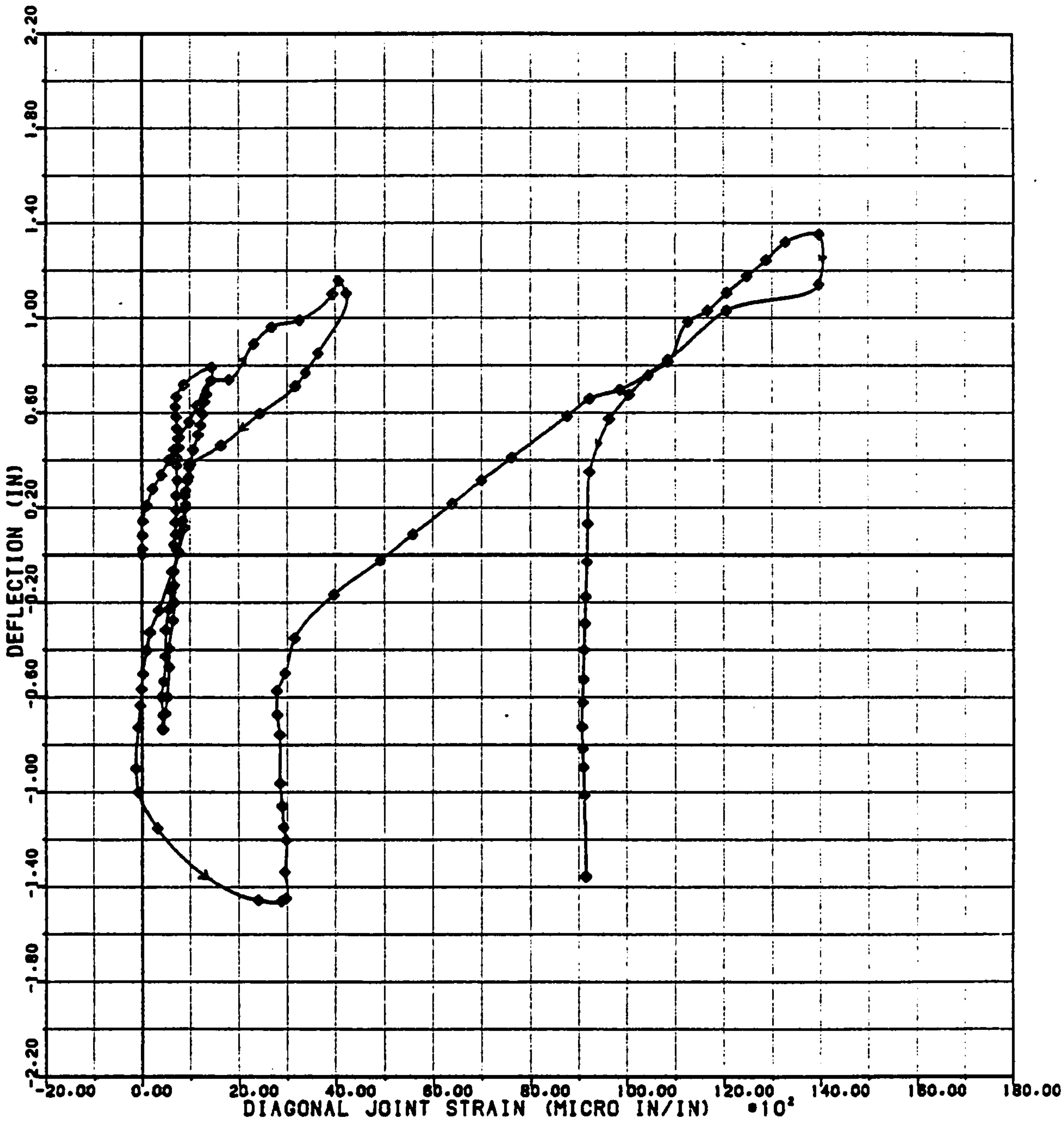

FIG. A 19a DIAGONAL JOINT STRAIN(LT-RB) VERSUS BEAM TIP DEFLECTION, SP.3

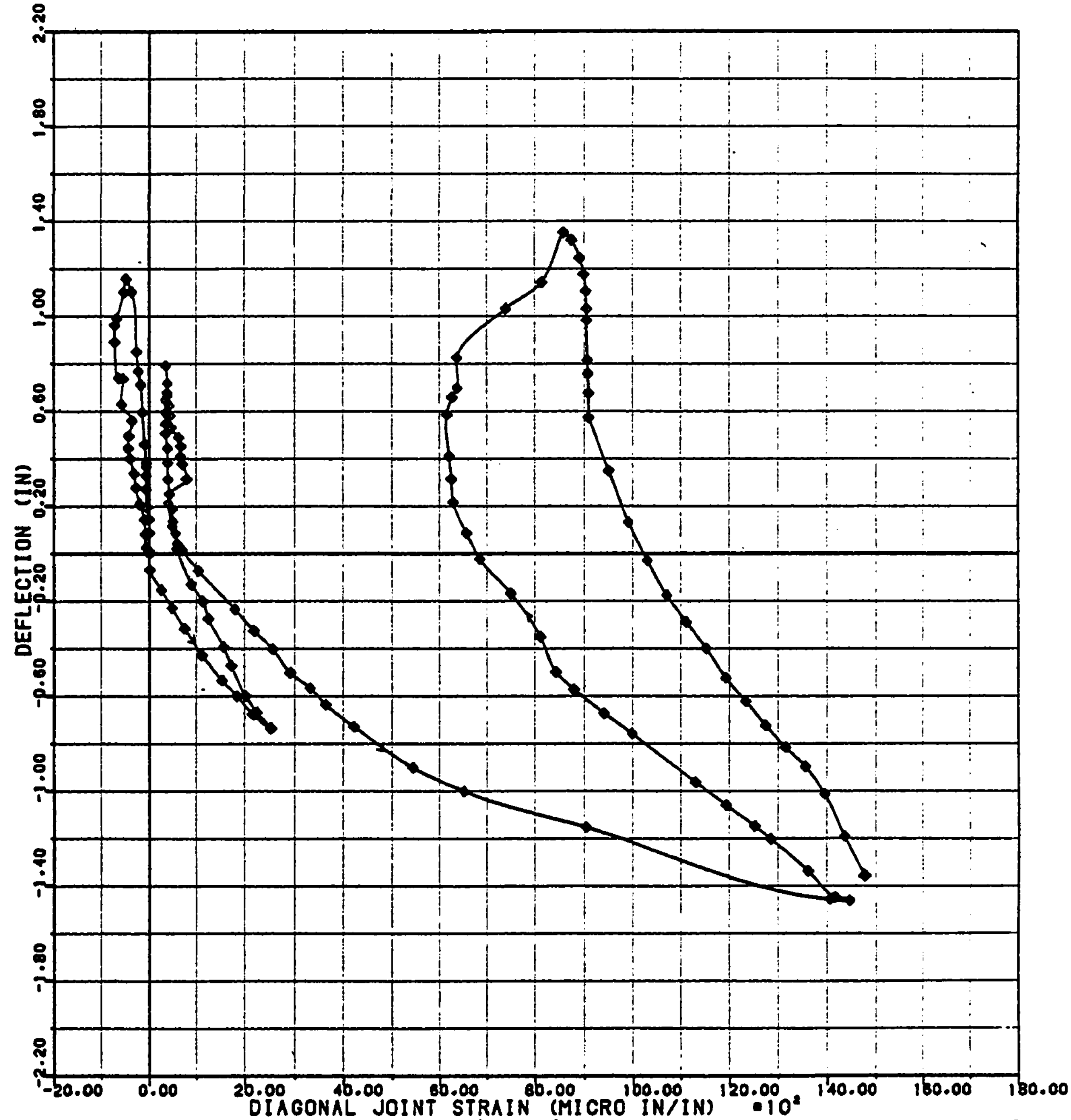

FIG A 19b DIAGONAL JOINT STRAIN(RT-LB) VERSUS BEAM TIP DEFLECTION, SP.3

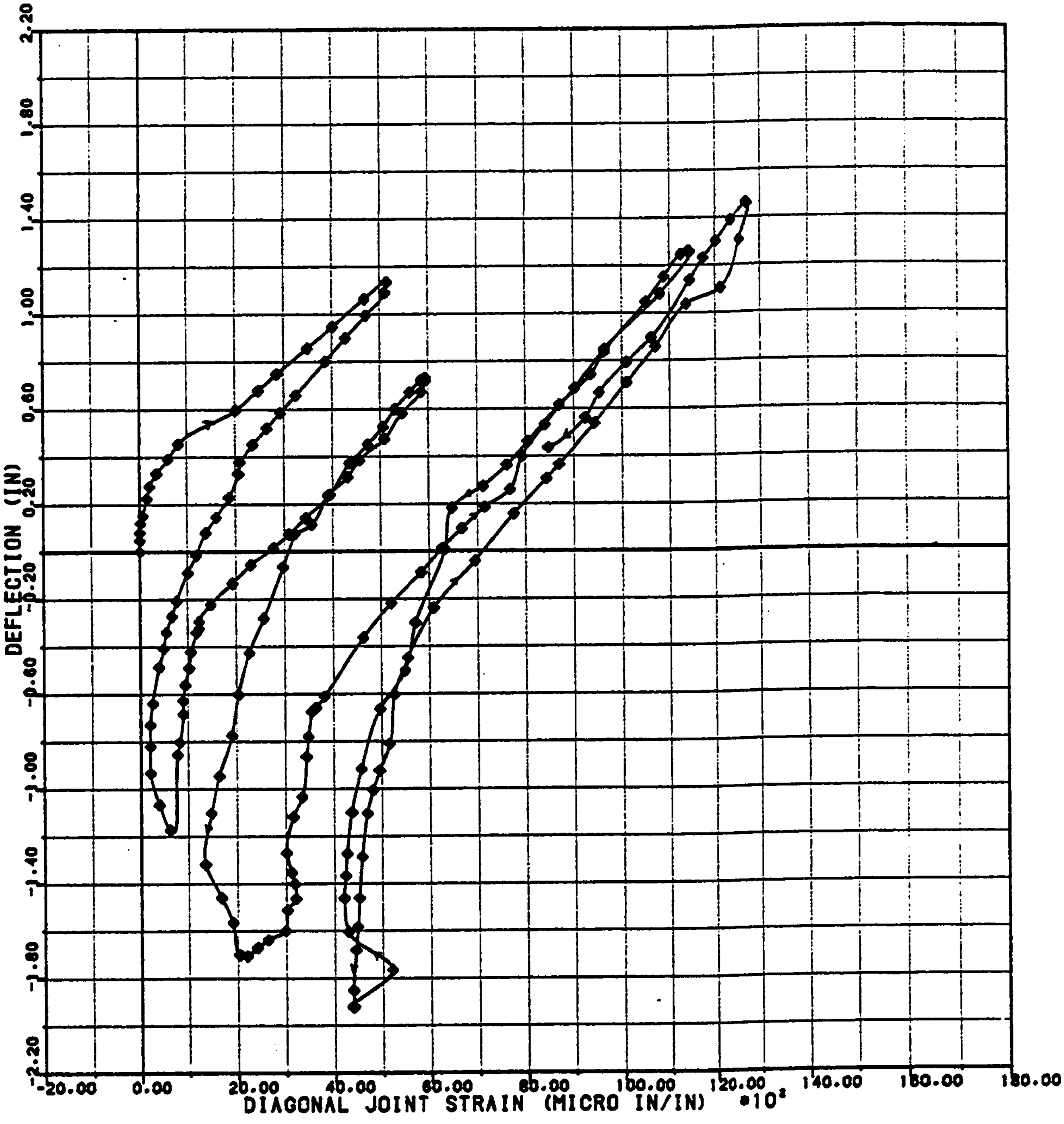

FIG. A20a DIAGONAL JOINT STRAIN(LT-RB) VERSUS BEAM TIP DEFLECTION, SP.4

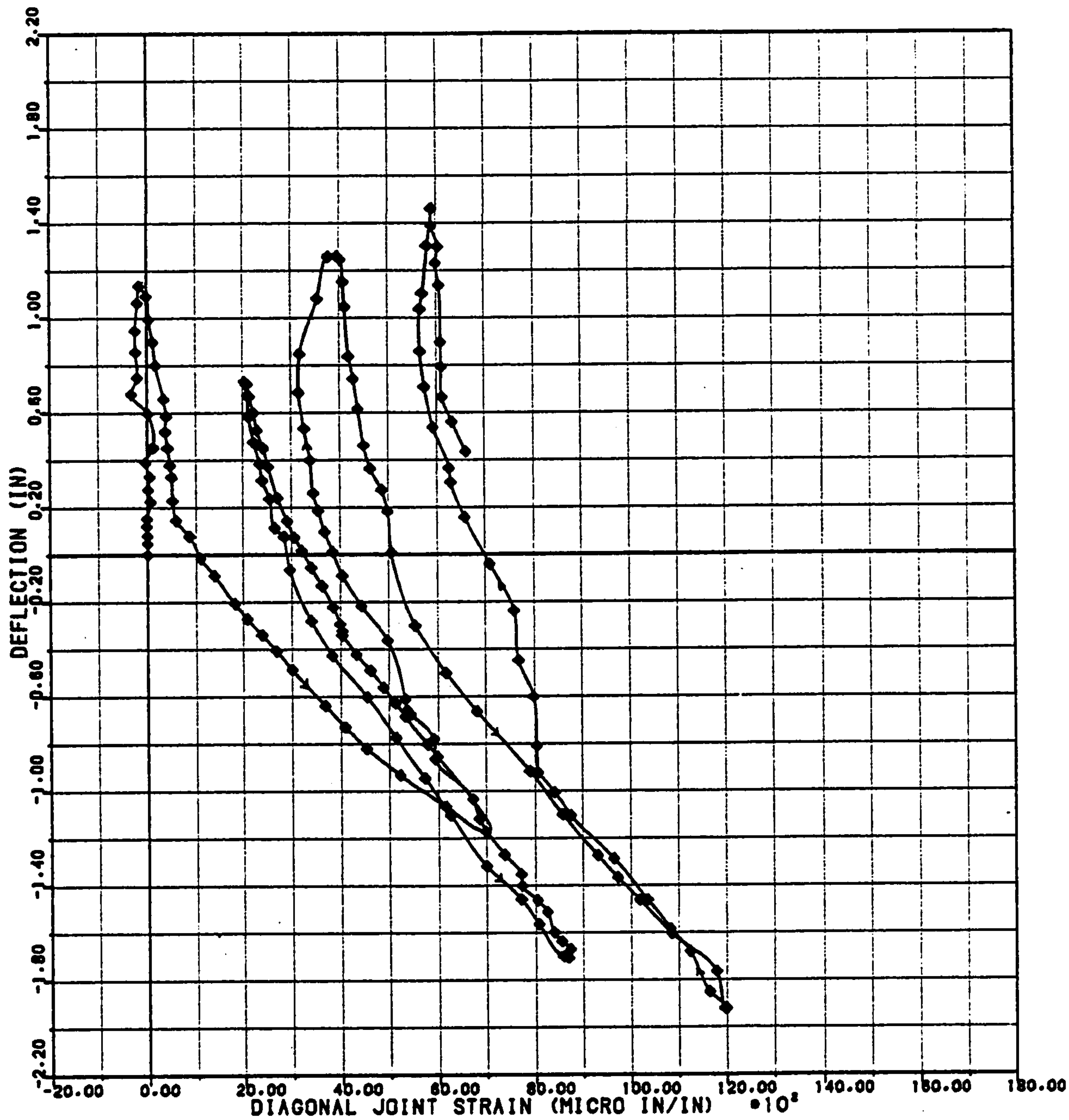

FIG. A20b DIAGONAL JOINT STRAIN(RT-LB) VERSUS BEAM TIP DEFLECTION,SP.4

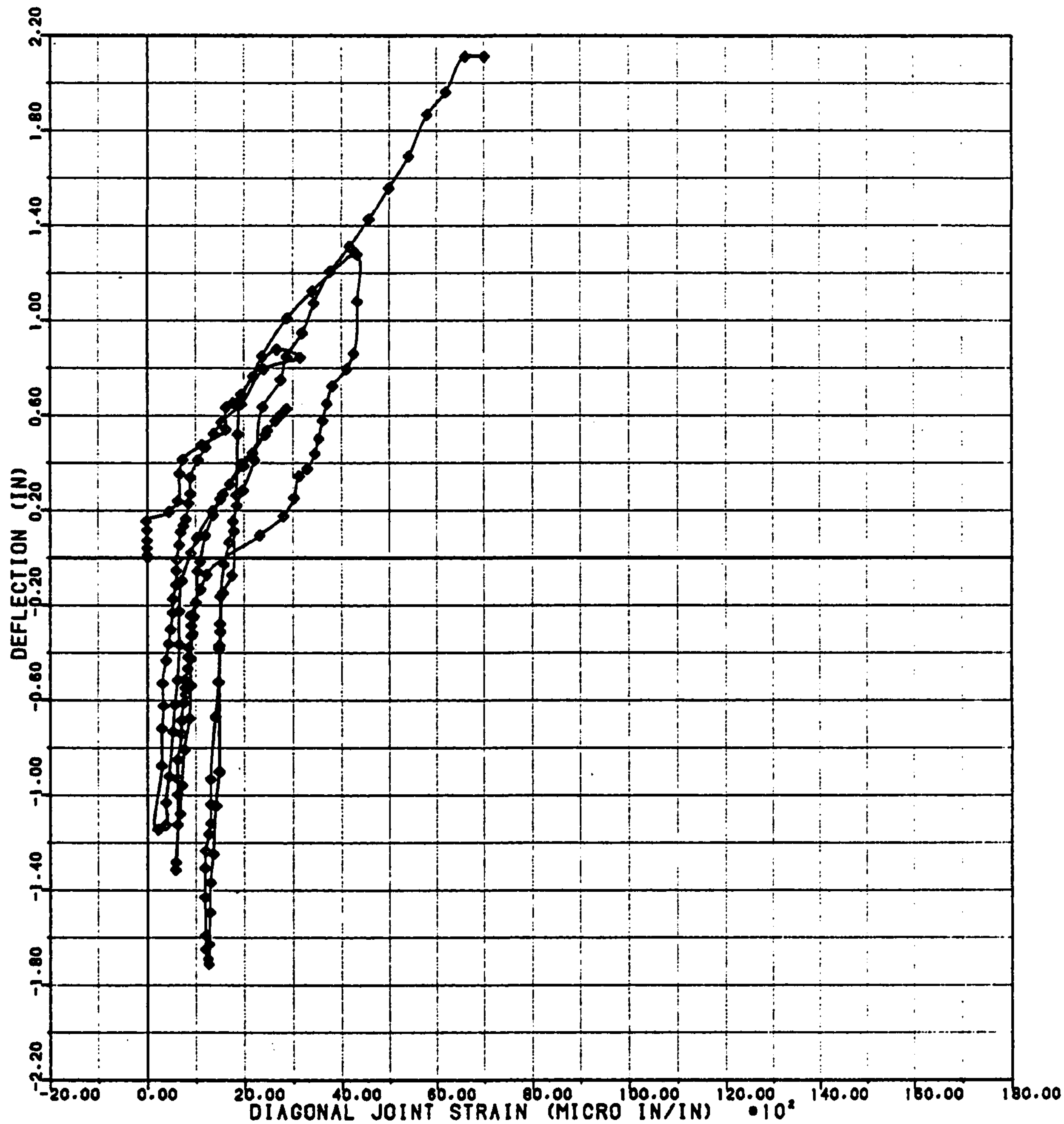

FIG. A 21a   DIAGONAL JOINT STRAIN(LT-RB) VERSUS BEAM TIP DEFLECTION, SP.5

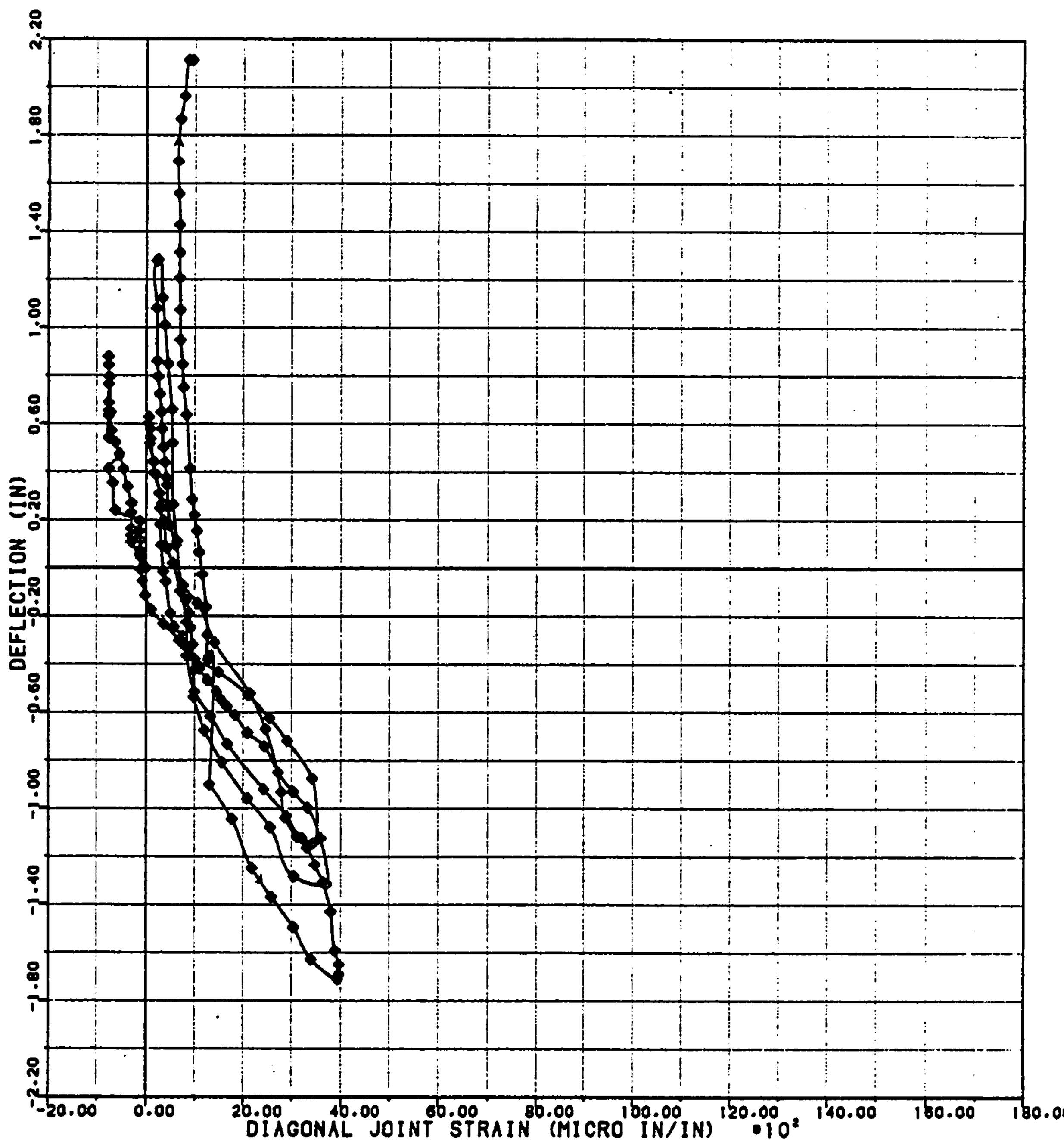

FIG. A21b DIAGONAL JOINT STRAIN(RT-LB) VERSUS BEAM TIP DEFLECTION, SP.5

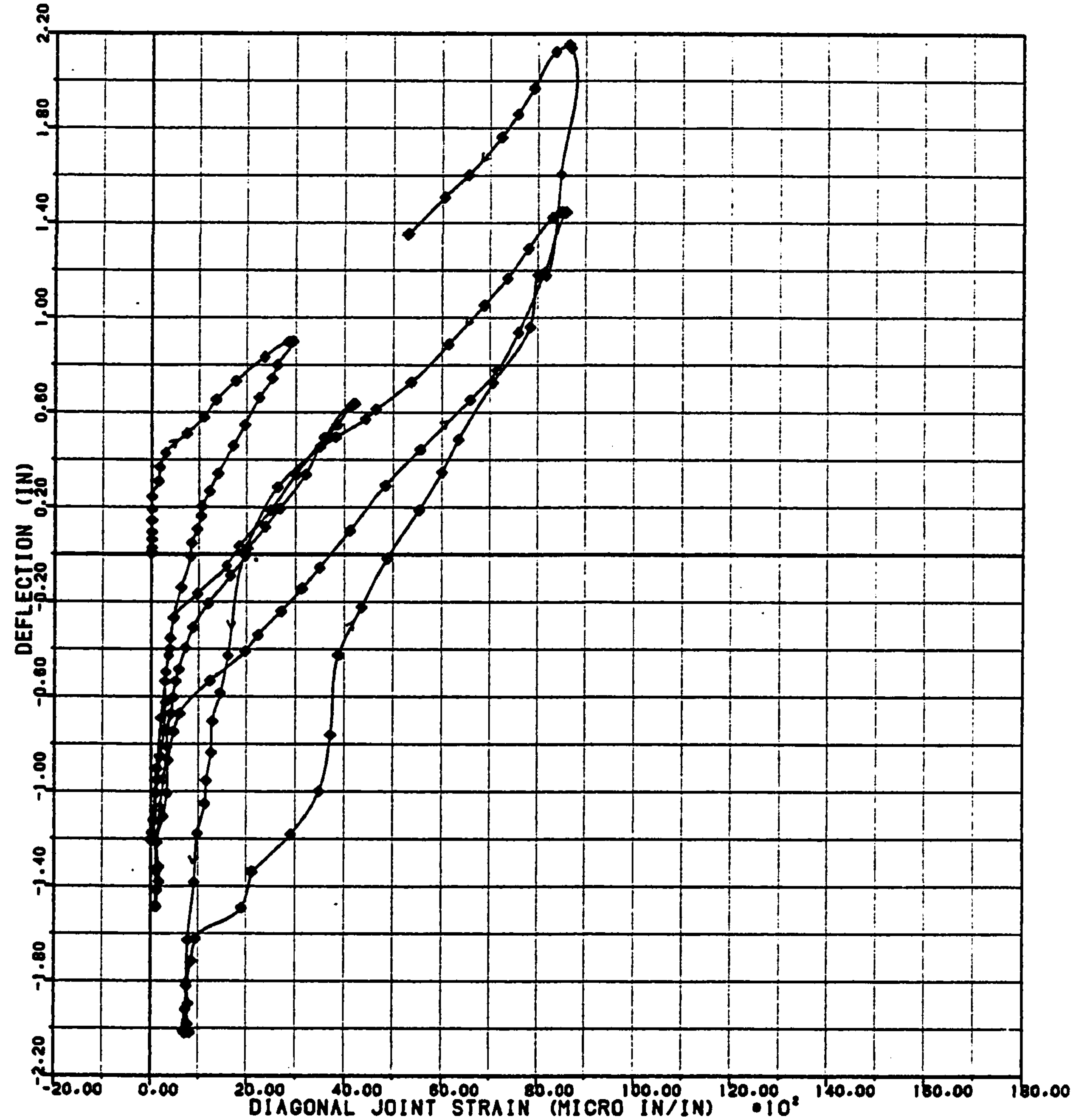

FIG. A22a DIAGONAL JOINT STRAIN(LT-RB) VERSUS BEAM TIP DEFLECTION, SP.6

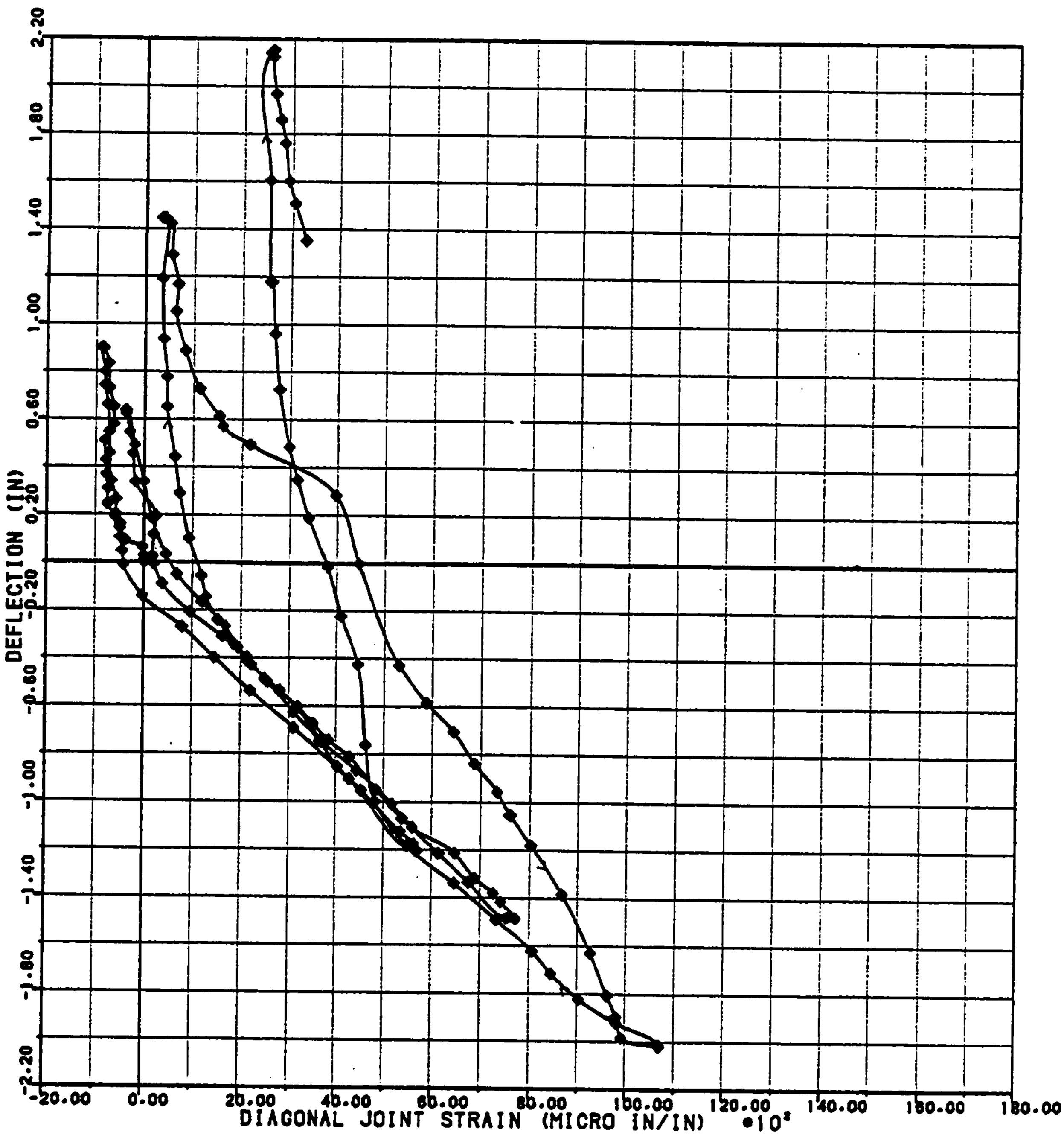

FIG. A22b DIAGONAL JOINT STRAIN(RT-LB) VERSUS BEAM TIP DEFLECTION, SP.6

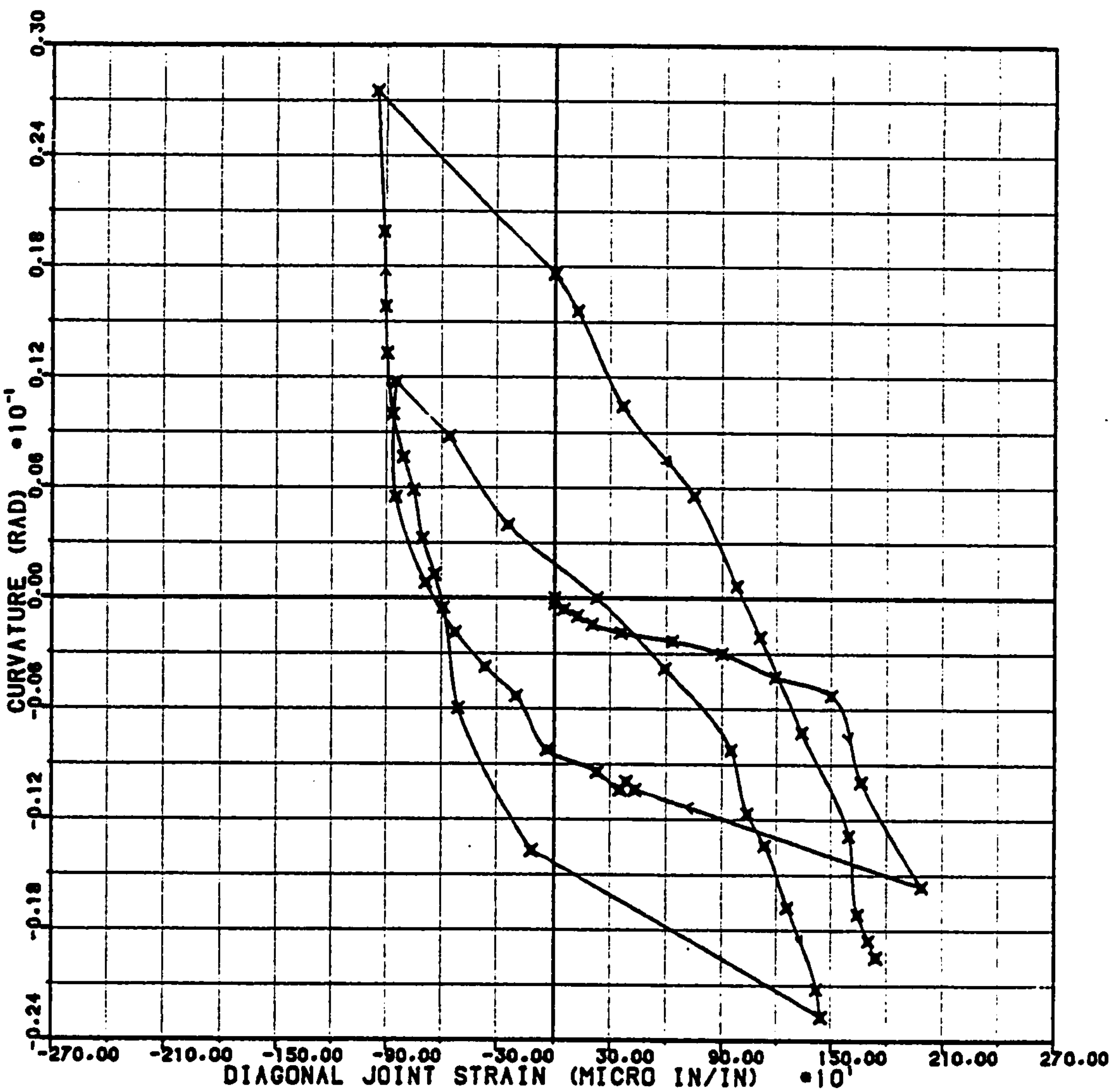

FIG. A23a DIAGONAL JOINT STRAIN(LT-RB) VERSUS BEAM CURVATURE, SPECIMEN 1

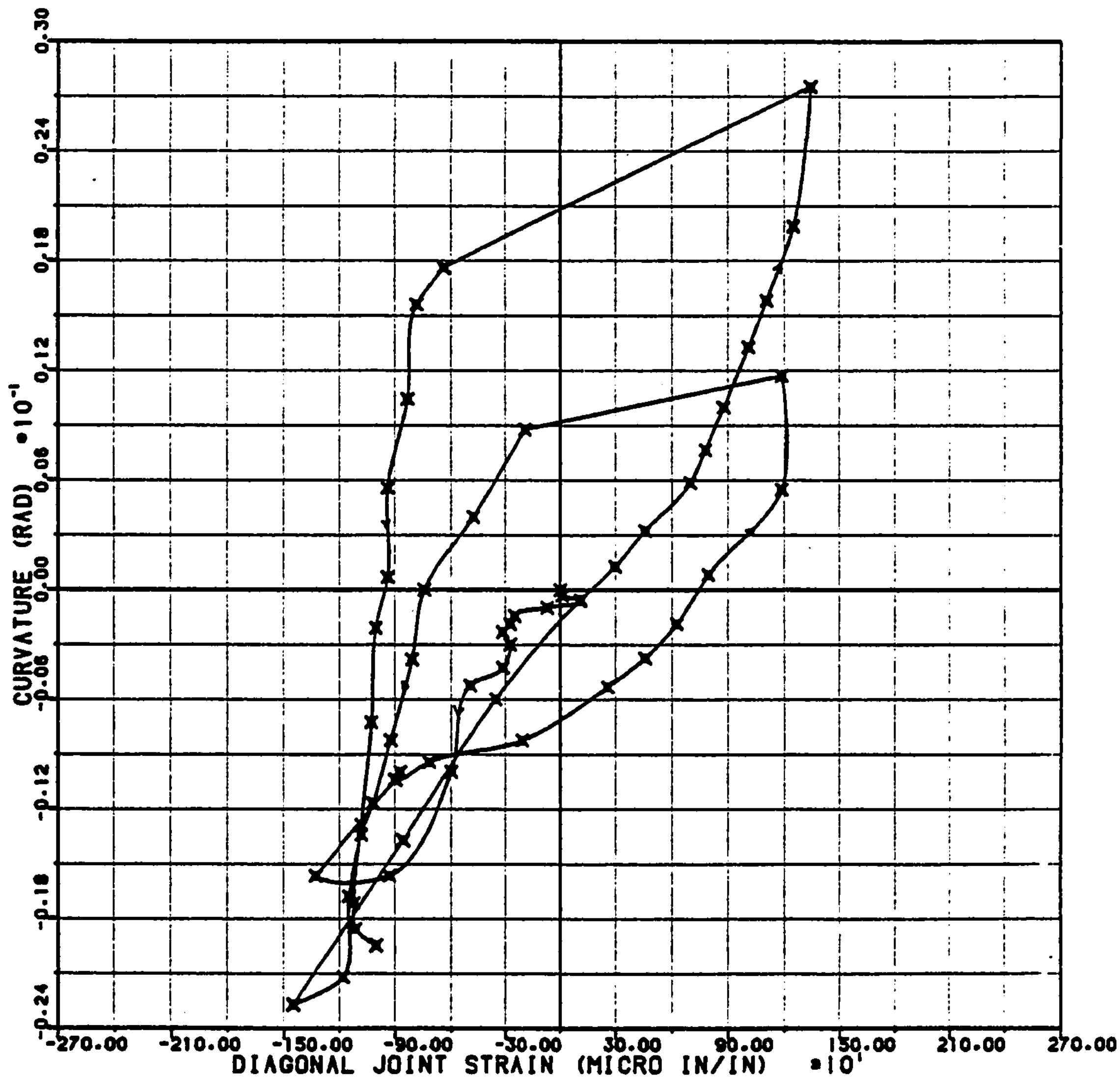

FIG. A23b DIAGONAL JOINT STRAIN(RT-LB) VERSUS BEAM CURVATURE, SPECIMEN 1

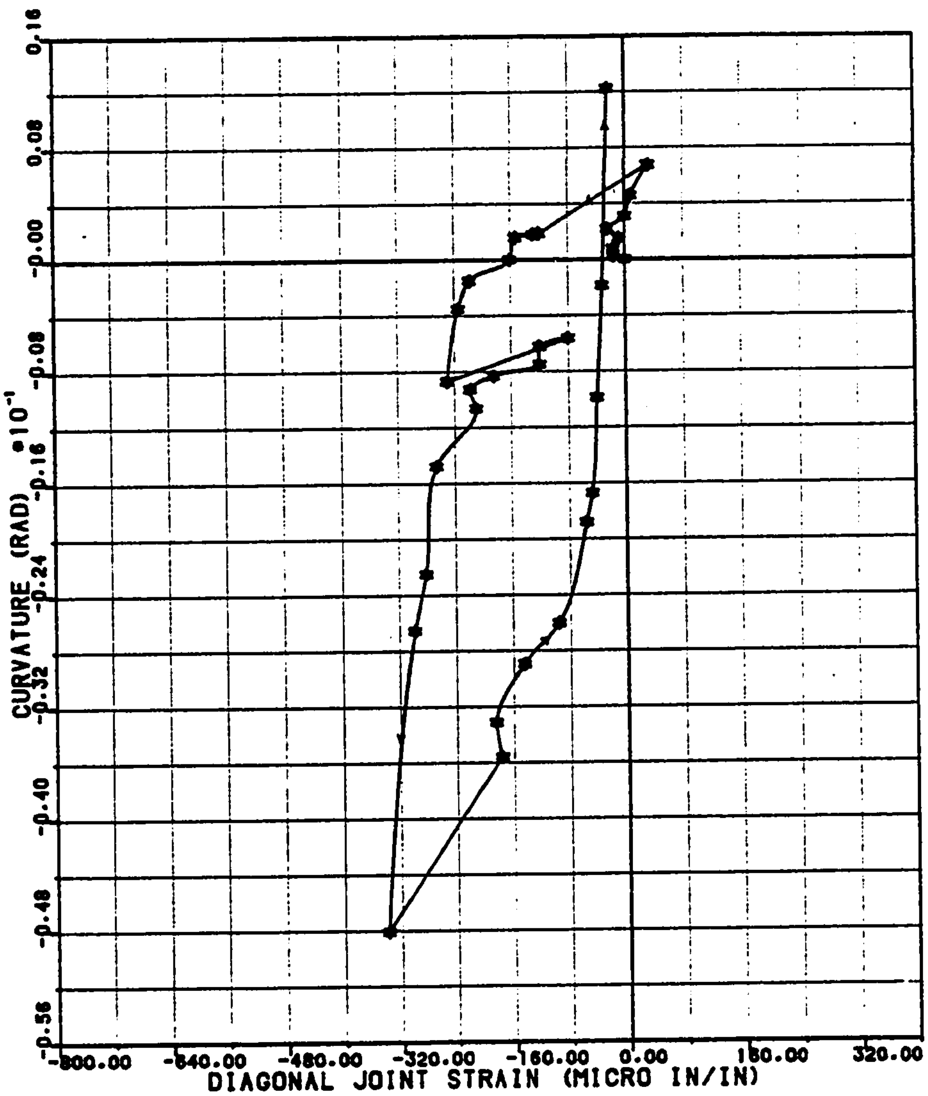

FIG. A24a DIAGONAL JOINT STRAIN(LT-RB) VERSUS BEAM CURVATURE, SPECIMEN 2

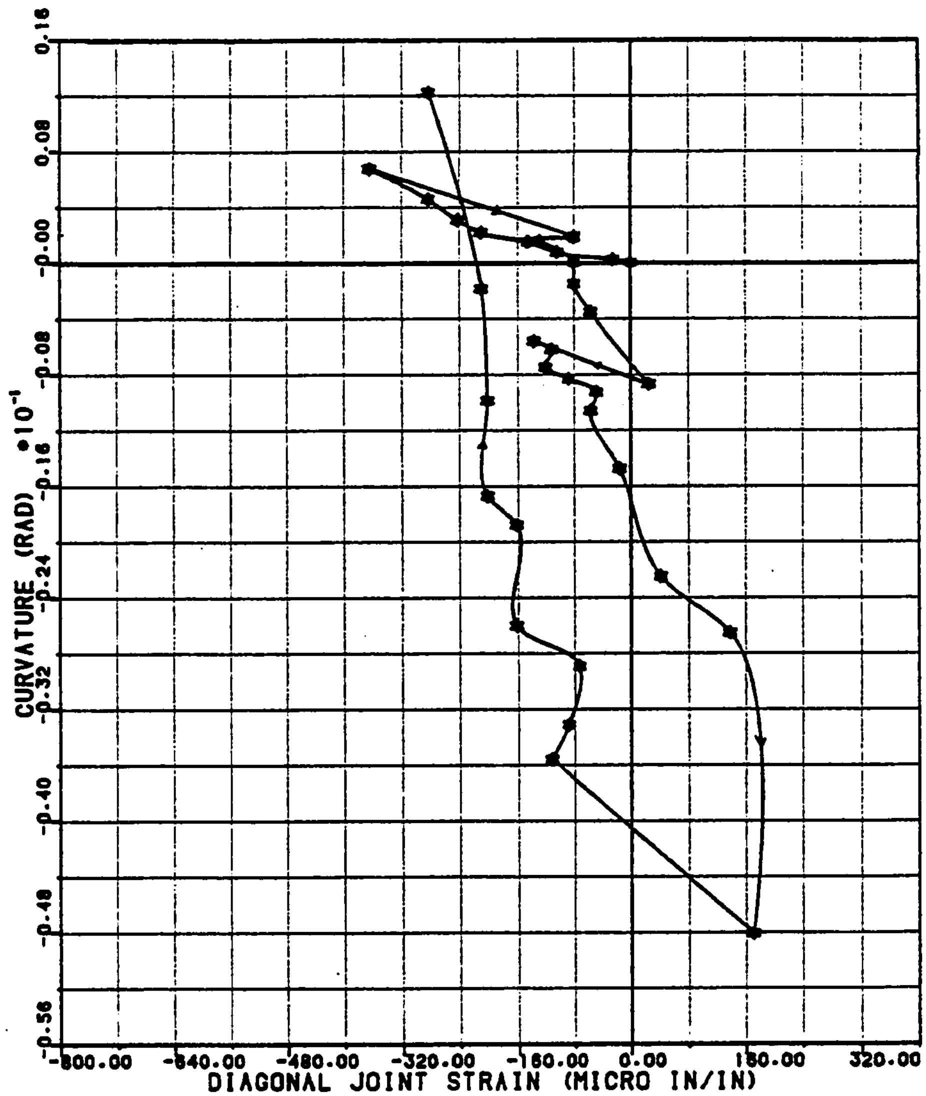

FIG. A24b DIAGONAL JOINT STRAIN(RT-LB) VERSUS BEAM CURVATURE, SPECIMEN 2

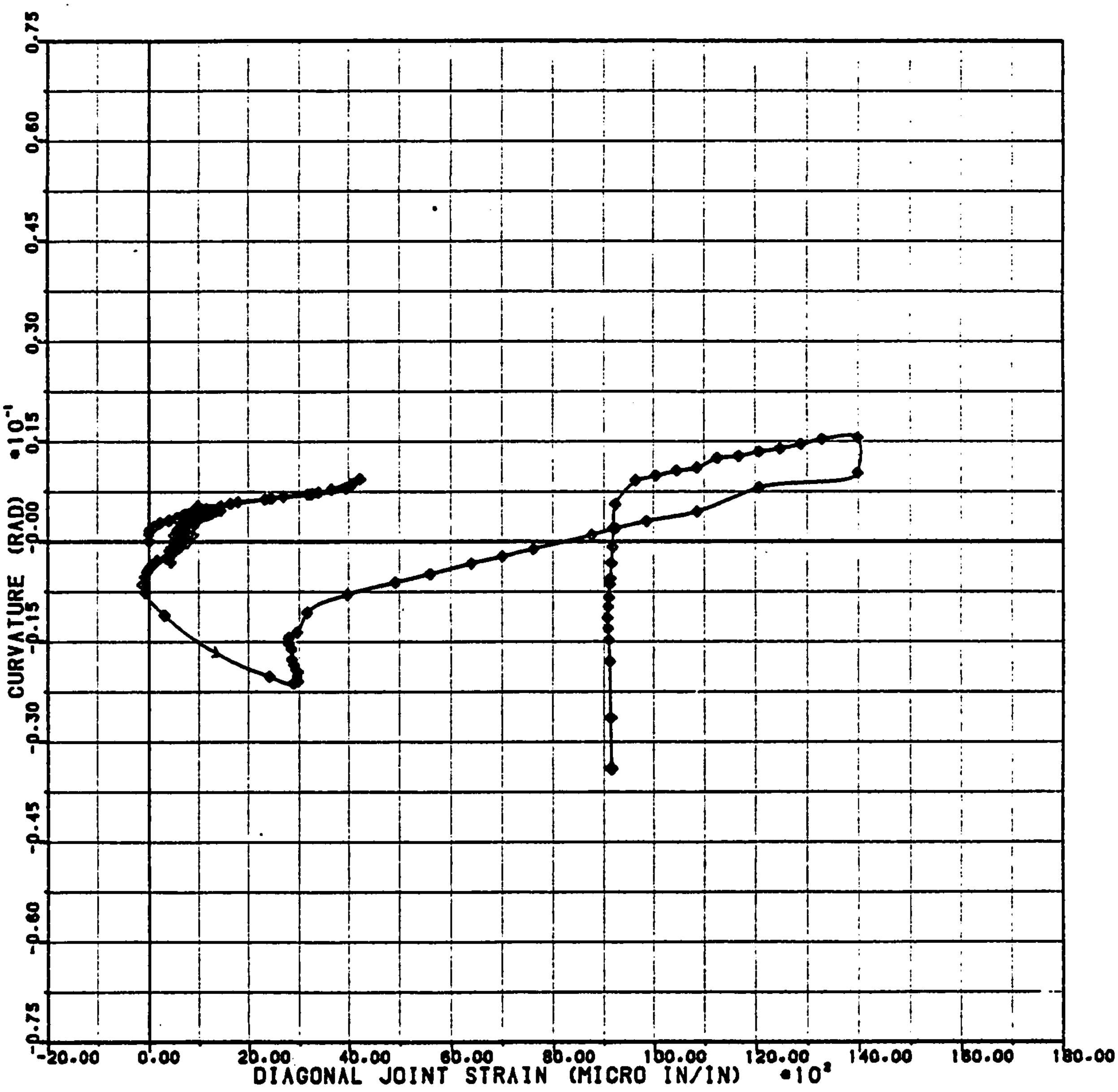

FIG. A25a DIAGONAL JOINT STRAIN(LT-RB) VERSUS BEAM CURVATURE, SPECIMEN 3

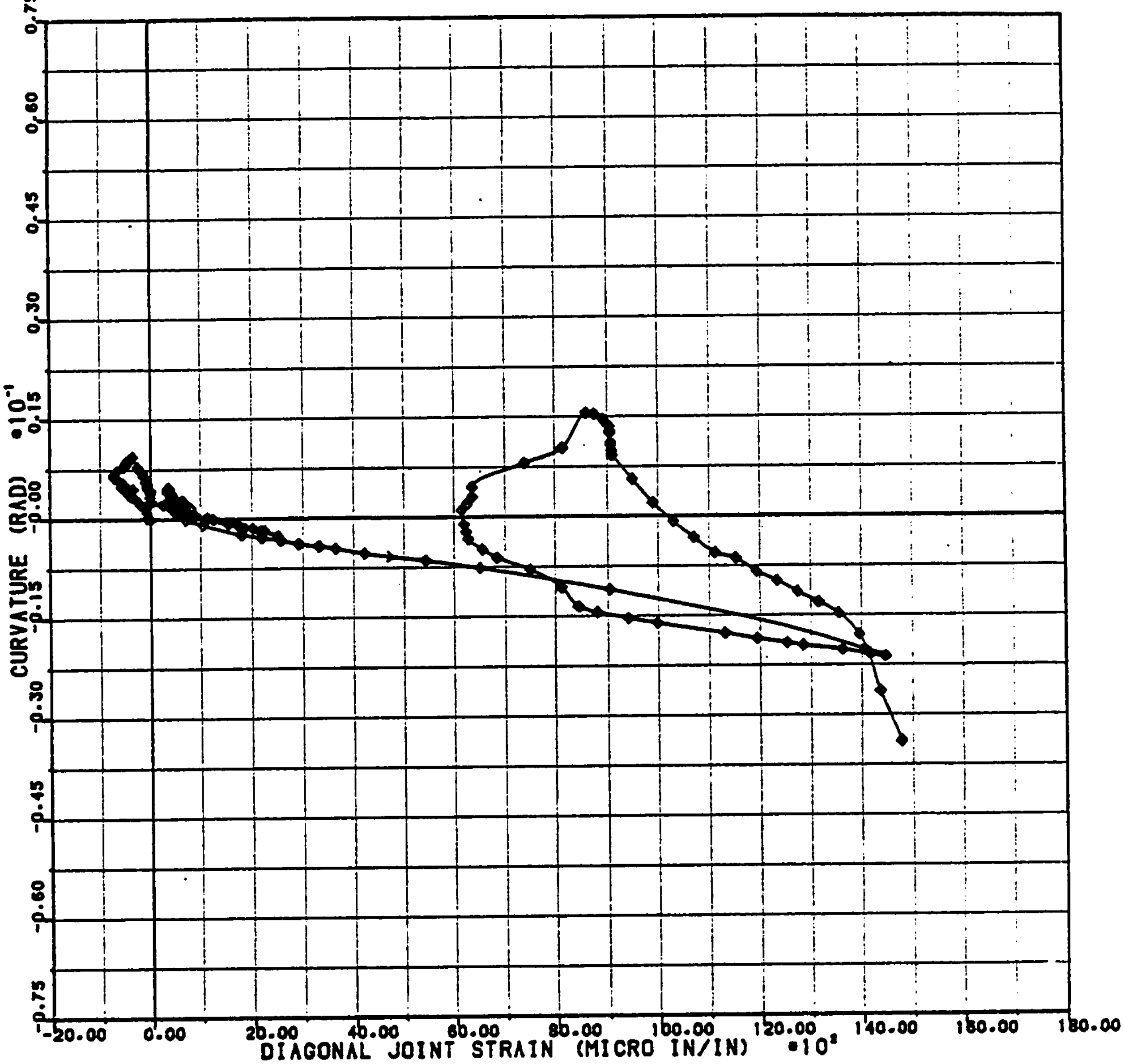

FIG. A25b DIAGONAL JOINT STRAIN(RT-LB) VERSUS BEAM CURVATURE, SPECIMEN 3

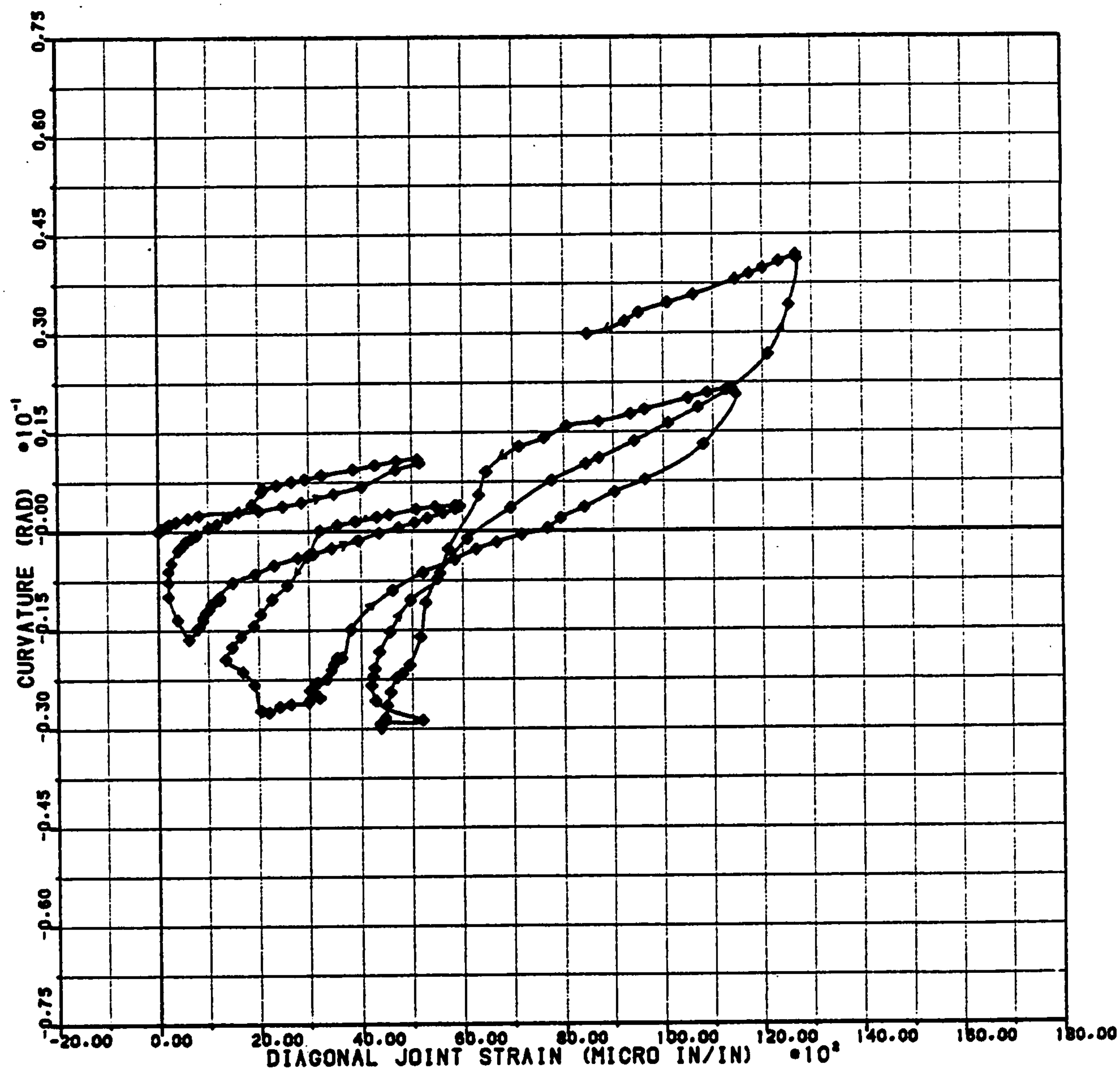

FIG. A26a DIAGONAL JOINT STRAIN(LT-RB) VERSUS BEAM CURVATURE, SPECIMEN 4

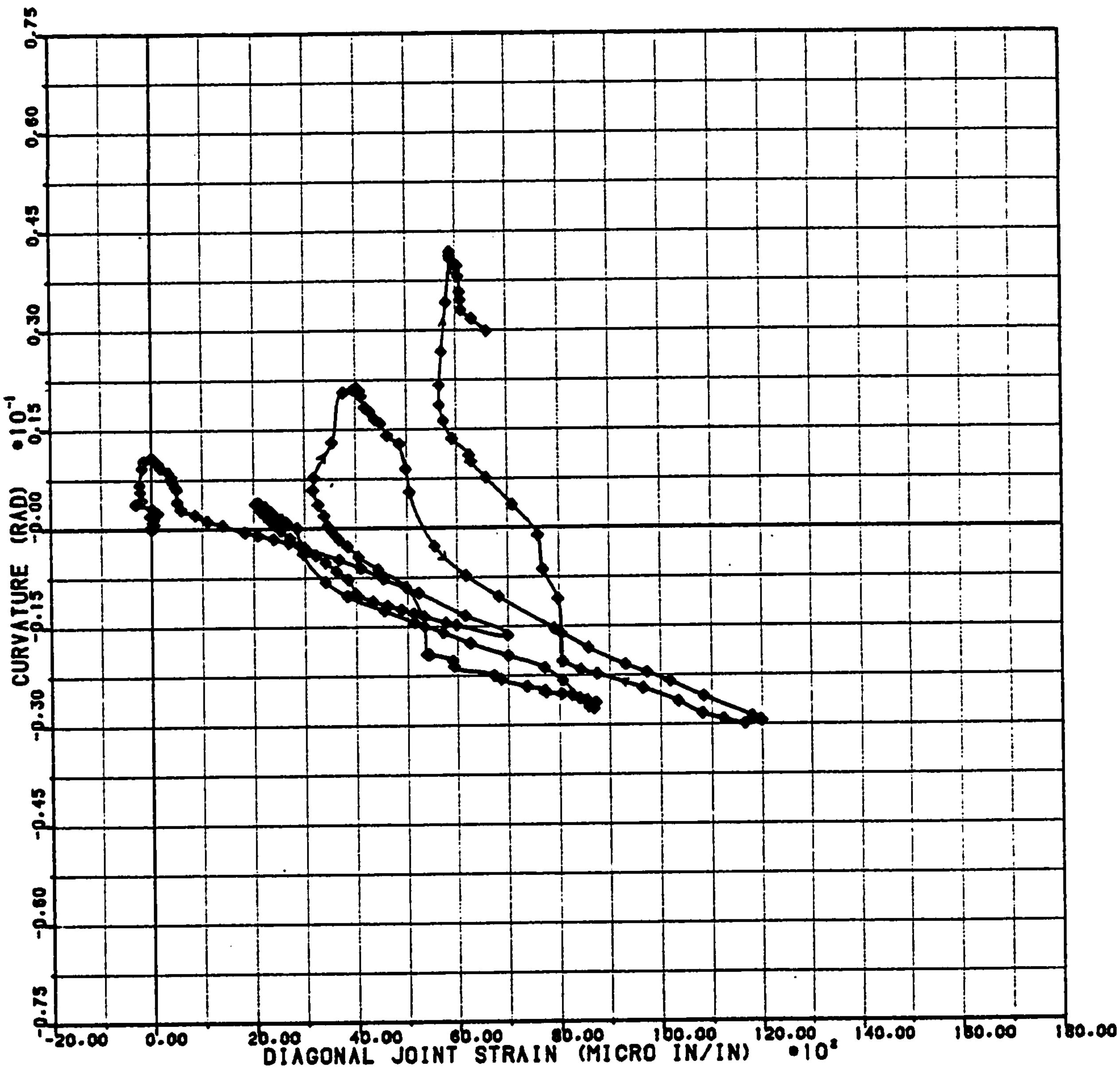

FIG. A26b DIAGONAL JOINT STRAIN(RT-LB) VERSUS BEAM CURVATURE, SPECIMEN 4

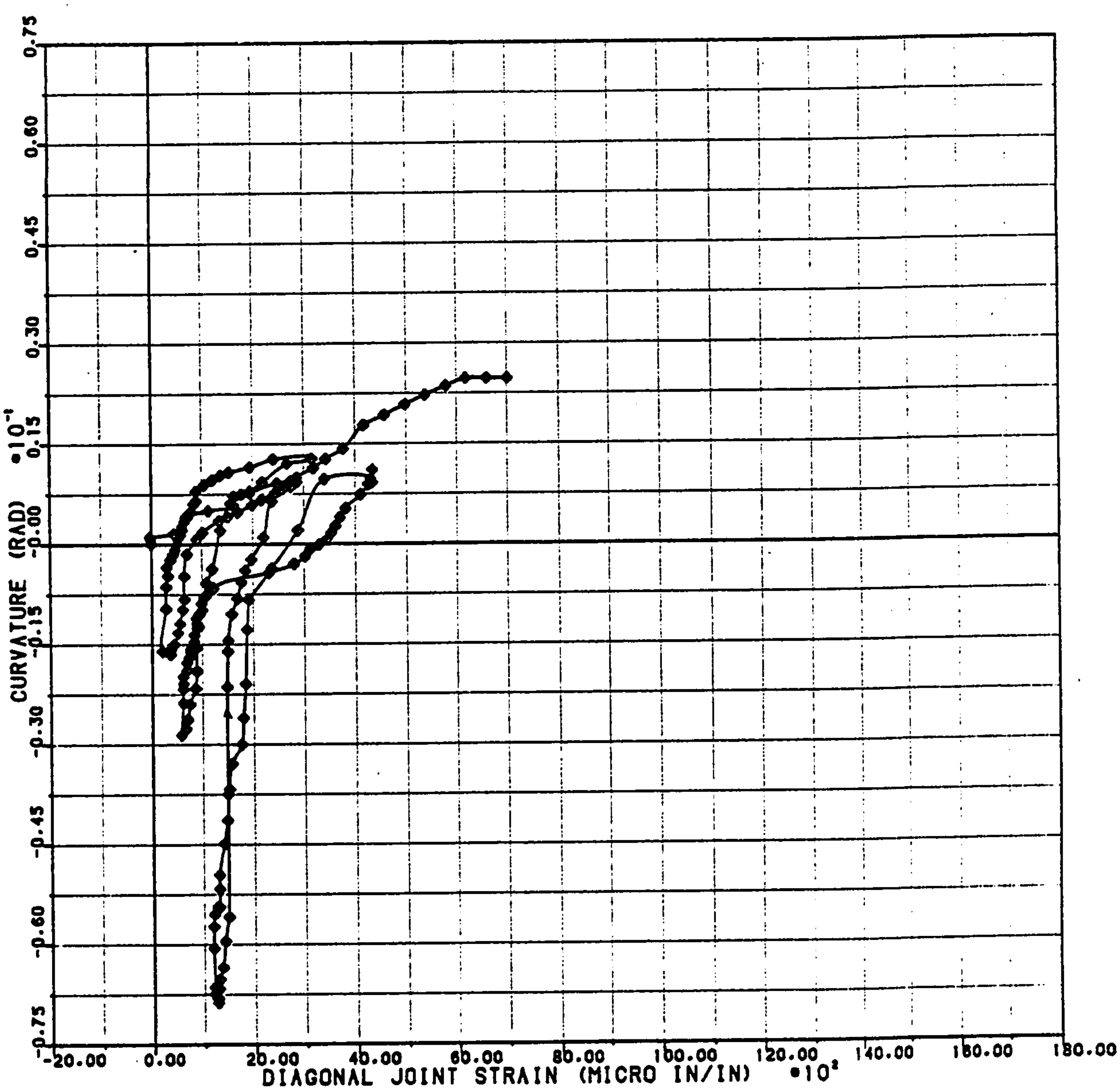

FIG. A27a DIAGONAL JOINT STRAIN(LT-RB) VERSUS BEAM CURVATURE, SPECIMEN 5

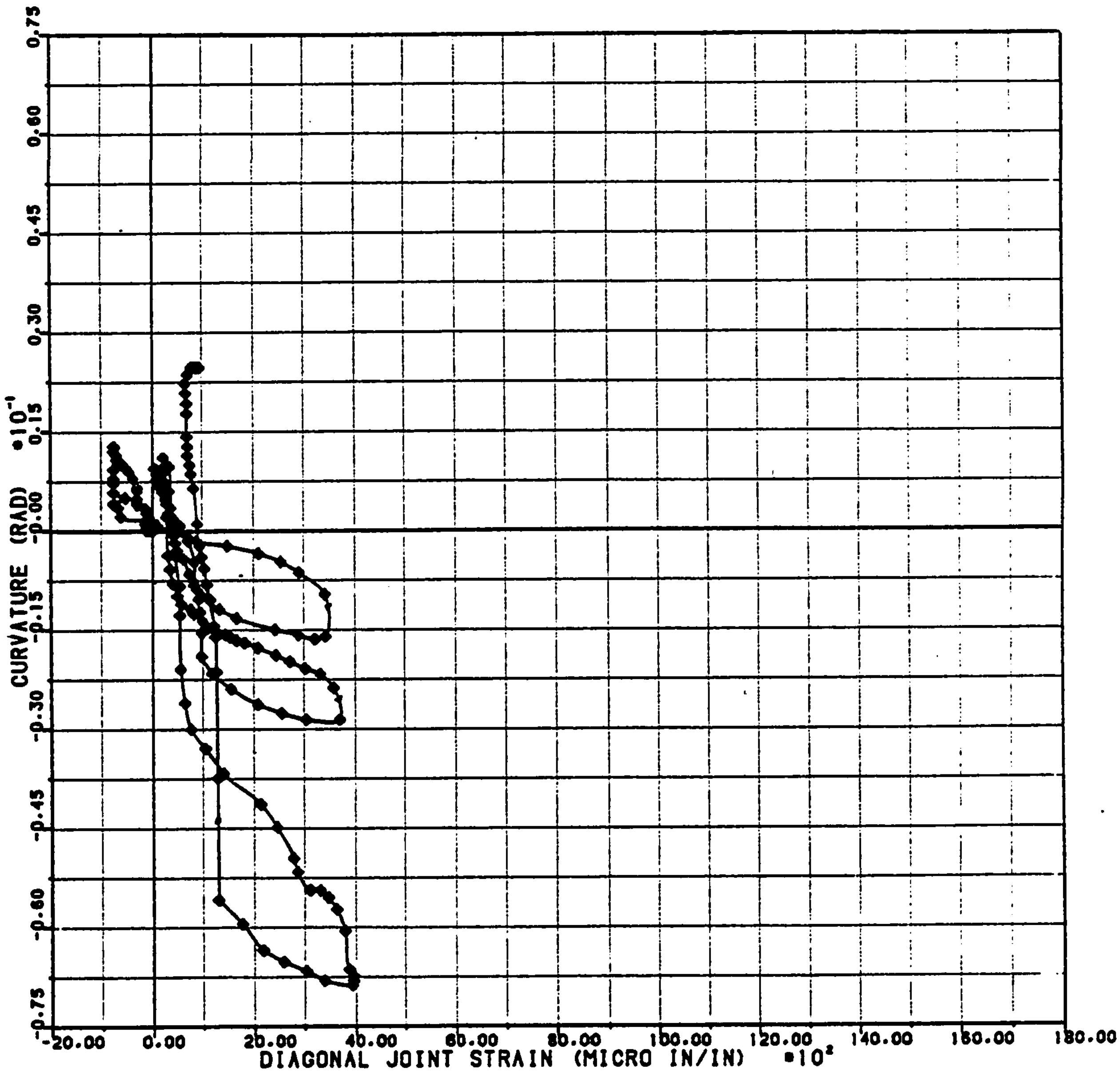

FIG. A27b DIAGONAL JOINT STRAIN(RT-LB) VERSUS BEAM CURVATURE, SPECIMEN 5

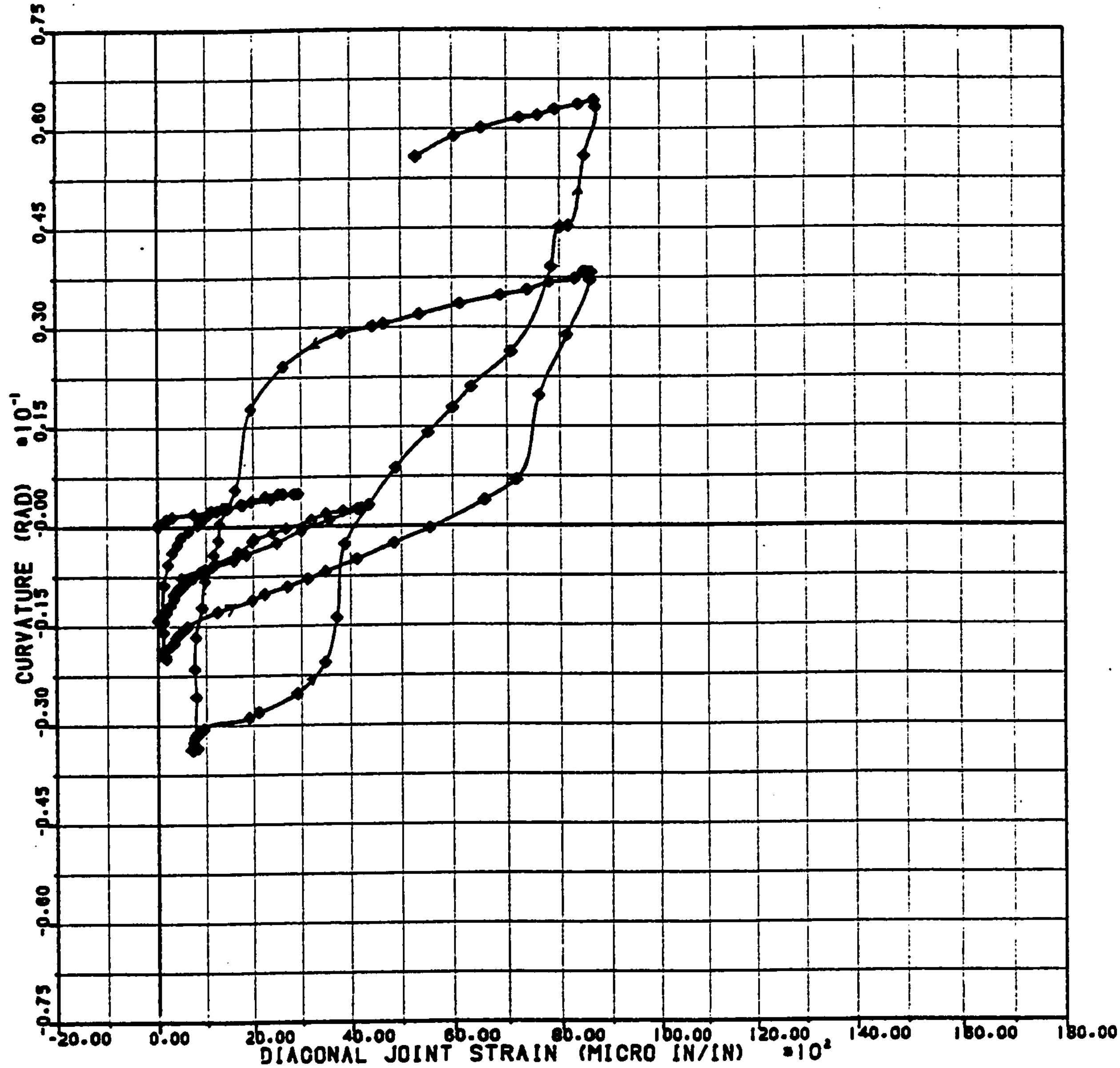

FIG. A28a DIAGONAL JOINT STRAIN(LT-RB) VERSUS BEAM CURVATURE, SPECIMEN 6

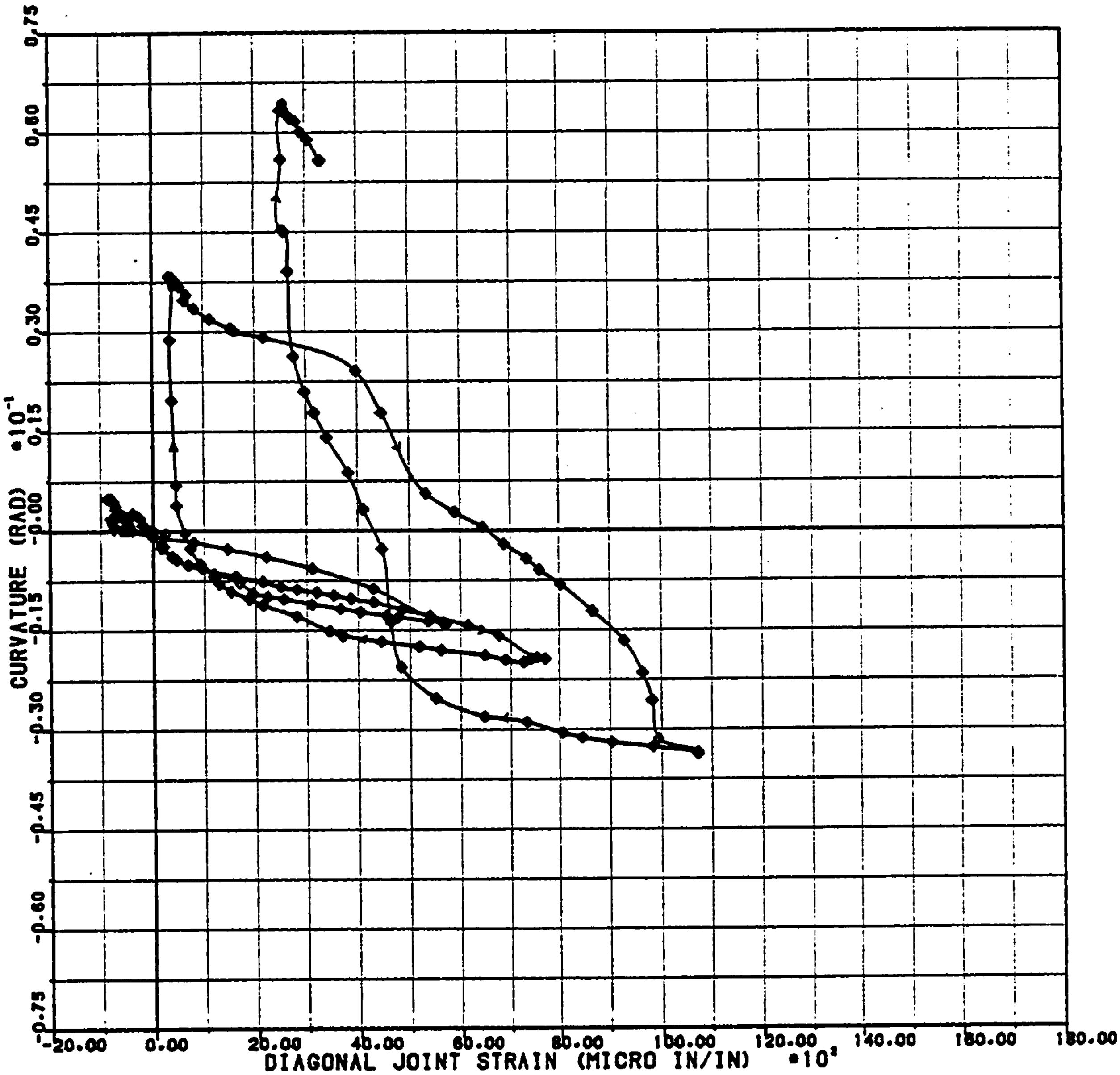

FIG. A28b DIAGONAL JOINT STRAIN(RT-LB) VERSUS BEAM CURVATURE, SPECIMEN 6

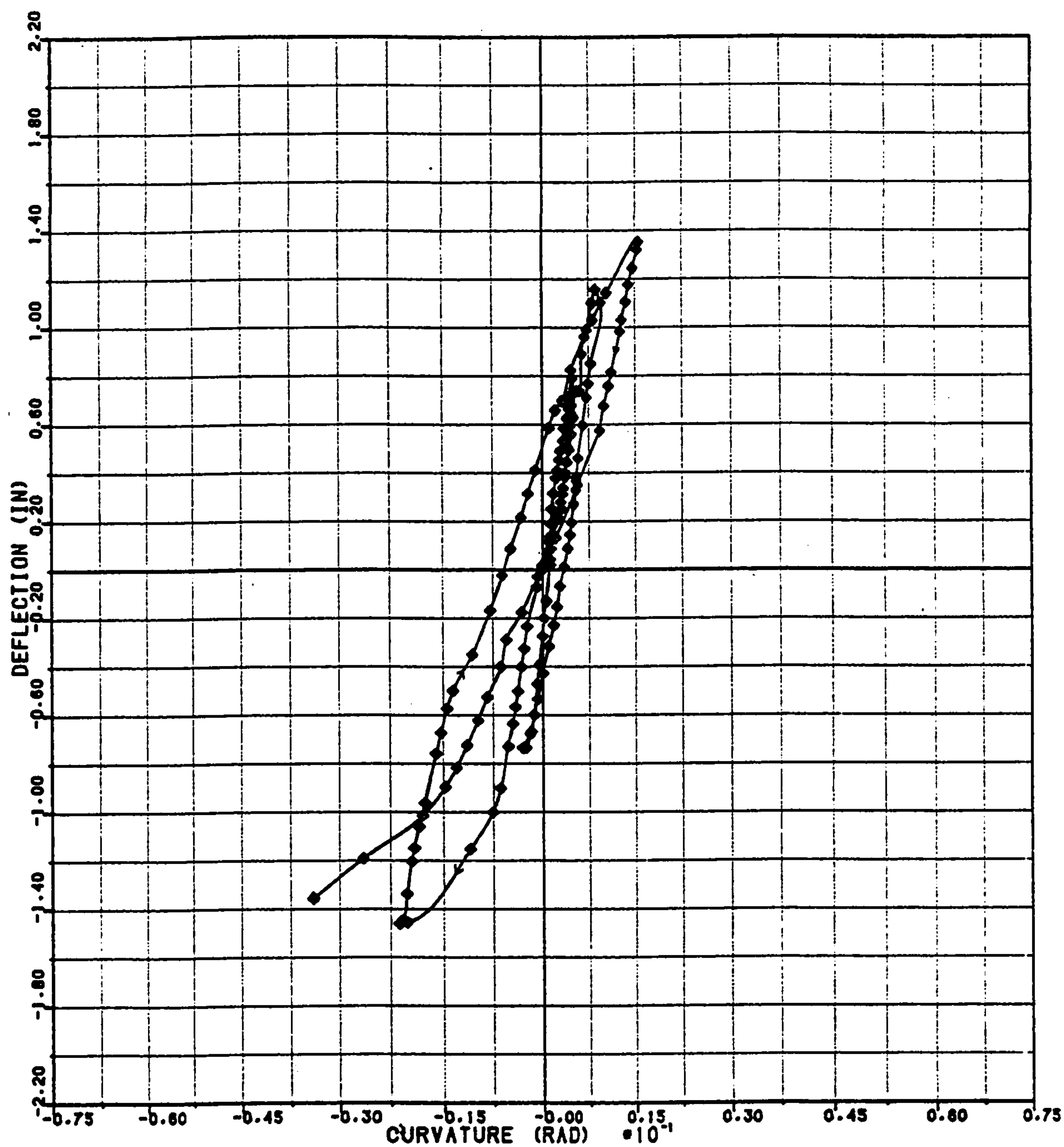

FIG. A29 BEAM CURVATURE VERSUS BEAM TIP DEFLECTION, SPECIMEN 3

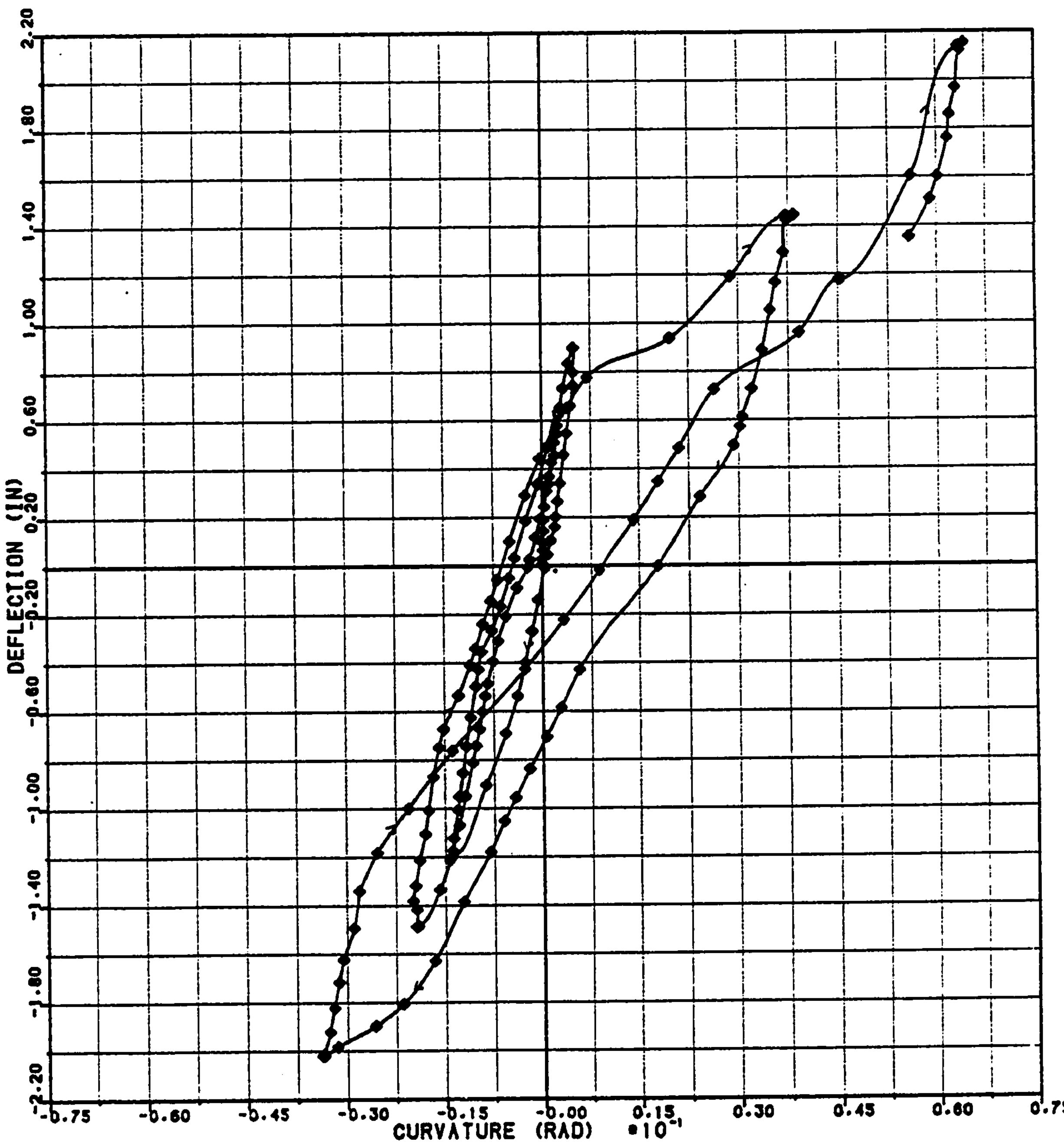

FIG. A30 BEAM CURVATURE VERSUS BEAM TIP DEFLECTION, SPECIMEN 4

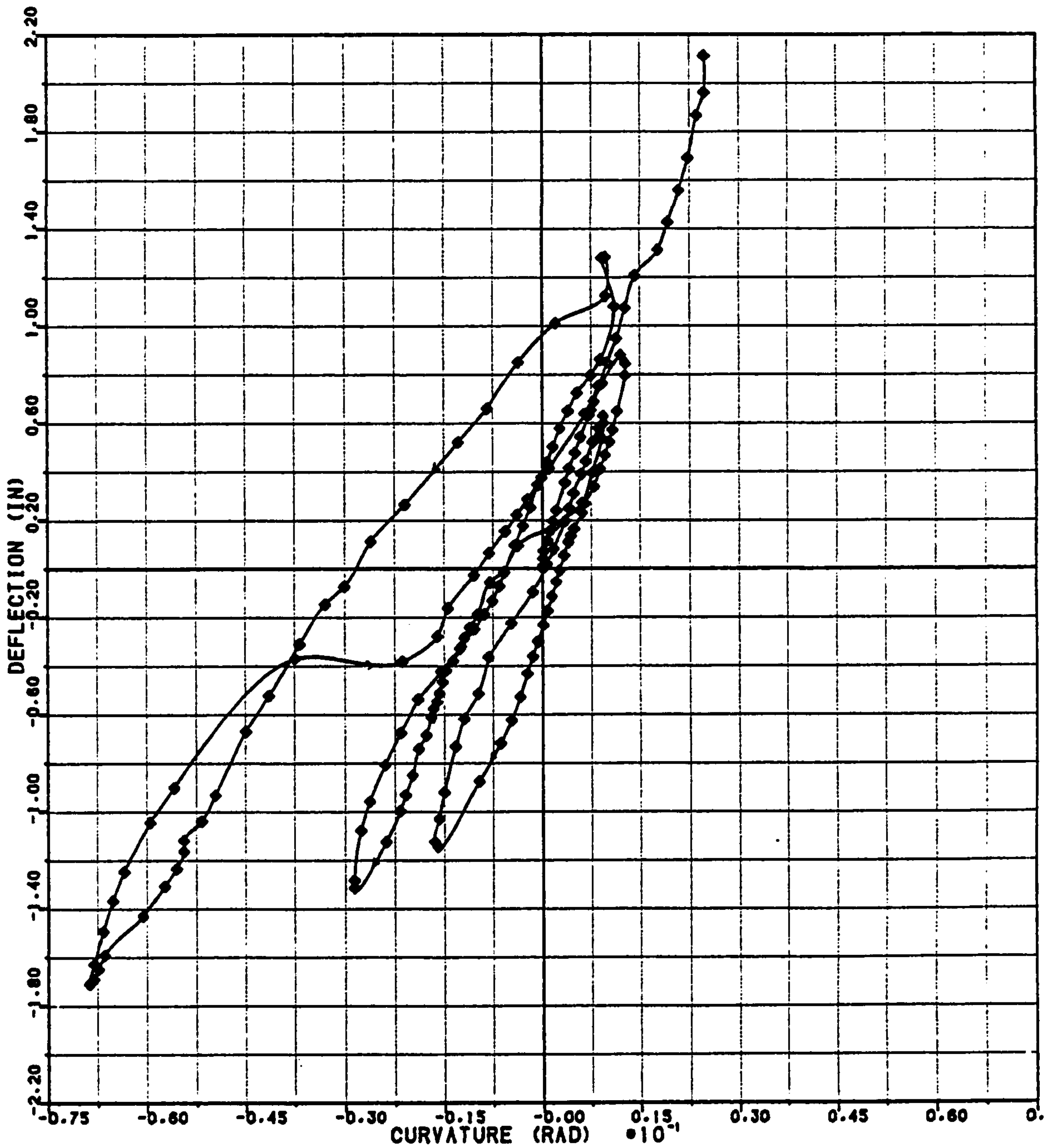

FIG. A31 BEAM CURVATURE VERSUS BEAM TIP DEFLECTION, SPECIMEN 5

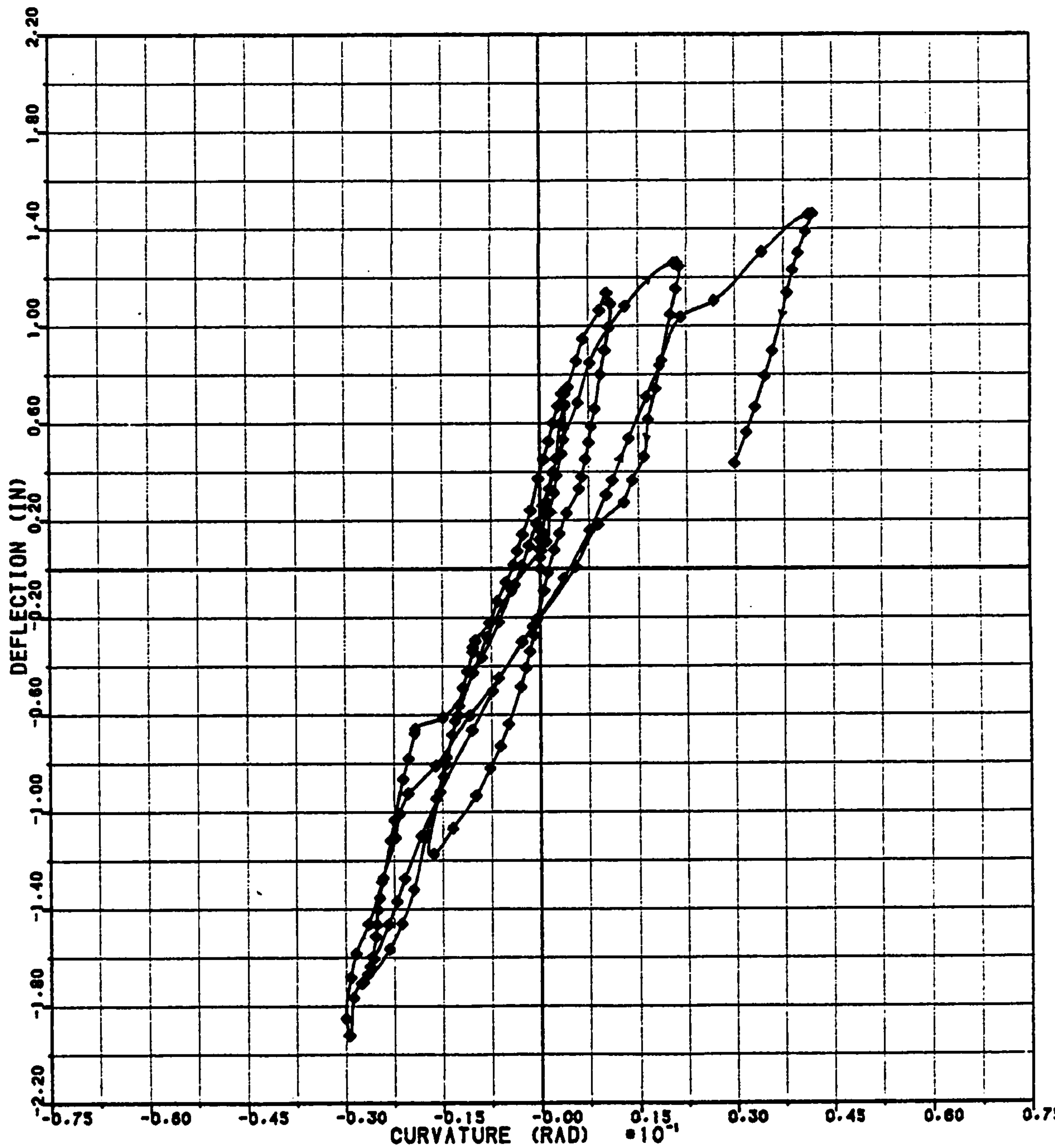

FIG. A32 BEAM CURVATURE VERSUS BEAM TIP DEFLECTION, SPECIMEN 6

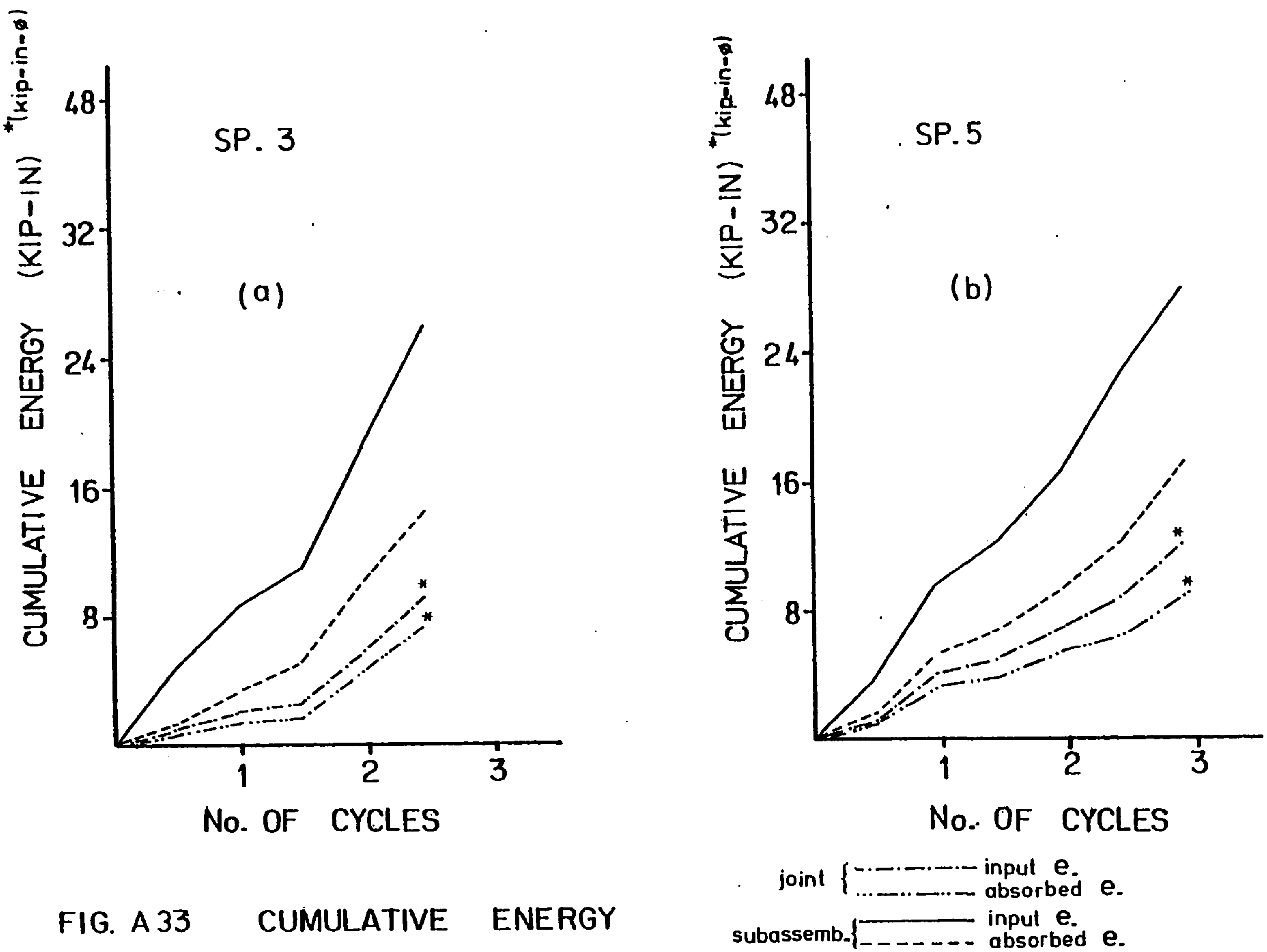

FIG. A 33 CUMULATIVE ENERGY

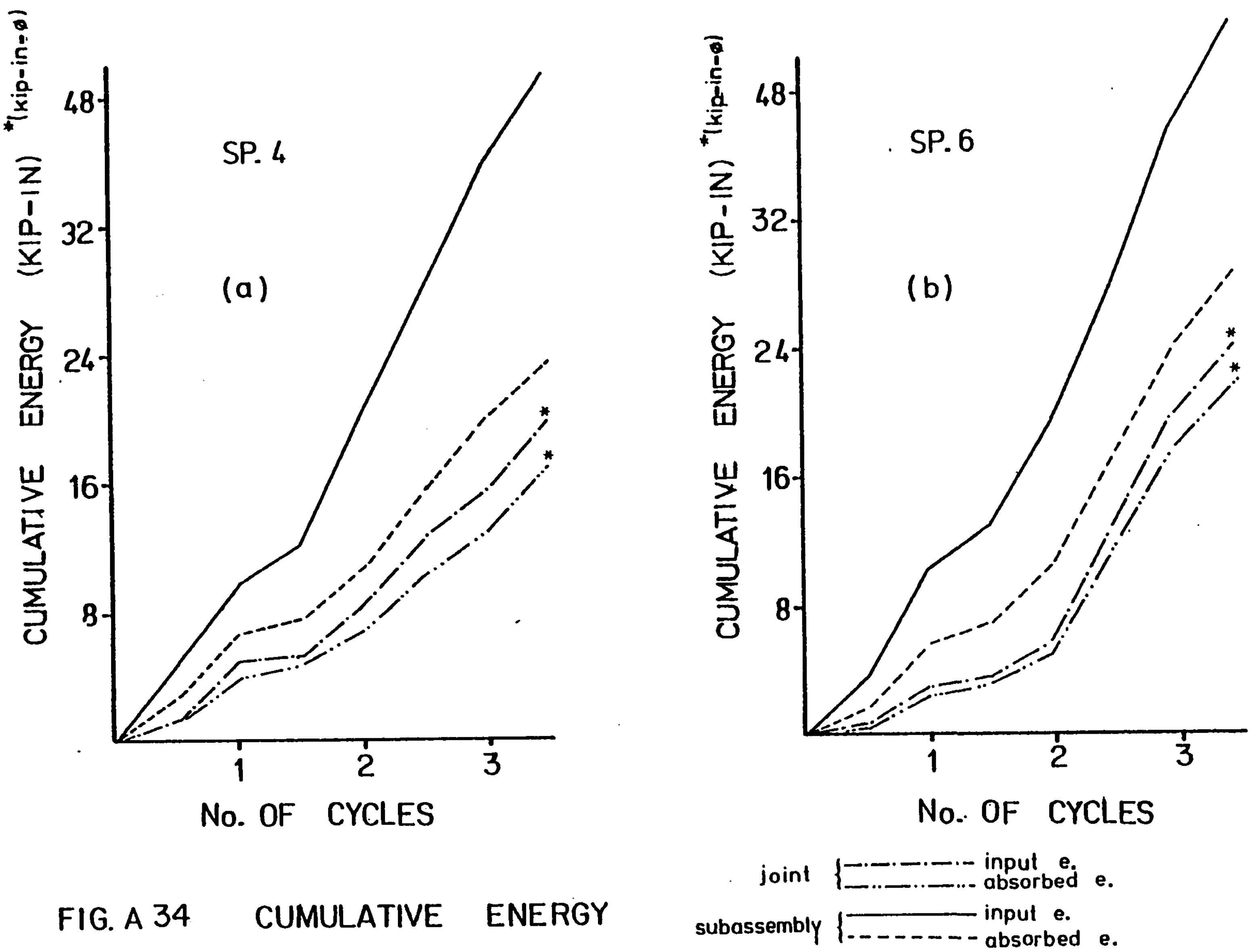

FIG. A 34 CUMULATIVE ENERGY

Appendix B

COMPUTER PROGRAM AND TYPICAL I/O OF SPECIMEN 6

```
CCCCCCCCCCCCCCCCCCCCCCCCCCCCCCCCCCCCCCCCCCCCCCCCCCCCCCCCCCCCCCCCCCC
C                                                                 C
C                                                                 C
C                      BEAM-COLUMN JOINT                          C
C                                                                 C
C                                                                 C
CCCCCCCCCCCCCCCCCCCCCCCCCCCCCCCCCCCCCCCCCCCCCCCCCCCCCCCCCCCCCCCCCCC
      REAL  PL(10,30), PR(10,30), DL(10,30), DR(10,30), LAST(30)
      REAL LX(10,30), GX(10,30), X1(10,30), X2(10,30), PLAST(30)
      REAL LY(10,30), GY(10,30), Y1(10,30), Y2(10,30), X(200), Y(200)
      REAL R1(10,30), R2(10,30), LR(10,30), RT(10,30), RB(10,30)
      REAL RLAST(30), GR(10,30), RR(200), R(200), MOM(200)
      REAL C5(10,30), C6(10,30), LC5(10,30), LC6(10,30), GC5(10,30)
      REAL GC6(10,30), C5LAST(30), C6LAST(30), CA5(200), CA6(200)
      REAL BIGX(10), BIGY(10), NC(10)
      REAL BIGMOM(10), BIGRR(10), BIGCA5(10), BIGCA6(10)
      INTEGER A
CCCCCCCCCCCCCCCCCCCCCCCCCCCCCCCCCCCCCCCCCCCCCCCCCCCCCCCCCCCCCCCCCCC
C                          NOTATION                               C
C                                                                 C
C  FIRST NOTATION                                                 C
C   P=LOAD DATA                           G=GLOBAL                C
C   D=DEFLECTION DATA                     L=LOCAL                 C
C   R=ROTATION                            X=DEFLECTION            C
C   C=DIAGONAL JOINT STRAIN               Y=LOAD                  C
C                                                                 C
C  SECOND NOTATION                                                C
C   L=LEFT                                1=LEFT OR TOP           C
C   R=RIGHT OR ROTATION                   2=RIGHT OR BOTTOM       C
C   B=BOTTOM                              X=DEFLECTION            C
C   T=TOP                                 Y=LOAD                  C
C   5=NORTHWEST-SOUTHEAST DIAGONAL                                C
C   6=NORTHEAST-SOUTHWEST DIAGONAL                                C
C                                                                 C
CCCCCCCCCCCCCCCCCCCCCCCCCCCCCCCCCCCCCCCCCCCCCCCCCCCCCCCCCCCCCCCCCCC
      READ (5,1) N, K, A
      READ (5,10) ((PL(I,J),J=1,K),I=1,N)
      READ (5,10) ((PR(I,J),J=1,K),I=1,N)
      READ (5,10) ((DL(I,J),J=1,K),I=1,N)
      READ (5,10) ((DR(I,J),J=1,K),I=1,N)
      READ (5,10) ((RT(I,J),J=1,K),I=1,N)
      READ (5,10) ((RB(I,J),J=1,K),I=1,N)
      READ (5,10) ((C5(I,J),J=1,K),I=1,N)
      READ (5,10) ((C6(I,J),J=1,K),I=1,N)
      WRITE (6,51)
   51 FORMAT ('1',30X,'INPUT RAW DATA')
      WRITE (6,55)
   55 FORMAT ('-','LEFT LOAD CELL READING')
      WRITE (6,11) ((PL(I,J),J=1,K),I=1,N)
      WRITE (6,53)
   53 FORMAT ('-','RIGHT LOAD CELL READING')
      WRITE (6,11) ((PR(I,J),J=1,K),I=1,N)
      WRITE (6,57)
   57 FORMAT ('-','LEFT DEFLECTION READING')
      WRITE (6,11) ((DL(I,J),J=1,K),I=1,N)
      WRITE (6,59)
   59 FORMAT ('-','RIGHT DEFLECTION READING')
      WRITE (6,11) ((DR(I,J),J=1,K),I=1,N)
      WRITE (6,61)
   61 FORMAT ('-','TOP ROTATION READING')
```

```
 63   FORMAT ('-','BOTTOM ROTATION READING')
      [illegible]
      WRITE (6,63)
 65   FORMAT ('-','LT-RB DIAGONAL JOINT CRACKS')
      WRITE (6,11) ((C5(I,J),J=1,K),I=1,N)
      WRITE (6,67)
 67   FORMAT ('-','LT-RB DIAGONAL JOINT CRACKS')
      WRITE (6,11) ((C6(I,J),J=1,K),I=1,N)
 1    FORMAT (2I5,I5)
 10   FORMAT (9F6.0)
 11   FORMAT (8X,9F9.0)
CCCCCCCCCCCCCCCCCCCCCCCCCCCCCCCCCCCCCCCCCCCCCCCCCCCCCCCCCCCCCCCCCCCCCCC
C                                                                     C
C                                                                     C
C              COLLECTION OF THE INITIAL VALUES                       C
C                                                                     C
C                                                                     C
CCCCCCCCCCCCCCCCCCCCCCCCCCCCCCCCCCCCCCCCCCCCCCCCCCCCCCCCCCCCCCCCCCCCCCC
      KK=K-1
      DO 4 I=1,N
      PLINI=PL(I,1)
      PRINI=PR(I,1)
      LINI=DL(I,1)
      PINI=DR(I,1)
      RTINI=RT(I,1)
      RBINI=RB(I,1)
      C5INI=C5(I,1)
      C6INI=C6(I,1)
CCCCCCCCCCCCCCCCCCCCCCCCCCCCCCCCCCCCCCCCCCCCCCCCCCCCCCCCCCCCCCCCCCCCCCC
C                                                                     C
C                                                                     C
C              FORMATION OF LOCAL COORDINATES                         C
C                                                                     C
C                                                                     C
CCCCCCCCCCCCCCCCCCCCCCCCCCCCCCCCCCCCCCCCCCCCCCCCCCCCCCCCCCCCCCCCCCCCCCC
      DO 2 J=1,KK
      X1(I,J)=0
      X2(I,J)=0
      LX(I,J)=0
      X1(I,J)=DL(I,J)-LINI
      X2(I,J)=RINI-DR(I,J)
      LX(I,J)=(X1(I,J)+X2(I,J))/2.
      Y1(I,J)=0
      Y2(I,J)=0
      LY(I,J)=0
      Y1(I,J)=PL(I,J)-PLINI
      Y2(I,J)=PR(I,J)-PRINI
      LY(I,J)=(Y1(I,J)+Y2(I,J))/2.
      R1(I,J)=0
      R2(I,J)=0
      LR(I,J)=0
      R1(I,J)=RT(I,J)-RTINI
      R2(I,J)=RBINI-RB(I,J)
      LR(I,J)=(R1(I,J)+R2(I,J))/2.
      LC5(I,J)=0
      LC6(I,J)=0
      LC5(I,J)=C5(I,J)-C5INI
      LC6(I,J)=C6(I,J)-C6INI
 2    CONTINUE
 4    CONTINUE
```

```
C                         COORDINATES                                       C
C                                                                           C
C                                                                           C
C                                                                           C
CCCCCCCCCCCCCCCCCCCCCCCCCCCCCCCCCCCCCCCCCCCCCCCCCCCCCCCCCCCCCCCCCCCCCCCCCCCCC
      M=1
      LAST (1)=0
      PLAST(1)=0
      RLAST(1)=0
      C5LAST(1)=0
      C6LAST(1)=0
      DO 8 I=1,N
      DO 6 J=1,KK
      GX(I,J)=LX(I,J)+LAST(M)
      GY(I,J)=LY(I,J)+PLAST(M)
      GR(I,J)=LR(I,J)+RLAST(M)
      GC5(I,J)=LC5(I,J)+C5LAST(M)
      GC6(I,J)=LC6(I,J)+C6LAST(M)
    6 CONTINUE
      M=I+1
      LAST (M)=GX(I,KK)
      PLAST (M)=GY(I,KK)
      RLAST(M)=GR(I,KK)
      C5LAST(M)=GC5(I,KK)
      C6LAST(M)=GC5(I,KK)
    8 CONTINUE
CCCCCCCCCCCCCCCCCCCCCCCCCCCCCCCCCCCCCCCCCCCCCCCCCCCCCCCCCCCCCCCCCCCCCCCCCCCCC
C                                                                           C
C                                                                           C
C          CORRECTING AND FINALIZING THE GLOBAL COORDINATES                 C
C                                                                           C
C                                                                           C
CCCCCCCCCCCCCCCCCCCCCCCCCCCCCCCCCCCCCCCCCCCCCCCCCCCCCCCCCCCCCCCCCCCCCCCCCCCCC
      WRITE (6,70)
   70 FORMAT('1','POINTS',3X,'DEFLECTION(IN)',2X,'LOAD(KIP)',2X,
     @'MOMENT(KIP-IN)',2X,'ROTATION(RAD)',2X,
     @'LT-BT,RT-LB DIAGONAL JOINT STRAIN')
      WRITE (6,71)
   71 FORMAT (' ',75X,'(MICRO IN/IN)')
      M=1
      DO 15 I=1,N
      DO 14 J=1,KK
      X(M)=GX(I,J)/1000.
      Y(M)=0.94*GY(I,J)/100.
      MOM(M)=A*Y(M)
      R(M)=GR(I,J)
      RR(M)=ATAN2(R(M),6670.)
      CA5(M)=3.1*GC5(I,J)
      CA6(M)=3.1*GC6(I,J)
      WRITE (6,7) M, X(M), Y(M), MOM(M), RR(M), CA5(M), CA6(M)
    7 FORMAT ('0',I5,F13.3,F13.2,F15.2,F14.3,5X,2F15.3)
      M=M+1
   14 CONTINUE
   15 CONTINUE
CCCCCCCCCCCCCCCCCCCCCCCCCCCCCCCCCCCCCCCCCCCCCCCCCCCCCCCCCCCCCCCCCCCCCCCCCCCCC
C                                                                           C
C                                                                           C
C               CALCULATIONS OF MAXIMUM POINTS AT EACH CYCLE                C
C                                                                           C
C                                                                           C
```

```
      MM=1
      BIGX(1)=0
      BIGMOM(1)=0
      BIGY(1)=0
      BIGRR(1)=0
      BIGCA5(1)=0
      BIGCA6(1)=0
      DO 25 I=1,N
      BIG1=0
      BIG2=0
      BIGM=0
      BIGROT=0
      BIG5=0
      BIG6=0
      DO 24 J=1,KK
      IF (ABS(X(MM)).GT.ABS(BIG1)) BIG1=X(MM)
      IF (ABS(Y(MM)).GT.ABS(BIG2)) BIG2=Y(MM)
      IF (ABS(MOM(MM)).GT.ABS(BIGM)) BIGM=MOM(MM)
      IF (ABS(RR(MM)).GT.ABS(BIGROT)) BIGROT=RR(MM)
      IF (ABS(CA5(MM)).GT.ABS(BIG5)) BIG5=CA5(MM)
      IF (ABS(CA6(MM)).GT.ABS(BIG6)) BIG6=CA6(MM)
      MM=MM+1
   24 CONTINUE
      NN=NN+1
      NC(NN)=(FLOAT(NN)-1.0)
      BIGX(NN)=BIG1
      BIGY(NN)=BIG2
      BIGMOM(NN)=BIGM
      BIGRR(NN)=BIGROT
      BIGCA5(NN)=BIG5
      BIGCA6(NN)=BIG6
   25 CONTINUE
      WRITE (6,73)
   73 FORMAT ('1','POINT',2X,'MAX. DEFLECTION',2X,'MAX. LOAD',
     @2X,'MAX. MOMENT',2X,'MAX. ROTATION',2X,
     @'MAX. DIAGONAL JOINT STRAIN')
      WRITE (6,72)
   72 FORMAT (14X,'(IN)',9X,'(KIP)',6X,'(KIP-IN)',7X,'(RAD)',
     @11X,'(MICRO IN/IN)')
      DO 27 NN=1,8
      NC(1)=0
      WRITE (6,23) NC(NN), BIGX(NN), BIGY(NN),
     @BIGMOM(NN), BIGRR(NN),BIGCA5(NN),BIGCA6(NN)
   23 FORMAT ('0',F4.0,F12.3,F15.2,F13.2,F13.3,4X,2F14.3)
   27 CONTINUE
CCCCCCCCCCCCCCCCCCCCCCCCCCCCCCCCCCCCCCCCCCCCCCCCCCCCCCCCCCCCCCCCCCCC
C                                                                  C
C                                                                  C
C                  SUBROUTINE CALLED FOR PLOTTINGS                 C
C                                                                  C
C                                                                  C
CCCCCCCCCCCCCCCCCCCCCCCCCCCCCCCCCCCCCCCCCCCCCCCCCCCCCCCCCCCCCCCCCCCC
      CALL MDPLO(X,MOM)
      CALL MRPLO(RR,MOM)
      CALL MC5PLO(CA5,MOM)
      CALL MC6PLO(CA6,MOM)
      CALL DRPLO(RR,X)
      CALL DC5PLO(CA5,X)
      CALL DC6PLO(CA6,X)
      CALL RC5PLO(CA5,RR)
```

```
0176      CALL LPRC(NC,BIGY)
0177      STOP
0178      END
```

```
      SUBROUTINE LPRD(X,Y)
      FAC=1.)
      CALL PLOTS(15.,15.)
      X(9)=0.0
      Y(9)=-1200.0/100.
      X(10)=10.0/(10.0*FAC)
      Y(10)=2400.0/(12.0*FAC)/100.
      CALL NEWPEN (4)
      CALL PLOT(0.0,0.0,-3)
      CALL AXIS(0.0,0.0,'NUMBER OF CYCLES',-16,10.0,0.0,X(9),X(10))
      CALL AXIS(0.0,0.0,'APPLIED LOAD (KIPS)',+19,12.0,90.0,Y(9),Y(10))
      CALL PLOT (0.0,(ABS(Y(9)/Y(10))),3)
      CALL PLOT ((10.0*FAC),(ABS(Y(9)/Y(10))),2)
      CALL PLOT ((ABS(X(9)/X(10))),0.0,3)
      CALL PLOT ((ABS(X(9)/X(10))),(12.0*FAC),2)
      CALL PLOT(0.0,(12.0*FAC),3)
      CALL PLOT((10.0*FAC),(12.0*FAC),2)
      CALL PLOT((10.0*FAC),0.0,2)
      CALL LINE(X,Y,8,1,0,1)
      CALL PLOT(0.0,0.0,999)
      RETURN
      END
```

```
      SUBROUTINE DEFL(X,Y)
      [illegible]
      FAC=1.0
      CALL FLOTS(15.,15.)
      X(9)=0.0
      Y(9)=-2400.0/1000.
      X(10)=1?.0/(10.0*FAC)
      Y(10)=4800.0/(12.0*FAC)/1000.
      CALL NEWPEN (4)
      CALL FLOT(2.0,2.0,-3)
      CALL AXIS(0.0,0.0,'NUMBER OF CYCLES',-16,10.0,0.0,X(9),X(10))
      CALL AXIS(10.0,0.0,'DEFLECTION (IN)',-15,12.0,90.0,Y(9),Y(10))
      CALL PLOT (0.0,(ABS(Y(9)/Y(10))),3)
      CALL FLOT ((10.0*FAC),(ABS(Y(9)/Y(10))),2)
      CALL FLOT ((ABS(X(9)/X(10))),0.0,3)
      CALL PLOT ((ABS(X(9)/X(10))),(12.0*FAC),2)
      CALL FLOT(0.0,(12.0*FAC),3)
      CALL FLOT((10.0*FAC),(12.0*FAC),2)
      CALL FLOT((10.0*FAC),0.0,2)
      CALL DASHL(X,Y,8,1)
      RETURN
      END
```

```
      SUBROUTINE RCSPLC(X,Y)
      DIMENSION [illegible]
      FAC=1.0
      CALL PLOTS(27.5,27.5)
      X(183)=-2000.
      Y(183)=-0.075
      X(184)=20000./(20.0*FAC)
      Y(184)=0.150/(20.0*FAC)
      CALL NEWPEN (4)
      CALL RECT (2.0,1.0,26.0,24.0,0.0,3)
      CALL PLOT(4.0,4.0,-3)
      CALL AXIS(0.0,0.0,'DIAGONAL JOINT STRAIN (MICRO IN/IN)',-35,20.0,
     &0.0,X(183),X(184))
      CALL AXIS(0.0,0.0,'CURVATURE (RAD)',+15,20.0,90.0,Y(183),Y(184))
      CALL PLOT (0.0,(ABS(Y(183)/Y(184))),3)
      CALL PLOT ((20.0*FAC),(ABS(Y(183)/Y(184))),2)
      CALL PLOT ((ABS(X(183)/X(184))),0.0,3)
      CALL PLOT ((ABS(X(183)/X(184))),(20.0*FAC),2)
      CALL PLOT(0.0,(20.0*FAC),3)
      CALL PLOT((20.0*FAC),(20.0*FAC),2)
      CALL PLOT((20.0*FAC),0.0,2)
      CALL FLINE(X,Y,-182,1,1,5)
      CALL NEWPEN (2)
      CALL GRID(0.0,0.0,1.0,1.0,20,20)
      CALL PLOT(0.0,0.0,999)
      RETURN
      END
```

```
      SUBROUTINE RCSPLO(X,Y)
      [illegible]
      FAC=1.0
      CALL PLOTS(27.5,27.5)
      X(133)=-2000.
      Y(183)=-0.075
      X(184)=20000./(20.0*FAC)
      Y(184)=0.150/(20.0*FAC)
      CALL NEWPEN (4)
      CALL RECT (2.0,1.0,26.0,24.0,0.0,3)
      CALL PLOT(4.0,4.0,-3)
      CALL AXIS(0.0,0.0,'DIAGONAL JOINT STRAIN (MICRO IN/IN)',-35,20.0,
     @0.0,X(183),X(184))
      CALL AXIS(0.0,0.0,'CURVATURE (RAD)',+15,20.0,90.0,Y(183),Y(184))
      CALL PLOT (0.0,(ABS(Y(193)/Y(184))),3)
      CALL PLOT ((20.0*FAC),(ABS(Y(183)/Y(184))),2)
      CALL PLOT ((ABS(X(183)/X(184))),0.0,3)
      CALL PLOT ((ABS(X(183)/X(184))),(20.0*FAC),2)
      CALL PLOT(0.0,(20.0*FAC),3)
      CALL PLOT((20.0*FAC),(20.0*FAC),2)
      CALL PLOT((20.0*FAC),0.0,2)
      CALL FLINE(X,Y,-182,1,1,5)
      CALL NEWPEN (2)
      CALL GRID (0.0,0.0,1.0,1.0,20,20)
      CALL PLOT(0.0,0.0,999)
      RETURN
      END
```

```
      SUBROUTINE DGRPLD(X,Y)
      [illegible]
      FAC=1.0
      CALL PLOTS(27.5,27.5)
      X(183)=-2600.
      Y(183)=-2.2
      X(184)=20000.7(20.0*FAC)
      Y(184)=4.4/(22.0*FAC)
      CALL NEWPEN (4)
      CALL RECT (2.0,1.0,26.0,24.0,0.0,3)
      CALL PLOT(4.0,3.0,-3)
      CALL AXIS(0.0,0.0,'DIAGONAL JOINT STRAIN (MICRO IN/IN)',-35,20.0,
     @0.0,X(183),X(184))
      CALL AXIS(0.0,0.0,'DEFLECTION (IN)',+15,22.0,90.0,Y(183),Y(184))
      CALL PLOT (0.0,(ABS(Y(183)/Y(184))),3)
      CALL PLOT ((20.0*FAC),(ABS(Y(183)/Y(184))),2)
      CALL PLOT ((ABS(X(183)/X(184))),0.0,3)
      CALL PLOT ((ABS(X(183)/X(184))),(22.0*FAC),2)
      CALL PLOT(0.0,(22.0*FAC),3)
      CALL PLOT((20.0*FAC),(22.0*FAC),2)
      CALL PLOT((20.0*FAC),0.0,2)
      CALL FLINE(X,Y,-182,1,1,5)
      CALL NEWPEN (2)
      CALL GRID (0.0,0.0,1.0,1.0,20,22)
      CALL PLOT(0.0,0.0,999)
      RETURN
      END
```

```
      SUBROUTINE DCSPLO(X,Y)
      [illegible]
      FAC=1.0
      CALL PLOTS(27.5,27.5)
      X(183)=-2000.
      Y(183)=-2.2
      X(184)=2000.0/(20.0*FAC)
      Y(184)=4.4/(22.0*FAC)
      CALL NEWPEN (4)
      CALL RECT (2.0,1.0,26.0,24.0,0.0,3)
      CALL PLOT(4.0,3.0,-3)
      CALL AXIS(0.0,0.0,'DIAGONAL JOINT STRAIN (MICRO IN/IN)',-35,20.0,
     @0.0,X(183),X(184))
      CALL AXIS(0.0,0.0,'DEFLECTION (IN)',+15,22.0,90.0,Y(183),Y(184))
      CALL PLOT (0.0,(ABS(Y(183)/Y(184))),3)
      CALL PLOT ((20.0*FAC),(ABS(Y(183)/Y(184))),2)
      CALL PLOT ((ABS(X(183)/X(184))),0.0,3)
      CALL PLOT ((ABS(X(183)/X(184))),(22.0*FAC),2)
      CALL PLOT(0.0,(22.0*FAC),3)
      CALL PLOT((20.0*FAC),(22.0*FAC),2)
      CALL PLOT((20.0*FAC),0.0,2)
      CALL FLINE(X,Y,-182,1,1,5)
      CALL NEWPEN (2)
      CALL GRID (0.0,0.0,1.0,1.0,20,22)
      CALL PLOT(0.0,0.0,999)
      RETURN
      END
```

```
      SUBROUTINE DRPLO(X,Y)
      [illegible]
      FAC=1.0
      CALL PLOTS(27.5,27.5)
      X(183)=-0.075
      Y(183)=-2.2
      X(184)=0.150/(20.0*FAC)
      Y(184)=4.4/(22.0*FAC)
      CALL NEWPEN (4)
      CALL RECT (2.0,1.0,26.0,24.0,0.0,3)
      CALL PLOT(4.0,3.0,-3)
      CALL AXIS(0.0,0.0,'CURVATURE (RAD)',-15,20.0,0.0,X(183),X(184))
      CALL AXIS(0.0,0.0,'DEFLECTION (IN)',+15,22.0,90.0,Y(183),Y(184))
      CALL PLOT (0.0,(ABS(Y(183)/Y(184))),3)
      CALL PLOT ((20.0*FAC),(ABS(Y(183)/Y(184))),2)
      CALL PLOT ((ABS(X(183)/X(184))),0.0,3)
      CALL PLOT ((ABS(X(183)/X(184))),(22.0*FAC),2)
      CALL PLOT(0.0,(22.0*FAC),3)
      CALL PLOT((20.0*FAC),(22.0*FAC),2)
      CALL PLOT((20.0*FAC),0.0,2)
      CALL FLINE(X,Y,-182,1,1,5)
      CALL NEWPEN (2)
      CALL GRID (0.0,0.0,1.0,1.0,20,22)
      CALL PLOT(0.0,0.0,999)
      RETURN
      END
```

```
      SUBROUTINE MC6PLO(X,Y)
      [illegible]
      FAC=1.0
      CALL PLOTS(27.5,27.5)
      X(183)=-2000.
      Y(183)=-30000./100.
      X(184)=20000./(20.0*FAC)
      Y(184)=60000./(20.0*FAC)/100.
      CALL NEWPEN (4)
      CALL RECT (2.0,1.0,26.0,24.0,0.0,3)
      CALL PLOT(4.0,4.0,-3)
      CALL AXIS(0.0,0.0,'DIAGONAL JOINT STRAIN (MICRO IN/IN)',-35,20.0,
     @0.0,X(183),X(184))
      CALL AXIS(0.0,0.0,'MOMENT (IN-KIPS)',+16,20.0,90.0,Y(183),Y(184))
      CALL PLOT (0.0,(ABS(Y(183)/Y(184))),3)
      CALL PLOT ((20.0*FAC),(ABS(Y(183)/Y(184))),2)
      CALL PLOT ((ABS(X(183)/X(184))),0.0,3)
      CALL PLOT ((ABS(X(183)/X(184))),(20.0*FAC),2)
      CALL PLOT(0.0,(20.0*FAC),3)
      CALL PLOT((20.0*FAC),(20.0*FAC),2)
      CALL PLOT((20.0*FAC),0.0,2)
      CALL FLINE(X,Y,-182,1,1,5)
      CALL NEWPEN (2)
      CALL GRID (0.0,0.0,1.0,1.0,20,20)
      CALL PLOT(0.0,0.0,999)
      RETURN
      END
```

```
      SUBROUTINE MCSPLO(X,Y)

      FAC=1.0
      CALL PLOTS(27.5,27.5)
      X(183)=-2000.
      Y(183)=-30000./100.
      X(184)=20000./(20.0*FAC)
      Y(184)=50000./(20.0*FAC)/100.
      CALL NEWPEN (4)
      CALL RECT (2.0,1.0,26.0,24.0,0.0,3)
      CALL PLOT(4.0,4.0,-3)
      CALL AXIS(0.0,0.0,'DIAGONAL JOINT STRAIN (MICRO IN/IN)',-35,20.0,
     @0.0,X(183),X(184))
      CALL AXIS(0.0,0.0,'MOMENT (IN-KIPS)',+16,20.0,90.0,Y(183),Y(184))
      CALL PLOT (0.0,(ABS(Y(183)/Y(184))),3)
      CALL PLOT ((20.0*FAC),(ABS(Y(183)/Y(184))),2)
      CALL PLOT ((ABS(X(183)/X(184))),0.0,3)
      CALL PLOT ((ABS(X(183)/X(184))),(20.0*FAC),2)
      CALL PLOT(0.0,(20.0*FAC),3)
      CALL PLOT((20.0*FAC),(20.0*FAC),2)
      CALL PLOT((20.0*FAC),0.0,2)
      CALL FLINE(X,Y,-182,1,1,5)
      CALL NEWPEN (2)
      CALL GRID (0.0,0.0,1.0,1.0,20,20)
      CALL PLOT(0.0,0.0,999)
      RETURN
      END
```

```
      SUBROUTINE MRPLO(X,Y)
      [illegible]
      FAC=1.0
      CALL PLOTS(27.5,27.5)
      X(183)=-0.075
      Y(183)=-30000./100.
      YM1=Y(183)/35.
      X(184)=0.150/(20.0*FAC)
      Y(184)=60000./(20.0*FAC)/100.
      CALL NEWPEN (4)
      YM2=Y(184)/35.
      CALL RECT (2.0,1.0,26.0,24.0,0.0,3)
      CALL PLOT(4.0,4.0,-3)
      CALL AXIS(0.0,0.0,'CURVATURE (RAD)',-15,20.0,0.0,X(183),X(184))
      CALL AXIS(0.0,0.0,'MOMENT (IN-KIPS)',+16,20.0,90.0,Y(183),Y(184))
      CALL AXIS (20.,0.0,'APPLIED LOAD (KIPS)',-19,20.0,90.0,YM1,YM2)
      CALL PLOT (0.0,(ABS(Y(183)/Y(184))),3)
      CALL PLOT ((20.0*FAC),(ABS(Y(183)/Y(184))),2)
      CALL PLOT ((ABS(X(183)/X(184))),0.0,3)
      CALL PLOT ((ABS(X(183)/X(184))),(20.0*FAC),2)
      CALL PLOT(0.0,(20.0*FAC),3)
      CALL PLOT((20.0*FAC),(20.0*FAC),2)
      CALL PLOT((20.0*FAC),0.0,2)
      CALL FLINE(X,Y,-182,1,1,5)
      CALL NEWPEN (2)
      CALL GRID (0.0,0.0,1.0,1.0,20,20)
      CALL PLOT(0.0,0.0,999)
      RETURN
      END
```

```
      SUBROUTINE MDPLO(X,Y)
      DIMENSION X(184),Y(184)
      FAC=1.0
      CALL PLOTS(27.5,27.5)
      X(183)=-2.2
      Y(183)=-30000./100.
      YM1=Y(183)/35.
      X(184)=3.4/(22.0*FAC)
      Y(184)=60000./(20.0*FAC)/100.
      YM2=Y(184)/35.
      CALL NEWPEN (4)
      CALL RECT (1.0,1.0,26.0,26.0,0.0,3)
      CALL PLOT(3.0,4.0,-3)
      CALL AXIS(0.0,0.0,'DEFLECTION (IN)',-15,22.0,0.0,X(183),X(184))
      CALL AXIS(22.0,0.0,'MOMENT (IN-KIPS)',-16,20.0,90.0,Y(183),Y(184))
      CALL AXIS (0.0,0.0,'APPLIED LOAD (KIPS)',+19,20.0,90.0,YM1,YM2)
      CALL PLOT (0.0,(ABS(Y(183)/Y(184))),3)
      CALL PLOT ((22.0*FAC),(ABS(Y(183)/Y(184))),2)
      CALL PLOT ((ABS(X(183)/X(184))),0.0,3)
      CALL PLOT ((ABS(X(183)/X(184))),(20.0*FAC),2)
      CALL PLOT(0.0,(20.0*FAC),3)
      CALL PLOT((22.0*FAC),(20.0*FAC),2)
      CALL PLOT((22.0*FAC),0.0,2)
      CALL FLINE(X,Y,-182,1,1,5)
      CALL NEWPEN (2)
      CALL GRID (0.0,0.0,1.0,1.0,22,20)
      CALL PLOT(0.0,0.0,999)
      RETURN
      END
```

LEFT LOAD CELL READING

7.	23.	51.	106.	149.	205.	251.	300.	360.
408.	452.	505.	555.	605.	650.	703.	730.	700.
597.	530.	430.	310.	218.	115.	53.	8.	2.
-6.	-50.	-104.	-156.	-203.	-302.	-388.	-475.	-561.
-657.	-753.	-830.	-778.	-747.	-683.	-554.	-503.	-395.
-289.	-186.	-93.	-49.	-9.	-9.	-9.	-9.	-9.
20.	58.	105.	160.	208.	305.	405.	504.	602.
574.	433.	339.	303.	201.	103.	58.	11.	11.
11.	11.	11.	11.	11.	11.	11.	11.	11.
0.	-20.	-49.	-94.	-150.	-205.	-267.	-304.	-353.
-404.	-450.	-502.	-603.	-590.	-780.	-824.	-363.	-306.
-703.	-756.	-666.	-537.	-360.	-267.	-155.	-56.	-1.
1.	33.	77.	122.	155.	205.	259.	310.	406.
521.	603.	706.	749.	805.	860.	890.	844.	758.
640.	574.	446.	342.	261.	149.	54.	1.	1.
0.	-26.	-54.	-100.	-142.	-206.	-256.	-303.	-355.
-410.	-455.	-513.	-592.	-697.	-650.	-597.	-512.	-503.
-494.	-496.	-458.	-368.	-282.	-216.	-131.	-61.	-5.
5.	47.	65.	71.	86.	113.	149.	203.	245.
307.	409.	500.	386.	386.	599.	637.	585.	483.
383.	293.	218.	118.	64.	6.	6.	6.	6.

RIGHT LOAD CELL READING

6.	22.	50.	102.	144.	202.	254.	313.	380.
436.	491.	558.	615.	670.	722.	777.	800.	771.
575.	504.	411.	298.	211.	110.	51.	5.	1.
-6.	-51.	-102.	-151.	-198.	-303.	-404.	-499.	-602.
-704.	-799.	-875.	-831.	-755.	-686.	-556.	-505.	-407.
-308.	-205.	-102.	-49.	-4.	-4.	-4.	-4.	-4.
13.	52.	100.	153.	197.	238.	379.	472.	562.
538.	573.	460.	351.	233.	116.	60.	5.	5.
5.	5.	5.	5.	5.	5.	5.	5.	5.
0.	-24.	-52.	-99.	-152.	-206.	-265.	-300.	-348.
-409.	-450.	-505.	-615.	-707.	-804.	-854.	-895.	-856.
-790.	-624.	-547.	-451.	-317.	-247.	-151.	-58.	-4.
1.	33.	77.	122.	154.	205.	252.	297.	380.
477.	550.	628.	670.	713.	744.	752.	696.	726.
741.	782.	606.	457.	326.	173.	61.	6.	1.
0.	-26.	-54.	-101.	-137.	-185.	-226.	-264.	-307.
-349.	-383.	-427.	-490.	-569.	-643.	-775.	-852.	-862.
-811.	-766.	-566.	-457.	-348.	-258.	-154.	-57.	-4.
5.	48.	65.	72.	88.	112.	150.	204.	244.
302.	396.	486.	664.	664.	609.	640.	586.	491.
388.	290.	213.	112.	58.	4.	4.	4.	4.

LEFT DEFLECTION READING

100.	110.	128.	154.	195.	245.	293.	349.	416.
477.	538.	622.	694.	771.	858.	972.	1042.	1047.
940.	885.	804.	691.	603.	485.	409.	342.	332.
-100.	-137.	-190.	-244.	-298.	-417.	-541.	-665.	-800.
-949.	-1143.	-1384.	-1386.	-1356.	-1307.	-1198.	-1147.	-1055.
-952.	-839.	-719.	-651.	-583.	-583.	-583.	-583.	-583.
100.	192.	293.	412.	495.	649.	800.	954.	1095.
1096.	1095.	1021.	931.	816.	670.	590.	497.	497.
497.	497.	497.	497.	497.	497.	497.	497.	497.
-109.	-131.	-209.	-320.	-415.	-496.	-582.	-630.	-693.
-750.	-825.	-892.	-1022.	-1133.	-1265.	-1362.	-1511.	-1515.
-1482.	-1432.	-1369.	-1273.	-1122.	-1036.	-909.	-774.	-685.

[illegible]	[illegible]	[illegible]	[illegible]	[illegible]	[illegible]	[illegible]	[illegible]	-1582.
-2875.	-2866.	-2760.	-2660.	-2554.	-2458.	-2326.	-2171.	-2045.
[illegible]	[illegible]	[illegible]	[illegible]	[illegible]	1220.	1419.	1615.	1767.
1895.	2124.	2349.	2671.	2571.	3105.	3753.	3771.	3795.
3594.	3487.	3392.	3246.	3146.	2995.	2995.	2995.	2995.
RIGHT DEFLECTION READING								
900.	891.	874.	840.	810.	761.	716.	665.	600.
543.	486.	434.	338.	268.	196.	105.	48.	47.
143.	209.	284.	400.	489.	605.	679.	740.	751.
-1900.	-1855.	-1796.	-1734.	-1674.	-1534.	-1398.	-1264.	-1123.
-963.	-736.	-373.	-374.	-401.	-456.	-530.	-638.	-745.
-860.	-986.	-1120.	-1193.	-1271.	-1271.	-1271.	-1271.	-1271.
1900.	1816.	1718.	1602.	1521.	1370.	1218.	1062.	914.
914.	940.	1021.	1113.	1232.	1373.	1449.	1539.	1539.
1539.	1539.	1539.	1539.	1539.	1539.	1539.	1539.	1539.
-1900.	-1867.	-1760.	-1655.	-1548.	-1458.	-1362.	-1309.	-1238.
-1165.	-1092.	-1018.	-873.	-745.	-587.	-440.	-291.	-290.
-398.	-419.	-431.	-597.	-661.	-769.	-921.	-1027.	-1192.
2900.	2836.	2711.	2598.	2534.	2440.	2346.	2262.	2112.
1930.	1779.	1549.	1402.	1197.	850.	503.	503.	503.
503.	550.	691.	820.	937.	1104.	1268.	1389.	1406.
-2700.	-2667.	-2600.	-2400.	-2118.	-1696.	-1540.	-1418.	-1283.
-1159.	-1058.	-922.	-697.	-416.	-250.	-225.	-220.	-210.
-210.	-214.	-293.	-392.	-497.	-589.	-716.	-366.	-994.
3700.	3544.	3359.	3121.	2789.	2583.	2373.	2160.	1993.
1345.	1591.	1348.	1232.	1232.	317.	392.	382.	468.
576.	689.	789.	962.	1051.	1210.	1210.	1210.	1210.
TOP ROTATION READING								
800.	800.	800.	801.	801.	802.	802.	803.	803.
803.	803.	803.	804.	805.	805.	808.	812.	813.
812.	812.	811.	809.	808.	807.	806.	805.	805.
804.	803.	798.	794.	791.	782.	773.	762.	748.
726.	688.	622.	622.	626.	629.	638.	641.	648.
655.	664.	674.	679.	685.	685.	685.	685.	685.
590.	708.	719.	728.	733.	745.	758.	768.	779.
779.	778.	776.	773.	768.	760.	755.	749.	749.
749.	749.	749.	749.	749.	749.	749.	749.	749.
745.	742.	725.	712.	702.	694.	686.	682.	677.
672.	666.	660.	647.	635.	618.	598.	555.	553.
553.	546.	551.	560.	571.	578.	583.	600.	609.
623.	630.	650.	663.	670.	679.	683.	696.	709.
724.	734.	743.	747.	747.	750.	755.	759.	758.
759.	757.	755.	752.	749.	742.	733.	726.	725.
720.	715.	702.	662.	640.	622.	611.	602.	593.
586.	580.	574.	569.	566.	542.	500.	436.	416.
417.	419.	432.	441.	451.	460.	472.	486.	495.
501.	526.	548.	558.	567.	578.	591.	607.	621.
533.	655.	675.	667.	690.	736.	820.	827.	826.
824.	821.	818.	812.	809.	804.	804.	804.	804.
BOTTOM ROTATION READING								
990.	990.	990.	990.	990.	990.	990.	989.	984.
979.	974.	965.	963.	958.	953.	944.	938.	938.
938.	938.	942.	949.	954.	961.	965.	968.	969.
974.	975.	978.	981.	984.	988.	992.	995.	997.
990.	1002.	1007.	1008.	1008.	1009.	1009.	1009.	1009.
1009.	1009.	1009.	1008.	1008.	1008.	1008.	1008.	1008.
1006.	1002.	995.	986.	980.	969.	957.	945.	935.
934.	934.	930.	938.	946.	955.	959.	965.	965.
[illegible]	[illegible]	[illegible]	[illegible]	[illegible]	[illegible]	[illegible]	[illegible]	[illegible]

997.	998.	999.	1001.	1002.	1004.	[illegible]	[illegible]	[illegible]
[illegible]	[illegible]	[illegible]	[illegible]	[illegible]	[illegible]	[illegible]	1007.	1007.
219.	[illegible]	[illegible]	[illegible]	[illegible]	526.	421.	409.	408.
408.	[illegible]	[illegible]	[illegible]	[illegible]	455.	467.	479.	481.
495.	495.	495.	523.	586.	730.	757.	778.	803.
825.	842.	865.	914.	971.	1011.	1025.	1038.	1045.
1050.	1051.	1050.	1050.	1050.	1050.	1040.	1043.	1038.
1028.	1016.	975.	895.	756.	688.	627.	572.	536.
506.	437.	306.	238.	238.	142.	127.	121.	128.
136.	145.	147.	162.	175.	212.	212.	212.	212.

LT-P3 DIAGONAL JOINT CRACKS

690.	690.	690.	690.	690.	690.	690.	690.	707.
710.	725.	780.	825.	855.	907.	980.	1040.	1051.
1012.	1000.	966.	930.	909.	860.	839.	819.	816.
802.	800.	790.	776.	773.	750.	730.	721.	708.
698.	687.	676.	671.	674.	679.	684.	688.	695.
705.	709.	710.	717.	722.	722.	722.	722.	722.
741.	751.	810.	885.	918.	998.	1061.	1132.	1207.
1211.	1209.	1165.	1123.	1086.	1022.	985.	939.	939.
939.	939.	939.	939.	939.	939.	939.	939.	939.
906.	909.	862.	805.	766.	747.	730.	722.	716.
710.	700.	700.	690.	681.	674.	672.	671.	671.
674.	679.	678.	672.	690.	700.	703.	717.	723.
761.	776.	834.	945.	977.	1037.	1088.	1133.	1210.
1300.	1388.	1515.	1585.	1639.	1706.	1762.	1764.	1753.
1746.	1725.	1665.	1611.	1551.	1460.	1365.	1276.	1249.
1208.	1181.	1105.	959.	874.	832.	812.	792.	789.
777.	773.	754.	746.	730.	727.	731.	730.	735.
723.	719.	724.	727.	739.	750.	868.	894.	862.
952.	1051.	1122.	1151.	1171.	1230.	1295.	1375.	1430.
1476.	1565.	1660.	1680.	1700.	1739.	1766.	1762.	1725.
1669.	1627.	1585.	1500.	1438.	1347.	1347.	1347.	1347.

LT-F3 DIAGONAL JOINT CRACKS

780.	780.	779.	776.	730.	717.	706.	686.	687.
683.	682.	679.	700.	700.	690.	687.	675.	671.
679.	679.	686.	690.	690.	695.	707.	707.	707.
681.	692.	693.	697.	700.	750.	851.	932.	1025.
1136.	1232.	1454.	1458.	1448.	1414.	1343.	1313.	1251.
1203.	1135.	1069.	1027.	992.	992.	992.	992.	992.
964.	932.	872.	809.	761.	745.	725.	700.	678.
676.	677.	687.	695.	702.	756.	750.	747.	747.
747.	747.	747.	747.	747.	747.	747.	747.	747.
762.	766.	787.	858.	939.	1003.	1048.	1086.	1134.
1174.	1215.	1270.	1338.	1406.	1498.	1574.	1671.	1691.
1656.	1637.	1590.	1539.	1432.	1380.	1288.	1195.	1126.
1068.	1037.	958.	876.	843.	800.	771.	759.	727.
703.	690.	670.	659.	660.	656.	662.	661.	660.
654.	675.	680.	696.	691.	715.	752.	802.	797.
794.	803.	873.	1095.	1156.	1262.	1332.	1400.	1453.
1511.	1543.	1596.	1675.	1750.	1794.	1816.	1830.	1327.
1927.	1927.	1817.	1720.	1648.	1600.	1510.	1403.	1280.
1192.	1073.	990.	965.	944.	900.	864.	813.	784.
761.	735.	723.	715.	710.	707.	706.	713.	712.
719.	732.	743.	754.	771.	801.	801.	801.	801.

(MICRO IN/IN)

1	0.0	0.0	0.0	0.0	0.0	0.0
2	0.009	0.15	5.26	0.0	0.0	0.0
3	0.027	0.41	14.48	0.0	0.0	-8.100
4	0.062	0.92	32.08	0.000	0.0	-32.400
5	0.092	1.32	46.06	0.000	0.0	-405.000
6	0.142	1.85	64.81	0.000	0.0	-510.300
7	0.198	2.31	80.93	0.000	0.0	-599.400
8	0.242	2.82	98.70	0.000	0.0	-761.400
9	0.308	3.42	119.59	0.001	137.700	-753.300
10	0.367	3.91	136.70	0.001	162.000	-785.700
11	0.426	4.37	152.98	0.001	283.500	-793.800
12	0.509	4.93	172.72	0.002	729.000	-818.100
13	0.578	5.44	190.33	0.002	1093.500	-648.000
14	0.651	5.93	207.60	0.003	1336.500	-648.000
15	0.731	6.39	223.56	0.003	1757.700	-729.000
16	0.833	6.39	241.32	0.004	2349.000	-753.300
17	0.897	7.13	249.55	0.005	2835.000	-850.500
18	0.900	6.85	239.84	0.005	2924.100	-882.900
19	0.798	5.45	190.66	0.005	2608.200	-818.100
20	0.742	4.80	167.95	0.005	2511.000	-818.100
21	0.650	3.89	136.21	0.004	2235.600	-761.400
22	0.545	2.80	97.88	0.004	1944.000	-729.000
23	0.457	1.96	68.43	0.003	1701.000	-729.000
24	0.340	1.00	34.87	0.003	1377.000	-688.500
25	0.265	0.43	14.97	0.002	1206.900	-591.300
26	0.201	0.0	0.0	0.002	1044.900	-591.300
27	0.201	0.0	0.0	0.002	1044.900	-591.300
28	0.160	-0.42	-14.64	0.002	1028.700	-502.200
29	0.104	-0.91	-31.91	0.001	947.700	-494.100
30	0.046	-1.39	-48.53	0.001	834.300	-461.700
31	-0.011	-1.83	-63.99	0.000	810.000	-437.400

33	-0.270	-3.67	-128.31	-0.002	481.700	785.700
34	-0.379	-4.52	-158.25	-0.003	388.800	1441.800
35	-0.537	-5.41	-189.34	-0.004	283.500	2195.100
36	-0.692	-6.34	-221.91	-0.006	202.500	3094.200
37	-0.905	-7.24	-253.33	-0.009	113.400	4276.797
38	-1.204	-7.96	-278.50	-0.014	24.300	5669.996
39	-1.205	-7.51	-262.71	-0.014	-16.200	5702.398
40	-1.176	-7.00	-245.10	-0.014	8.100	5621.398
41	-1.124	-6.38	-223.23	-0.014	48.500	5345.996
42	-1.008	-5.16	-180.62	-0.013	89.100	4770.898
43	-0.953	-4.68	-163.84	-0.013	121.500	4527.898
44	-0.854	-3.71	-129.95	-0.012	178.200	4025.700
45	-0.745	-2.75	-96.23	-0.012	259.200	3636.900
46	-0.625	-1.76	-62.35	-0.011	291.600	3036.100
47	-0.498	-0.86	-30.10	-0.010	299.700	2543.400
48	-0.428	-0.40	-14.15	-0.010	356.400	2211.300
49	-0.355	-0.00	-0.16	-0.009	396.900	1927.800
50	-0.355	-0.00	-0.16	-0.009	396.900	1927.800
51	-0.355	-0.00	-0.16	-0.009	396.900	1927.800
52	-0.355	-0.00	-0.16	-0.009	396.900	1927.800
53	-0.355	-0.00	-0.16	-0.009	396.900	1927.800
54	-0.257	0.36	12.50	-0.008	477.900	1668.600
55	-0.167	0.80	28.13	-0.006	955.800	1192.600
56	-0.050	1.31	45.90	-0.005	1563.300	672.300
57	0.032	1.74	61.03	-0.004	1830.600	445.500
58	0.184	2.63	91.96	-0.003	2478.600	153.900
59	0.336	3.52	123.37	-0.001	2988.900	-8.100
60	0.491	4.43	154.96	0.001	3564.000	-210.600
61	0.635	5.31	185.88	0.003	4171.496	-388.800
62	0.636	5.07	177.33	0.003	4203.898	-405.000
63	0.622	4.80	168.12	0.003	4114.797	-396.900
64	0.545	3.83	133.90	0.002	3831.300	-315.900
65	0.454	2.91	101.99	0.002	3491.100	-251.100

67	[illegible]	[illegible]	[illegible]	-0.000	2673.000	248.000
68	0.115	0.37	13.82	-0.001	2373.300	134.400
69	0.024	-0.08	-2.96	-0.002	2000.700	170.100
70	0.024	-0.03	-2.96	-0.002	2000.700	170.100
71	0.024	-0.08	-2.96	-0.002	2000.700	170.100
72	0.024	-0.08	-2.96	-0.002	2000.700	170.100
73	0.024	-0.08	-2.96	-0.002	2000.700	170.100
74	0.024	-0.08	-2.96	-0.002	2000.700	170.100
75	0.024	-0.08	-2.96	-0.002	2000.700	170.100
76	0.024	-0.08	-2.96	-0.002	2000.700	170.100
77	0.024	-0.08	-2.96	-0.002	2000.700	170.100
78	0.024	-0.08	-2.96	-0.002	2000.700	170.100
79	0.024	-0.08	-2.96	-0.002	2000.700	170.100
80	-0.108	-0.29	-10.20	-0.002	1952.100	202.500
81	-0.090	-0.56	-19.58	-0.004	1644.300	372.600
82	-0.208	-0.99	-34.71	-0.006	1182.600	947.700
83	-0.309	-1.50	-52.64	-0.007	866.700	1603.800
84	-0.395	-2.02	-70.57	-0.008	712.800	2122.200
85	-0.486	-2.56	-90.47	-0.008	575.100	2486.700
86	-0.536	-2.92	-102.32	-0.009	510.300	2794.500
87	-0.603	-3.38	-118.28	-0.009	461.700	3183.300
88	-0.673	-3.36	-135.22	-0.010	413.100	3507.300
89	-0.742	-4.31	-151.01	-0.010	332.100	3839.400
90	-0.813	-4.82	-168.61	-0.011	332.100	4284.898
91	-0.950	-5.81	-203.32	-0.012	251.100	4835.699
92	-1.070	-6.65	-232.77	-0.013	178.200	5386.496
93	1.215	-7.53	-263.53	-0.014	121.500	6131.699
94	-1.337	-7.97	-278.99	-0.016	105.300	6747.297
95	-1.436	-8.35	-292.15	-0.019	97.200	7532.996
96	-1.438	-7.90	-276.36	-0.019	97.200	7694.996
97	-1.418	-7.10	-248.56	-0.019	121.500	7411.496
98	-1.382	-6.57	229.97	-0.020	162.000	7257.598
99	-1.320	-5.79	-202.50	-0.020	153.900	6876.898

101	-1.106	-3.27	-114.33	-0.018	251.100	5597.098
102	-1.009	-2.50	-87.51	-0.018	332.100	5175.898
103	-0.876	-1.32	-53.50	-0.017	355.400	4430.699
104	-0.749	-0.62	-21.71	-0.016	469.800	3677.400
105	-0.749	-0.62	-21.71	-0.016	469.800	3677.400
106	-0.673	-0.32	-11.19	-0.015	591.300	3426.300
107	-0.535	0.09	3.29	-0.013	1223.100	2786.400
108	-0.410	0.52	13.09	-0.011	1960.200	2122.200
109	-0.341	0.92	28.79	-0.010	2219.400	1854.900
110	-0.240	1.30	45.40	-0.009	2705.400	1506.600
111	-0.144	1.77	62.02	-0.008	3118.500	1271.700
112	-0.057	2.22	77.81	-0.007	3483.000	1174.500
113	0.039	3.06	107.25	-0.005	4106.699	915.300
114	0.289	4.06	142.13	-0.003	4835.699	720.900
115	0.441	4.79	167.63	-0.000	5548.496	615.600
116	0.651	5.64	197.40	0.004	6577.199	453.600
117	0.777	6.04	211.38	0.007	7144.199	445.500
118	0.936	6.50	227.67	0.020	7581.598	372.600
119	1.190	6.91	241.81	0.029	8124.297	340.200
120	1.441	7.09	248.07	0.037	8577.898	338.800
121	1.445	6.61	231.29	0.038	8594.098	380.700
122	1.446	6.34	222.07	0.038	8504.996	372.600
123	1.444	5.86	205.13	0.038	8448.297	324.000
124	1.421	5.74	201.02	0.037	8278.199	494.100
125	1.290	4.31	151.01	0.037	7792.199	534.600
126	1.166	3.13	109.39	0.036	7354.797	664.200
127	1.051	2.13	74.52	0.035	6868.797	623.700
128	0.887	0.88	30.93	0.033	6131.699	618.100
129	0.727	-0.09	-3.13	0.032	5362.199	1117.800
130	0.611	-0.60	-20.89	0.031	4641.297	1522.800
131	0.611	-0.60	-20.89	0.031	4641.297	1522.800
132	0.571	-0.84	-29.45	0.030	4422.598	1595.700
133	0.494	-1.10	-33.66	0.029	3807.000	2162.700

135	-0.003	-1.91	-66.79	0.018	1935.900	4454.996
136	-0.428	-2.43	-85.21	0.006	1595.700	5313.598
137	-0.535	-2.86	-100.18	0.003	1433.700	5880.598
138	-0.706	-3.26	-114.16	0.000	1271.700	6431.398
139	-0.838	-3.71	-129.79	-0.002	1247.400	6860.699
140	-0.957	-4.16	-145.75	-0.004	1150.200	7330.496
141	-1.053	-4.54	-158.74	-0.006	1117.800	7539.699
142	-1.180	-5.01	-175.52	-0.008	963.900	8016.996
143	-1.385	-5.68	-198.88	-0.012	899.100	8658.898
144	-1.629	-6.55	-229.15	-0.017	769.500	9266.398
145	-1.807	-6.81	-233.52	-0.022	745.200	9622.797
146	-1.897	-7.05	-246.59	-0.026	777.600	9800.996
147	-1.984	-7.01	-245.27	-0.031	769.500	9914.398
148	-2.019	-7.01	-245.43	-0.033	810.000	10700.098
149	-2.021	-6.73	-235.56	-0.034	712.800	10700.098
150	-2.014	-6.53	-228.49	-0.034	680.400	10700.098
151	-1.922	-5.41	-189.34	-0.033	720.900	9809.098
152	-1.822	-4.47	-156.60	-0.032	745.200	9023.398
153	-1.717	-3.56	-124.53	-0.031	842.400	8440.199
154	-1.623	-2.82	-98.86	-0.031	931.500	8051.398
155	-1.493	-1.94	-67.77	-0.029	1887.300	7322.398
156	-1.341	-1.15	-40.30	-0.028	2097.900	6455.699
157	-1.341	-1.15	-40.30	-0.028	2097.900	6455.699
158	-1.183	-0.75	-26.32	-0.025	2899.800	5491.797
159	-1.001	-0.59	-20.56	-0.021	3474.900	4819.496
160	-0.763	-0.53	-18.42	-0.014	3709.800	4616.996
161	-0.426	-0.38	-13.32	-0.003	3871.800	4446.898
162	-0.222	-0.14	-4.93	0.003	4349.699	4090.500
163	-0.018	0.21	7.24	0.009	4876.199	3798.900
164	0.186	0.71	25.00	0.014	5524.199	3385.800
165	0.346	1.10	38.49	0.018	5993.996	3150.900
166	0.483	1.66	58.23	0.021	6342.297	2964.600
167	0.725	2.59	90.47	0.026	7063.199	2754.000

169	1.178	3.74	130.78	0.045	7994.699	2592.000
170	1.178	3.74	130.78	0.045	8156.699	2551.500
171	1.603	4.48	156.77	0.056	8472.598	2527.200
172	2.139	4.80	168.12	0.063	8691.297	2519.100
173	2.153	4.31	150.68	0.064	8658.898	2575.800
174	2.122	3.38	118.28	0.064	8359.199	2567.700
175	1.968	2.43	84.88	0.063	7905.598	2624.400
176	1.858	1.54	53.96	0.062	7565.398	2729.700
177	1.760	0.83	28.95	0.062	7225.199	2818.600
178	1.601	-0.12	-4.11	0.060	6536.699	2907.900
179	1.506	-0.63	-21.88	0.059	6034.496	3045.600
180	1.351	-1.15	-40.30	0.056	5297.398	3288.600
181	1.351	-1.15	-40.30	0.056	5297.398	3288.600
182	1.351	-1.15	-40.30	0.056	5297.398	3288.600

POINT	MAX. DEFLECTION (IN)	MAX. LOAD (KIP)	MAX. MOMENT (KIP-IN)	MAX. ROTATION (RAD)	MAX. DIAGONAL JOINT STRAIN (MICRO IN/IN)	
0.	0.0	0.0	0.0	0.0	0.0	0.0
1.	0.900	7.13	249.55	0.005	2924.100	-882.900
2.	-1.205	-7.96	-278.50	-0.014	1044.900	5702.398
3.	0.636	5.31	185.88	-0.009	4203.898	1927.800
4.	-1.488	-8.35	-292.15	-0.020	2000.700	7694.996
5.	1.445	7.09	248.07	0.038	8594.098	3677.400
6.	2.021	-7.05	-246.59	-0.034	4641.297	10700.098
7.	2.153	4.80	168.12	0.064	8691.297	6455.699

Appendix C

THE DESIGN OF SPECIMEN 1

GIVEN:

$f'_c = 4{,}000$ psi ; $f_y = 60{,}000$ psi ; ρ(design)= 0.015

DESIGN A INTERIOR BEAM-COLUMN JOINT.

CHOOSING BEAM DIMENSION:

b=5.25in. ; d=5.25in. ; h=6.25in.(cover=0.5in.)

use 3#3 top bars; As=0.33 in^2 ; $\rho_{top}=0.012$

2#3 bottom bars; As'=0.22 in^2 ; $\rho_{bottom}=0.008$

$\rho_{min}=200/f_y=0.003$; $\rho_{max}= 1/2\ \rho_b =0.024$

DETERMINING THE LENGTH OF THE 'ARM' (beam)

$L/h \leq 21$; $L \leq 10.9$ ft.; use 6.67 ft.(from end to end)

(due to some difficulties encountered in the testing frame, it was decided to use 3ft. beam for the rest of the specimens)

CHOOSING COLUMN DIMENSION:

b=8.00in. ; d=6.06in. ; h=7.0in.

use 10#3 bars; As=1.10 in^2 ; $\rho_{col}=0.023$

$\rho_{col.max}=0.06$; $\rho_{col.min}=0.01$

DETERMINING THE LENGTH OF THE COLUMN

$L/r \leq 22$, where r=0.30h; $L \leq 46.2$ in.

use L=3.5 ft. (=42.0 in.)

JOINT CAPACITY

(Type 2 interior joint)

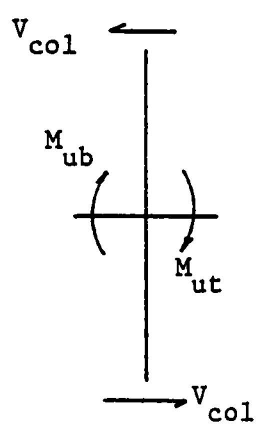

Shear: Forces in joint

Beam Moment $M_{ult} = \alpha$ Ast f_y (d-a/2)

where α=1.25; d=5.25 in.

a_t = 1.11 in. ; M_{ut}= 9.69 K-ft.

a_b = 0.74 in. ; M_{ub}= 6.70 K-ft.

$$V_{col} = \frac{M_{ut} + M_{ub}}{L_{col}} = 4.69 \text{ K}$$

SHEAR STRESS IN JOINT

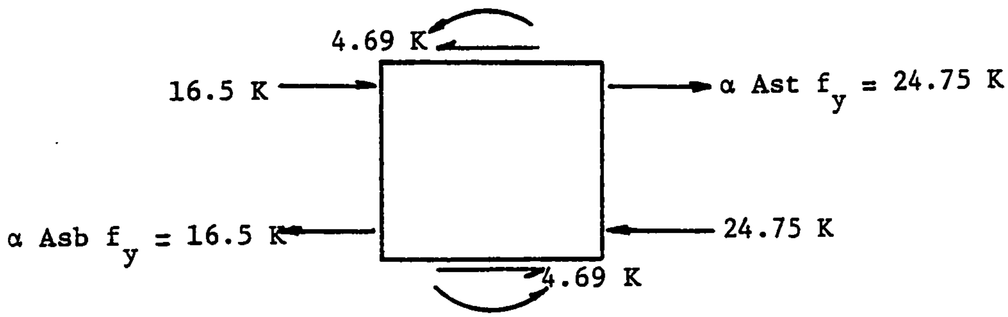

Vu = 24.75   16.50 - 4.69 = 36.56 K

Column: b_{eff} = 7.0 in. ; d = 6.06 in.

b < ¾ col. width

$Acv = b_{eff}\, d = 7.0(6.06) = 42.44\ in^2$

$$v_u = \frac{Vu}{\phi\ Acv} = \frac{36.56\ (1000)}{0.85\ (42.44)} = 1013.47\ psi < 20\sqrt{f'_c}\quad OK$$

JOINT SHEAR

Shear carried by concrete

β=1.0 ; γ=1.0 ; Nu/Ag=0

$$v_c = 3.5\ \beta\ \gamma\ \sqrt{f'_c\ (1 + 0.002(Nu/Ag))} = 221.36\ psi.$$

$$v_u - v_c = 1013.47 - 221.36 = 792.11 < 15\sqrt{f'_c}$$

Transverse steel for shear

$$\frac{Av\ f_y\ d}{S} = (v_u - v_c)\ Acv$$

$$\frac{3(0.05)(60)(6.06)}{S} = 0.792(42.44)$$

S = 1.62 in.

Use 3#2 at 1.25 in. spacing at the joint

BEAM STIRRUPS

$M_{tot} = M_{ut} + M_{ub} = 16.34$ K-ft. = 196.68 K-in.

$$\text{Load } P = \frac{M_{tot}}{arm} = \frac{196.68}{80} = 2.46 \text{ K.} \quad \{ \text{ Pe,equivalent} = 5.61 \text{ K } \}$$

$$v_u = \frac{Vu}{\phi\ b\ d} = 213.42 \text{ psi.}$$

$$v_c = 2\sqrt{f'_c} = 126.5 \text{ psi.}$$

$$Av = \frac{(v_u - v_c)\ b_w\ s}{f_y} \rightarrow \quad s_1 = 13.1 \text{ in.}$$

$$s_2 = \frac{Av\ f_y}{50\ b_w} = 22.86 \text{ in.}$$

$s_3 = d/2 = 2.6$ in. ← control

Use #2 closed ties in 2.5 in. spacing.

COLUMN TIES

$s_1 = 16\ d_{b_1} = 16(0.375) = 6$ in. ← control

$s_2 = 48\ d_s = 48(0.250) = 12$ in.

$s_3 = h_{min} = 7$ in.

Use #2 closed ties in 6.0 in. spacing.

Note: Necessary checks have been made to satisfy the design specification (A.C.I. 318/71 and Committee 352) for other specimens.